Response to RC1

The authors used GLASS CDRs data and Google Earth Engine platform and produced the long-term continuous land cover dataset from 1982 to 2015. This is a very valuable dataset for further applications in the analyses of energy and carbon dynamics and the global land surface modelling. However, I have some concerns about the data processing in the classification, accuracy assessment and the interpretation of the land cover change results. I think these problems must be solved / addressed before publication.

We thank the reviewer for the comments and thoughtful review. Please find our detailed response along with the suggested changes to our manuscript below.

1. Differences between forest and tree cover

The authors used vegetation cover fraction (VCF) data from Song et al. 2018. However, in their paper, they specified "tree cover" increase. This is not equal to forest increase. Usually, the forest is defined by canopy closure (e.g. tree cover fraction >10% in FAO, >25% in Hansen et al. 2013), tree height and minimum area. The authors showed that a lot of forest increase occurred in Siberia (Fig. 10) and was from grassland (Fig. 11). This could be artificial considering the coarse resolution (5 km) and poor ability of land cover mapping for mosaic pixels (see below) in the methods used in this study. For example, there is 5 ha forest with tree cover fraction of 35%, and the tree cover fraction increased to 45% because of better growth (e.g. longer growing season, CO2) in the same 5 ha forest. In this case, we cannot say the forest area increased 5 ha x 10% = 0.5 ha because it is the same 5 ha forest but with denser tree cover. Therefore, I doubt that there is confusion of these concepts in this manuscript and maybe in the classification system. The authors briefly mentioned this issue on L450-454, but this really needs to be clarified, assessed and solved.

Response 1:

Thank you for your advice. It should be pointed out that our classification target is land cover class, not vegetation cover percentage information. Our land cover products belong to the hard classification and give each mapping unit a single land cover class. VCF is only used as features that assist in the land cover classification, which is introduced as prior probability, and only one of many factors that affect the final classification result. Although based on VCF information, our results are not the same.

The classification system we used is from FROM-GLC_v2 (Li et al., 2017). Considering the quality of the data and the separability of classes, our products include 7 land cover classes, cropland, forest, grassland, shrubland, tundra, barren land, and snow and ice (Table 1). Among them, the forest is also defined and distinguished by canopy closure. The forest is defined under the condition that tree cover≥10% and height> 5m. We have updated the description of the classification system in our manuscript.

Table 1: Classification system, with 7 Level 1 classes and 21 Level 2 classes.

Level 1 class	Level 2 class	Description
Cropland	Rice paddy Greenhouse Other farmland Orchard Bare farmland	
Forest	Broadleaf, leaf-on Broadleaf, leaf-off Needle-leaf, leaf-on Needle-leaf, leaf-off Mixed leaf type, leaf-on Mixed leaf type, leaf-off	Tree cover≥10%; Height>5m; For mixed leaf, neither coniferous nor broadleaf types exceed 60%
Grassland	Pasture, leaf-on Natural grassland, leaf-on Grassland, leaf-off	Canopy cover≥20%
Shrubland	Shrub cover, leaf-on Shrub cover, leaf-off	Canopy cover≥20%; Height<5m
Tundra	Shrub and brush tundra Herbaceous tundra	
Barren land	Barren land	Vegetation cover<10%
Snow/Ice	Snow Ice	

We agree with you that forest increase may exist under the condition that you described. This is an inevitable problem in hard classification. What we call forest increase is the change of land cover class in our classification results under our 5km coarse resolution classification system. Limited to a spatial resolution of 5km, there are many mixed mapping units. For these mixed units, the estimation of hard classification will cause a large deviation. This is a common problem in hard classification. Similar problems also exist in land cover data prediction with higher spatial resolution. At coarse resolution, accurate estimates may be better with cover percentage data.

Change in manuscript:

We have updated the description to our used classification system in Table 1.

2. The majority land cover in a 0.05 deg pixel

The majority method in a coarse resolution (5 km) may work for some pure pixels but is expected to work poorly for the mosaic pixels with high heterogeneity or similar fraction of different vegetation types. For example, in a 5 km pixel with 43% tree cover, 44% grass and 13% others in the first year, it became 45% tree cover, 44% grass and 11% of others in the second year simply because of the good climate. If I understood correctly, this pixel would be classified as grassland in

the first year and forest in the second year, and thus there is a 25 km2 land cover change from grassland to forest. This may also partly explain the strong forest increase in Siberia, high variations in the temporal land cover dynamics in Fig. 8 and the high uncertainties in the intensive LCC regions (e.g. savanna in Africa).

Response 2:

Thanks for your comment. For mosaic pixels, especially mosaic pixels of vegetation, hard classification does have such disadvantages. The classification system used in the MODIS-based land cover product has included some mosaic classes, such as the Forest / Cropland Mosaics, Natural Herbaceous / Croplands Mosaics and Herbaceous Croplands defined in the FAO-Land Cover Classification System land use (LCCS2) system, which also reflects the difficulty and disadvantage of hard classification in coarse resolution to a certain extent. However, for these mosaic classes in the MODIS-based land cover product, hard classification is still used. Although at individual pixel level this is unavoidable when land cover data are aggregated over large areas the extreme cases as raised by the reviewer would usually be averaged out.

Despite of the disadvantage, the way that hard classification presents information is more direct. In many applications, researchers prefer to use the results of hard classification.

Besides, the scheme we used to aggregate and extract coarse-resolution samples from fine-resolution data is one of the common used schemes (DeFries et al., 1998;Wang et al., 2016). Under the framework of hard classification, there does not seem to be a better solution.

As for the LCC area reflected in the product, there are some places, as you said, that may be affected by the hard classification method. However, there are also many areas where the LCC is correctly reflected, such as the forest area of the Amazon region cut back. It should be pointed out that the LCC information in our results has uncertainty, especially the regions with high variability in LCC.

Change in manuscript:

We have added a reminder to data users about the uncertainty of our products.

3. Accuracy of change detection

The authors only assessed the accuracy for year 2015, not mentioning that the uncertainty of FROM-GLC_v2 was not propagated. First, the same product was used for training the classification system and for the accuracy assessment. Although the samples in the same product may be not overlapped, we cannot exclude the coherence since both are from FROM-GLC_v2. So, some independent evaluation dataset would be helpful. Second, an important feature of this continuous land cover maps is the temporal dynamics. So, the change detection needs to be further validated / evaluated in addition to the one-year classification accuracy assessment. This part is currently lacking in this work.

Response 3:

Thank you for your useful comment. In this revision, we collected a new independent test sample and performed the accuracy assessment. To prove the impact of change detection, we further compared the accuracies with and without change detection.

Specifically, we collected 2431 randomly distributed 5km sample points in different years around the world. According to the majority principle, we manually interpreted the land cover class of each sample as an independent test sample. Besides, to verify the accuracy of the change detection method, we also compared the classification accuracy before and after the change detection. The temporal distribution of the newly collected test samples is shown in Fig. 1, and the geographical distribution is shown in Fig. 2.

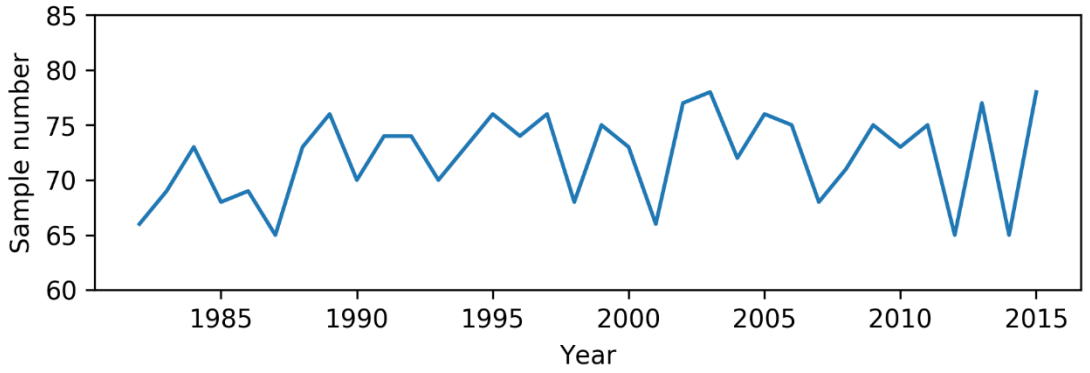

Figure 1: The temporal distribution of the newly collected test sample.

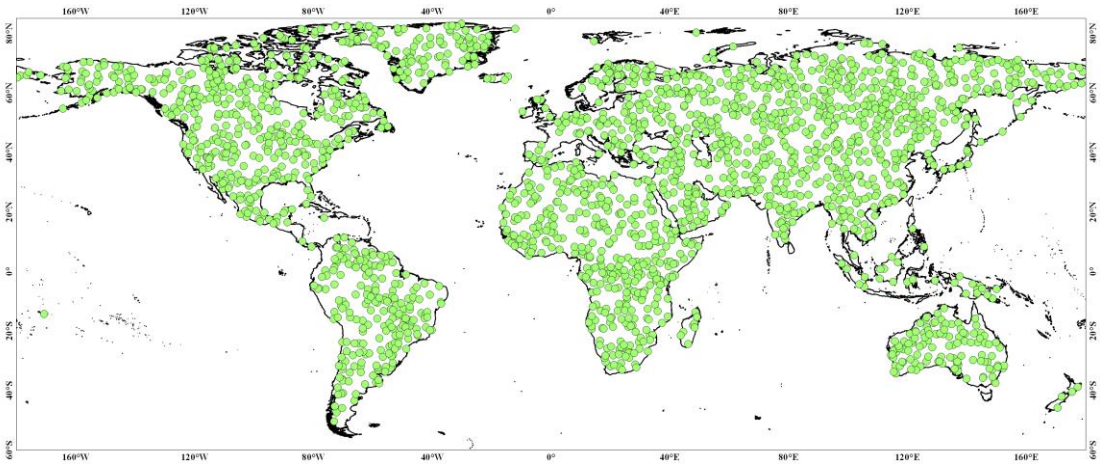

Figure 2: The geographical distribution of random test sample.

The new assessment result is shown in Table 3 and Table 4. It shows that OA of GLASS-GLC without change detection is 81.28%, and OA with change detection is 82.81%. This reflects the reliability of GLASS-GLC since the test samples are randomly distributed along the spatial and temporal dimensions, and also confirm the significance and effectiveness of the change detection method.

Table 3: Classification accuracy of GLASS-GLC without change detection under 2431 independent test samples. (Overall accuracy = 81.28 %, UA = User's Accuracy and PA = Producer's Accuracy)

Class	Cropland	Forest	Grassland	Shrubland	Tundra	Barren land	Snow/ice	Total number	UA
Cropland	257	21	34	15	0	31	0	358	71.79%
Forest	35	620	45	27	22	1	1	751	82.56%
Grassland	17	26	248	12	3	19	4	329	75.38%
Shrubland	7	6	10	154	9	12	0	198	77.78%
Tundra	0	9	11	12	250	3	0	285	87.72%
Barren land	4	1	13	14	5	355	6	398	89.20%
Snow/ice	0	4	3	0	0	13	92	112	82.14%
Total number	320	687	364	234	289	434	103	2431	
PA	80.31%	90.25%	68.13%	65.81%	86.51%	81.80%	89.32%		81.28%

Table 4: Classification accuracy of GLASS-GLC with change detection under 2431 independent test samples. (Overall accuracy =82.81 %, UA = User's Accuracy and PA = Producer's Accuracy)

Class	Cropland	Forest	Grassland	Shrubland	Tundra	Barren land	Snow/ice	Total number	UA
Cropland	262	19	32	20	0	25	0	358	73.18%
Forest	33	637	29	28	24	0	0	751	84.82%
Grassland	24	24	254	6	13	8	0	329	77.20%
Shrubland	12	3	11	159	6	7	0	198	80.30%
Tundra	0	12	9	4	250	10	0	285	87.72%
Barren land	5	1	17	8	7	357	3	398	89.70%
Snow/ice	0	5	6	0	0	7	94	112	83.93%
Total number	336	701	358	225	300	414	97	2431	
PA	77.98%	90.87%	70.95%	70.67%	83.33%	86.23%	96.91%		82.81%

Change in manuscript:

We have added the new accuracy assessment result in the manuscript.

4. Comparison with other datasets

A suggestion for the evaluation may be to compare the total area, spatial and temporal changes with other datasets e.g. ESA-CCI 300 m, Hansen forest, FAO and some cropland datasets. This would help to verify the mapping results in this study and to understand their differences. It would also help to define the possible applications of this dataset (e.g. whether it can be used for carbon accounting, land modeling).

Response 4:

Thank you for your advice. Comparison with other land cover products is a very good way to reflect product quality and accuracy. For this reason, in addition to the classification accuracy obtained by several evaluation methods, we compared other available land cover products with our products. Although there are some differences in the classification system of different products, it can still reflect the reliability of our products in general.

We inter-compared GLASS-GLC with other available global land cover products with a relatively long time series. Land cover products from MODIS and the ESA-CCI were used. The MODIS-based global land cover products come from Collection 6 (C6) MODIS Land Cover Type (MLCT) products (Sulla-Menashe et al., 2019), and are supervised classification results from 2001 to 2016. Considering the comparability to our classification system, the FAO-Land Cover Classification System land use (LCCS2) layer was used. The corresponding relationships of classes are listed as follows, and the class names we used are the latter: barren - barren land, permanent snow and ice – snow/ice, all kinds of forest – forest, forest/cropland mosaics and natural herbaceous/cropland mosaic – cropland, natural herbaceous and herbaceous cropland – grassland, shrubland - shrubland. The ESA-CCI global land cover products (Bontemps et al., 2013) are 300m resolution yearly products ranging from 1992 to 2015. The products were developed using the GlobCover unsupervised classification chain and merging multiple available Earth observation products based on the GlobCover products of the ESA (Liu et al., 2018). Referring to the class relationships in (Liu et al., 2018), we cross-walked classes including cropland, forest, grassland, shrubland, barren land and snow/ice.

Apart from land cover products, we also compared GLASS-GLC with the Food and Agricultural Organization of the United Nations statistical data (FAOSTAT) on cropland and forest (forest land) classes, which are the main sources of country-level land cover data for many applications. The annual FAOSTAT data set on cropland we used ranged from 1982 to 2015, and that on forest we used ranged from 1990 to 2015.

We made an inter-comparison between classes including cropland, forest, grassland, shrubland, barren land and snow/ice. The main inter-comparison is the area corresponding to the top 50 countries in each class. Besides, to compare the accuracy of different products, test samples from FLUXNET site data in 2015 are given for independent accuracy assessment.

The assessment results of MODIS-based land cover products and ESA-CCI land cover products based on test samples from FLUXNET site data are shown in Table 6 and Table 7, respectively. The overall accuracies of ESA-CCI products and MODIS-based products are 73.90% and 80.38% in 2015, respectively. Compared to these, The overall accuracy of GLASS-GLC (82.10%, Table 5) is superior. Although the cross-walk of the different classification systems may be slightly different, It can still reflect the high accuracy of our GLASS-GLC products.

Table 5: Classification accuracy of GLASS-GLC in 2015 based on FLUXNET test sample. (Overall accuracy = 82.10 %, UA = User's Accuracy and PA = Producer's Accuracy)

Class	Cropland	Forest	Grassland	Shrubland	Tundra	Barren land	Snow/ice	Total number	UA
Cropland	**63**	5	17	1	0	0	0	86	73.26 %
Forest	13	**243**	9	2	0	0	0	267	91.01 %
Grassland	8	21	**91**	2	0	2	0	124	73.39 %
Shrubland	7	3	0	**19**	0	0	0	29	65.52 %
Tundra	0	3	0	0	**14**	0	0	17	82.35 %
Barren land	0	1	0	0	0	**1**	0	2	50.00 %
Snow/ice	0	0	0	0	0	0	**0**	0	-
Total number	91	276	117	24	14	3	0	**525**	
PA	69.23 %	88.04 %	77.78 %	79.17 %	100.00 %	33.33 %	-		**82.10 %**

Table 6: Classification accuracy of the MODIS-based land cover product in 2015 based on FLUXNET test sample. (Overall accuracy = 82.10 %, UA = User's Accuracy and PA = Producer's Accuracy)

Class	Cropland	Forest	Grassland	Shrubland	Tundra	Barren land	Snow/ice	Total number	UA
Cropland	**7**	5	73	0	0	0	0	85	8.24%
Forest	1	**261**	5	0	0	0	0	267	97.75%
Grassland	1	15	**108**	1	0	0	0	125	86.40%
Shrubland	0	9	9	**11**	0	0	0	29	37.93%
Tundra	0	3	6	8	**0**	0	0	17	-
Barren land	0	0	1	0	0	**1**	0	2	50.00%
Snow/ice	0	0	0	0	0	0	**0**	0	-
Total number	9	293	202	20	0	1	0	**525**	
PA	77.78%	89.08%	53.47%	55.00%	-	100.00%	-		**73.90%**

Table 7: Classification accuracy of the ESA-CCI land cover product in 2015 based on FLUXNET test sample. (Overall accuracy = 82.10 %, UA = User's Accuracy and PA = Producer's Accuracy)

Class	Cropland	Forest	Grassland	Shrubland	Tundra	Barren land	Snow/ice	Total number	UA
Cropland	**81**	1	4	0	0	0	0	86	94.19%
Forest	11	**246**	4	5	0	1	0	267	92.13%
Grassland	28	7	**76**	5	0	8	0	124	61.29%
Shrubland	2	7	1	**19**	0	0	0	29	65.52%
Tundra	0	3	9	0	**0**	5	0	17	-
Barren land	0	0	2	0	0	**0**	0	2	0.00%
Snow/ice	0	0	0	0	0	0	**0**	0	-
Total number	122	264	96	29	0	14	0	**525**	
PA	66.39%	93.18%	79.17%	65.52%	-	0.00%	-		**80.38%**

Figure 3 shows an inter-comparison with MODIS-based products, Figure 4 with ESA-CCI products and Figure 5 with FAOSTAT. The scatter plots and the linear fit lines reflect the results in 2015, and the box plots represent the distribution of R^2 of the annual linear fit lines for each class. It can be seen that various classes in several different products are relatively equivalent although they are under different classification systems. In comparison with MODIS-based products, the results of 2001-2015 for cropland, forest and snow/ice have high R^2. In comparison with ESA-CCI products, the mean R^2 of the linear fit lines of forest, grassland and snow/ice from 1992 to 2015 reach 0.99, 0.82, and 0.98, respectively, while the R^2 for shrubland is low. The inter-comparison of some other classes is poor, which may be caused by differences in the class definition in various classification systems. For instance, our classification system incorporates tundra, while the other two did not. Compared with FAOSTAT, the mean R^2 of the linear fit lines of cropland and forest is 0.82, and 0.87, respectively. In general, our GLASS-GLC products have a reasonable consistency with other products and statistics and the difference are not significant.

What's more, the duration of GLASS-GLC is much longer than MODIS-based and ESA-CC land cover products (as shown in Fig. 6). The comparison with other data illustrates the reliability and superiority of GLASS-GLC.

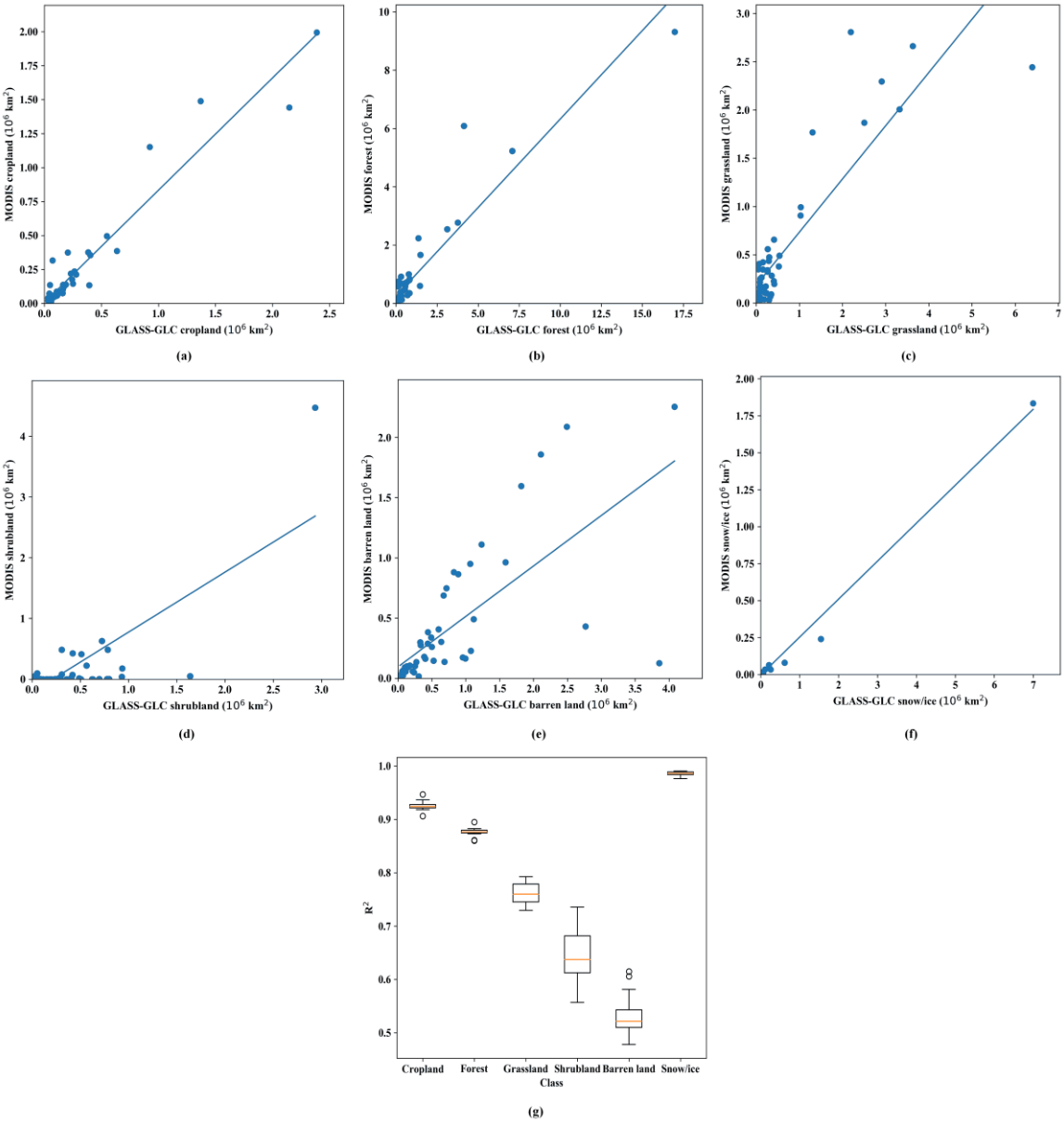

Figure 3: Inter-comparison with the MODIS-based land cover product, (a) cropland circa 2015, (b) forest circa 2015, (c) grassland circa 2015, (d) shrubland circa 2015, (e) barren land circa 2015 and (f) snow/ice circa 2015; (g) mean R2 of the annual linear fit lines for all years (2001-2015).

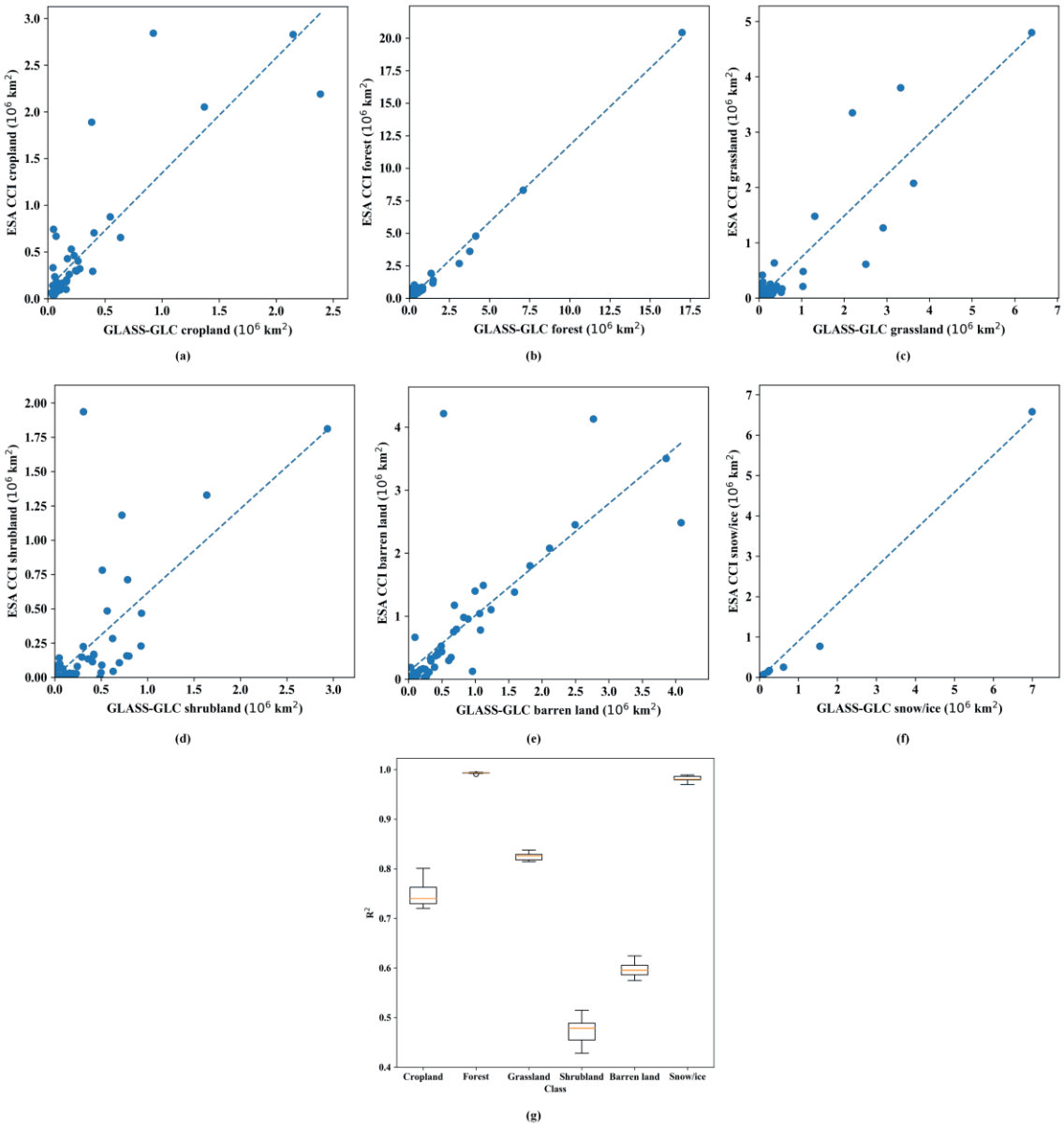

Figure 4: Inter-comparison with the ESA-CCI land cover product, (a) cropland circa 2015, (b) forest circa 2015, (c) grassland circa 2015, (d) shrubland circa 2015, (e) barren land circa 2015 and (f) snow/ice circa 2015; (g) mean R2 of the annual linear fit lines for all years (1992-2015).

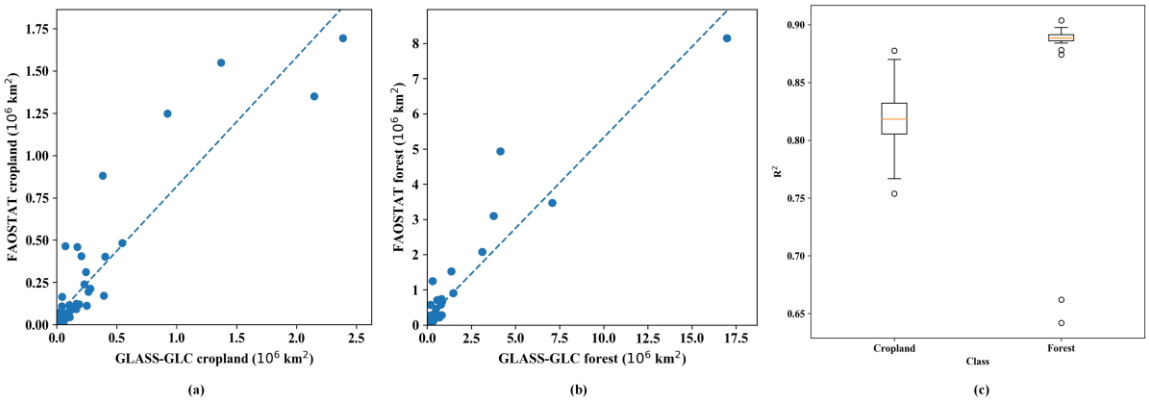

Figure 5: Inter-comparison with the FAOSTAT data set, (a) cropland circa 2015, (b) forest circa 2015, (c) mean R2 of the annual linear fit lines of cropland for years 1982-2015 and forest for years 1990-2015.

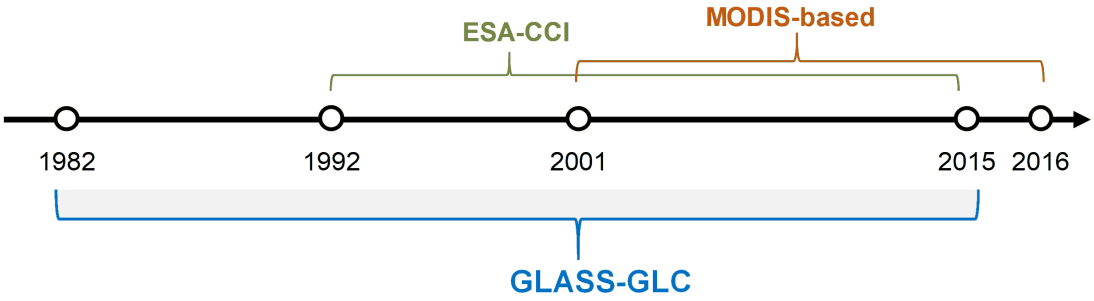

Figure 6: The duration of different land cover products, including GLASS-GLC, MODIS-based land cover products and ESA-CCI land cover products.

Change in manuscript:

We have included comparison results with other land cover data in the manuscript to help show the reliability and effectiveness of our products.

5. Superficial and fragmented interpretations of reasons for LCC

The authors made a lot of figures and tables to show the spatial and temporal changes and also reasons for such changes. These sections are not well organized and lack some internal logics. What I learned is only some fragmented information. The reasons for the LCC are not very solid (see my detailed comments below). Just taking one example, the author mentioned several times of "greening" and its effects on LCC. However, greening is very far away from LCC. It may only be caused by more leaves and extended growing season. We don't know whether this increased productivity was converted to carbon stock or leaded to a land cover transition from grass to forest. The increased carbon uptake by greening may just release back to the atmosphere through the enhanced respiration due to increased temperature. So, I would suggest being cautious when interpreting the reasons for the LCC. In fact, I don't think these sections are necessary for this manuscript. Adding comparisons with other datasets and discussing the differences between various data and the reasons (e.g. data sources, classification methods) would be enough for a nice data

paper. The reasons for LCC can be separated to another paper after adding more analyses. Putting it here only attenuate the main objective of this manuscript.

Response 5:

Thank you for your comment. The interpretations of reasons for LCC are just some examples of our attempts to apply our product for further analysis, not the main focus of this paper. The focus of this article is on the presentation and quality assessment of our produced GLASS-GLC data products. To this end, we have added more content on accuracy assessment and product inter-comparison, to better demonstrate the reliability and uncertainty of our products. As for the reasons for LCC, we will analyze and discuss in more detail in a subsequent paper.

Change in manuscript:

We have supplemented the sections of accuracy assessment and data inter-comparison.

6. Writing
Language needs further improvements. A lot of sentences are difficult to understand, and some sentences are broken in the context. Please polish the language during revision.

Response 6:

Thanks for your suggestion.

Change in manuscript:

We have polished our language with a native English consultant.

Specific comments:
L19: report how many classes

Response s1:

The classification system consists of 7 classes, including cropland, forest, grassland, shrubland, tundra, barren land, snow/ice, as shown in Table 1 in the manuscript.

Change in manuscript:

We have added the information in the corresponding place as you suggested.

L20: 85% accuracy based on what?

Response s2:

It was based on 23459 test samples in 2015. And the overall accuracy of the produced GLASS-GLC CDR in 2015 is 86.51 %. The test samples come from the 30 m resolution FROM-GLC_v2 test sample set (Li et al., 2017).

To give a more effective assessment, we also performed an accuracy assessment using FLUXNET site data and the newly collected independent test samples, and we supplemented this part of the results.

Change in manuscript:

We have updated the detail in the corresponding place.

L22: how can you separate afforestation and forest expansion?

Response s3:

The data products we produce can only provide information at the observation level. For example, the information we can obtain here is only forest gain. While the specific causes of these LCCs should be analyzed and investigated separately, we cannot distinguish afforestation and natural expansion of forests.

Change in manuscript:

We have modified our description according to our study.

L23: land degradation? did you mean grassland loss? if it is degradation, it may still be grassland.

Response s4:

Yes, we do mean by grassland loss. At the individual mapping unit level, we cannot detect land degradation.

Change in manuscript:

We have changed the word “land degradation” to “grassland loss”.

L25: greening is not directly related to LCC. very complex processes behind.

Response s5:

Greening is indeed a very complex process. Here, we mainly refer to vegetation gain such as forest gain in our results, which can only be used as evidence from the perspective of remote sensing and mapping. Thanks for pointing it out.

Change in manuscript:

We have corrected our expression.

L37: What is “surface attributes”?

Response s6:

It refers to the characteristics and properties of the Earth surface. The change of land cover would change the status of the Earth surface.

Change in manuscript:

We have changed the word “attributes” to “characteristics”.

L44: too strong statement

Response s7:

Thank you for your reminding.

Change in manuscript:

We have modified our expression.

L70: “which will…” useless half sentence

Response s8:

Many thanks.

Change in manuscript:

We have rechecked the sentence and deleted it.

L75: not clear “more prone to consistency and data volume”, rephrase

Response s9:

What we mean here was that Landsat data has a higher spatial resolution, but it also meets some problems including obvious cloud contamination, data inconsistency caused by multiple generations of sensors and relatively larger data volume because of the high resolution.

Change in manuscript:

We have changed it to detailed description.

L87: “Because of…” duplicate

Response s10:

Thanks for your comment.

Change in manuscript:

We have changed the used “Because of” to “Due to”.

L91: analyses

Response s11:

Thank you for correcting us.

Change in manuscript:

We have changed the word.

L136: explain if you have level 2 class and how they were derived

Response s12:

There are no Level 2 classes in our results. Considering the resolution and separability of GLASS data, only Level 1 classes are included. The description of Level 2 classes comes from the original design in the FROM-GLC classification system (Gong et al., 2013). It was listed in Table 1 to better show the meaning of each Level 1 class. In the future, we will try to produce land cover products

with a more detailed classification system.

L142: “2013-2015” is it a one-year map or three maps each for a year?

Response s13:

It was a one-year map, not three maps. Due to the problem of data quality, the Landsat data in one year usually cannot meet the need for land cover mapping on a global scale. The production of the FROM-GLC_v2 map took advantage of data from 2013 to 2015. And it can roughly be called circa 2015 (Li et al., 2017).

L145: “with a limited …” not clear what it is.

Response s14:

When generating random points in ArcGIS with the “create random points” tool, we limited the spatial interval among points greater than 0.1° by setting the parameter “minimum allowed distance” as 0.1.

Change in manuscript:

We changed our description.

L147: “class distribution” do you mean “percentage of each class”?

Response s15:

Yes. It means the percentage of each class.

Change in manuscript:

We have changed the description.

L158: what is end-number? end of what?

Response s16:

It is called end-member. Due to the complexity of ground objects and the limited spatial resolution of various sensors, the information contained in a pixel of remote sensing images is the mixture of information of many ground objects, hence resulting in mixed pixels (Zhang et al., 2011). It is

assumed that there are pure land cover types known as basic mixing elements (known as end-member) that cannot be further decomposed in the imaged area, and the process of finding these end-members is referred to endmember extraction (Plaza et al., 2002). Here, to reduce the systematic deviation of AVHRR products, we correct the GLASS data with MODIS products based on end-members (Song et al., 2018).

L162: Is the smaller fluctuation the truth? Something you expected?

Response s17:

It is a trade-off. The purpose of data correction was to correct the original remotely sensed data to a higher consistency, especially in the temporal dimension. Remotely sensed data is easy to be affected by many random and systematic factors such as the atmospheric environment and sensor situation. The values it reflects were usually not those of the real and direct surface conditions. What's more, many fake inter-annual variations exist in remotely sensed data (Friedl et al., 2010). This will cause much trouble and disturbance especially in the use of time-series remotely sensed data. Though the variations may be caused by phenological changes, other interfering factors exist, and the trade-off is more beneficial in general.

The correction process carried out belongs to one of the data pre-processing processes in time-series land cover mapping (Gómez et al., 2016), which was to mitigate and deal with these aspects and to produce more consistent data for use.

L172: How is the performance of you trained random forest classifier? OOB R2 or independent evaluation dataset?

Response s18:

The OOB accuracy of our random forest classifier reached to 87.12%.

Change in manuscript:

We have added this information in the manuscript.

L174: what are the other parameters and the default values?

Response s19:

The specific parameters are listed as follows. The number of trees was 200, the out-of-bag mode is on. The number of variables per split was set to 0, as the square root of the number of variables. The minimum size of a terminal node was 1, the fraction of input to bag per tree was 0.5, and the random

seed was 0.

Table 8 Specific parameters of the random forest classifier

Parameter	**Value**
Number of trees	200
Number of variables per split	0
Minimum size of a terminal node	1
Fraction of input to bag per tree	0.5
Whether the classifier should run in out-of-bag mode	True
Random seed	0

Change in manuscript:

We have listed the above parameter values in the manuscript.

L179: “the mode of…” not clear

Response s20:

The mode here refers to the class label that has the highest frequency in the segmented period with the calculated breakpoints. To improve the time consistency in the classification results, we use the mode class label to replace all the class labels in the period.

Change in manuscript:

We have updated our expression.

L186: How about the heterogeneous pixels? Not assessed at all?

Response s21:

Thanks for your question. In the newly collected independent test sample set, we use random points, with no difference between homogeneous and heterogeneous pixels. Therefore, the new assessment results include heterogeneous pixels.

L190: “class distribution”

Response s22:

Thanks for your reminding.

Change in manuscript:

We have changed the description.

L206: It is OK to fit a linear trend, but you cannot say to remove … because it may be caused by the actual LCC

Response s23:

Thanks for your advice. Our purpose was to fit a linear trend for better extraction of the land cover change trend in the long time-series land cover data. The fluctuations in the land cover were generally seen as an abnormal condition caused by climate conditions and phenological changes since the land cover is stable in most areas in the world across years, but they can be caused by the actual land cover change as you said.

Change in manuscript:

We have changed the description.

L212: why is summed?

Response s24:

Because we wanted to ensure the significance of the land cover change trend. For each pixel in the land cover map of each class, the original 0.05 ° pixel is labeled with 0 or 1 (belonging to the class or not), and such categorical data (not continuous data) cannot be statistically hypothesized. In order to carry out the hypothesis test, some studies used downscaling (Wang et al., 2016). By downscaling, the categorical label data can be summed up as the area ratio of the class (numerical data) in a greater statistical area, thus a statistical hypothesis test can be performed to verify the significance of land cover change.

L213: what is “annual change in slope of area ration”?

Response s25:

We are sorry for making a slip in writing. It is in fact “annual change slope of area ratio” estimated from a Theil-Sen estimator. More specifically, it represents the speed of land cover change.

Change in manuscript:

We have corrected it.

L219: why only statistically significant change was included? It is still area change even the trend is not significant. The way you process data exaggerate the changes.

Response s26:

Yes, there are certain shortcomings in doing so. But relatively speaking, this is a better strategy. Because it usually exists fake inter-annual land cover change in time-series land cover mapping studies (Sulla-Menashe et al., 2019) caused by many kinds of factors as explained in the above. Although there may be some real land cover change, to ensure the significance and reduce the uncertainty we did not include those into the statistics.

L223-224: Again, why only change mask?

Response s27:

Because we want to ensure the statistical significance and reduce the uncertainty caused by classification noises to detect more robust long-term land cover change trends.

L225: “direct” duplicate

Response s28:

Thank you for your comment.

Change in manuscript:

We have deleted the word.

L242: Need to explain UA and PA for non-remote-sensing readers; explain what the column and row names refer to.

Response s29:

Thanks for reminding. UA and PA represent user’s accuracy and producer’s accuracy respectively. They are two metrics reflecting the accuracy of classification. UA = corrected classified sample number / total sample number in the classification, PA = corrected classified sample number / total sample number in test sample.

Change in manuscript:

We explained the abbreviations in the titles of the corresponding tables.

L245: “Grassland is …” , from Table 3, they are shrubland and forest

Response s30:

It was concluded from the row dimension with the user’s accuracy. But as for the producer’s accuracy, it is as what you said.

L248: samples

Response s31:

Many thanks.

Change in manuscript:

We have corrected the word.

L255: these are regions with intensive LCC

Response s32:

Some regions such as Africa show relatively intensive LCC. There may be more mosaic pixels in these places in Africa, which may also lead to high uncertainty

For other regions with relatively high uncertainty, their locations are close to the continent edge which may be one of the reasons. The uncertainty map was reported based on the interpolation of test samples, the uncertainty values near the edges where test samples are rarely distributed would be affected to some degree.

L259: “variation curves” temporal changes

Response s33:

Thank you very much for your kindness.

Change in manuscript:

We have changed the phrase.

L260: Why so strong forest increase from 2006-2008? is it real?

Response s34:

We think it should be carefully treated. Since we do not have sufficient reference data, we cannot be sure if this is real or artifacts. The fluctuations in the curves can be seen as one of the representations of the uncertainty using coarse-resolution remotely sensed data.

L262: what about cropland? why so high variations, especially in 1994, 1999?

Response s35:

Cropland showed a slightly increasing trend, but not significantly. The high variations also reflect some kind of uncertainty introduced by the input data.

L263: Fig. 9, explain the meaning of your boxplot, mean, median, IQR, 90%, max, min? Why use the ratio, instead of total change area which is more straightforward?

Response s36:

The box extends from the first (lower) quartile (Q1) to third (upper) quartile (Q3) values of the data, with a line indicating the median. The whiskers extend from the box to show the range of the data. The upper whisker extends to the last datum less than Q3 + 1.5 * IQR, and the lower whisker extends to the first datum greater than Q1 - 1.5 * IQR. Flier points are those past the end of the whiskers. We wanted to use the change ratio to better reflect that how much percentage of global land cover changed in one year exactly like other studies (Friedl et al., 2010;Sulla-Menashe et al., 2019).

Change in manuscript:

We have added the corresponding introduction.

L263: “different time periods” the gross change each year or on the difference between the first and the last year in each period?

Response s37:

The annual ratio of the global land cover change area to the global total terrestrial area is plotted in

Fig. 9, but in a form of boxplot organized in a 5-year interval (a) and 10-year interval (b).

Change in manuscript:

We have revised our description.

L267: It's interesting to see a very likely decreasing trend of total LCC area.

Response s38:

Yes, and it was what our results showed.

L270: Fig. 10: The text and subplots in the figure is too small to read. I would suggest to only show the main land cover types and put the others to SI

Response s39:

Thanks for your suggestion.

Change in manuscript:

We have moved the low percentage classes such as shrubland, tundra and snow/ice to the supplementary information part.

L271: why only significant LCC? is it really necessary? why not just sum all?

Response s40:

In our opinion, the statistical test is necessary to lower the uncertainty in the long time-series land cover mapping results, especially for 0.05° such coarse resolution data.

L287: Table 5-10: too detailed, may put into SI and merge these results in a plot with different subplots

Response s41:

Thank you for the advice.

Change in manuscript:

We have reorganized the tables and put some into the supplementary information part.

L299: In In

Response s42:

Thanks for your correction.

Change in manuscript:

We have deleted the extra word.

L304-308: see my comments on greening above

Response s43:

Thanks again.

Change in manuscript:

We have deleted the corresponding part.

L309: need to note the high uncertainty from Fig. 7

Response s44:

Thank you for your valuable comment.

Change in manuscript:

We have added the note in the manuscript.

L310-311: greening again

Response s45:

Thanks again.

Change in manuscript:

We have deleted the corresponding part.

L313: Look at Fig. 10 and 11, significant grassland changed to forest in your dataset in the high latitudes

Response s46:

Yes, it is.

L316-317: why barren land decrease implies the desertification effects?

Response s47:

We may not expressed it clearly. What we mean was the management efforts to the desertification.

Change in manuscript:

We have updated the description.

L321: what is a coupling effect? non-relevant sentence

Response s48:

Thank you for the comment. What we mean was that natural and human factors usually had a significant joint effect on land cover change. Both aspects contribute to making a difference.

Change in manuscript:

We have revised the sentence.

L324 and all below: referring a or b when you report something. Why no explanations on the transitions from grassland to forest, which is the most obvious pattern in your figure

Response s49:

Thanks for your suggestion. This may be related to the shortcomings of the hard classification we adopted. As you pointed out above, the forest may become denser and the land cover class may change. But the interpretations of these phenomena are not the main focus of this paper.

L338: too strong statement. surface greening is not something that you can directly interpreted from LCC.

Response s50:

Thanks for your comment.

Change in manuscript:

We have changed the word.

L345: “natural vegetation” managed forest or pasture are not natural vegetation

Response s51:

Thank you for the comment. We used the wrong word.

Change in manuscript:

We have deleted the word “natural”.

L346: how about reforestation?

Response s52:

Yes, human activities also include reforestation. The focus of this paper is still on data product introduction and evaluation, we will weaken this part of the introduction.

Change in manuscript:

We have revised our description to avoid the ambiguity.

L355: shy subtropical mountain system is also high?

Response s53:

Figure 6 shows the division of eco-regions from FAO, where regions in the orange color belong to subtropical mountain system. Referring to Fig. 5, they overlaps some regions with a relatively high human impact level, such as Spain, central China, east America and South Africa. These regions may bias the overall results.

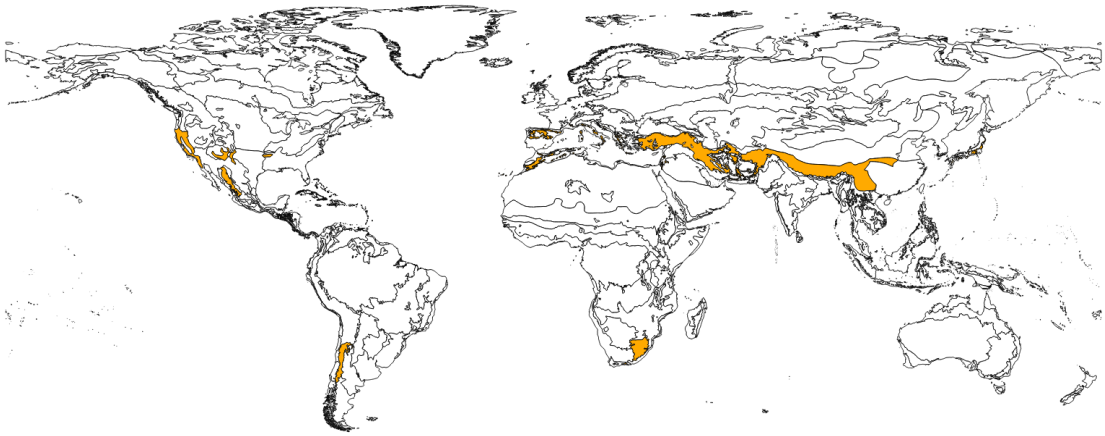

Figure 6 Subtropical mountain system eco-regions from FAO.

L363: Fig. 15 is very misleading with only >0 and <0. Why not give gradient of change?

Response s54:

Thank you very much for your suggestion. Here, we do so because we want to more intuitively reflect the information about where gain or loss occurred.

L365 and below: again, give the subplot title when you describing the results.

Response s55:

Thanks again.

Change in manuscript:

We have added the information as you suggested.

L381: Do you have evidence that global warming will increase vegetation in tropics?!

Response s56:

This part of the analysis is not the focus of this paper.

L383-384: Oil palm plantations are forest or crop in your classification system? I am not sure whether you can distinguish them!

Response s55:

We are sorry for it. In our classification system, oil palm plantations are forest.

Change in manuscript:

We have adjusted the sentence.

L399: Is that partly why you detected forest increase at the expense of grassland?

Response s57:

We are afraid not. Mongolia and Inner Mongolia of China mostly belong to semi-arid regions. The land cover types there should be grassland or barren land. It should have nothing to do with the forest.

L421-423: yes, this is the main defect of this product.

Response s58:

Yes. This is also one of the common problems of hard classification.

L435: This is definitely something that has to be done in this work.

Response s59:

Thank you for your advice. In order to specifically evaluate the magnitude of the errors introduced by our training samples, we randomly selected 500 samples from the training samples for manual interpretation and evaluation, and the assessment accuracy was 92.26%. It shows that the training samples we generate this way are sufficient for our data production.

Change in manuscript:

L441: what about the heterogeneous pixels?

Response s60:

We have added new samples for comprehensive independent accuracy assessment, where heterogeneous samples are also included.

L460: NDVI and LAI increase not equal to forest increase

Response s61:

Indeed it is. NDVI and LAI are features that help forest classification, and we are not strict in saying so here.

Change in manuscript:

We have updated our words.

L455-463: not helping but expose the weakness of the product

Response s62:

Thanks for your comment.

Change in manuscript:

We have deleted the corresponding part.

L464-465: This contradicts that you said forest loss in SE Asia is due to oil palm plantations

Response s63:

We are sorry for it. In our classification system, oil palm plantations are forests.

L466-467: need more explanations to justify the reasons for doing this.

Response s64:

As mentioned above, this is the result of our trade-off. There are too many uncertain factors in remote sensing. In contrast, suppressing some real fluctuations in LCC, and performing post-processing in the time dimension can make data products more reliable, less uncertain and less noisy. And the accuracy improvement brought by change detection illustrates the effectiveness of doing so.

References

Bontemps, S., Defourny, P., Radoux, J., Van Bogaert, E., Lamarche, C., Achard, F., Mayaux, P., Boettcher, M., Brockmann, C., and Kirches, G.: Consistent global land cover maps for climate modelling

communities: Current achievements of the ESA's land cover CCI, Proceedings of the ESA Living Planet Symposium, Edimburgh, 2013, 9-13,

DeFries, R. S., Hansen, M., Townshend, J. R. G., and Sohlberg, R.: Global land cover classifications at 8 km spatial resolution: the use of training data derived from Landsat imagery in decision tree classifiers, International Journal of Remote Sensing, 19, 3141-3168, https://doi.org/10.1080/014311698214235, 1998.

Friedl, M. A., Sulla-Menashe, D., Tan, B., Schneider, A., Ramankutty, N., Sibley, A., and Huang, X.: MODIS Collection 5 global land cover: Algorithm refinements and characterization of new datasets, Remote Sensing of Environment, 114, 168-182, https://doi.org/10.1016/j.rse.2009.08.016, 2010.

Gómez, C., White, J. C., and Wulder, M. A.: Optical remotely sensed time series data for land cover classification: A review, ISPRS Journal of Photogrammetry and Remote Sensing, 116, 55-72, https://doi.org/10.1016/j.isprsjprs.2016.03.008, 2016.

Gong, P., Wang, J., Yu, L., Zhao, Y., Zhao, Y., Liang, L., Niu, Z., Huang, X., Fu, H., and Liu, S.: Finer resolution observation and monitoring of global land cover: First mapping results with Landsat TM and ETM+ data, International Journal of Remote Sensing, 34, 2607-2654, https://doi.org/10.1080/01431161.2012.748992, 2013.

Li, C., Gong, P., Wang, J., Zhu, Z., Biging, G. S., Yuan, C., Hu, T., Zhang, H., Wang, Q., Li, X., Liu, X., Xu, Y., Guo, J., Liu, C., Hackman, K. O., Zhang, M., Cheng, Y., Yu, L., Yang, J., Huang, H., and Clinton, N.: The first all-season sample set for mapping global land cover with Landsat-8 data, Science Bulletin, 62, 508-515, https://doi.org/10.1016/j.scib.2017.03.011, 2017.

Liu, X., Yu, L., Li, W., Peng, D., Zhong, L., Li, L., Xin, Q., Lu, H., Yu, C., and Gong, P.: Comparison of country-level cropland areas between ESA-CCI land cover maps and FAOSTAT data, International Journal of Remote Sensing, 1-15, https://doi.org/10.1080/01431161.2018.1465613, 2018.

Plaza, A., Martínez, P., Pérez, R., and Plaza, J.: Spatial/spectral endmember extraction by multidimensional morphological operations, IEEE transactions on geoscience and remote sensing, 40, 2025-2041, https://doi.org/10.1109/TGRS.2002.802494, 2002.

Song, X.-P., Hansen, M. C., Stehman, S. V., Potapov, P. V., Tyukavina, A., Vermote, E. F., and Townshend, J. R.: Global land change from 1982 to 2016, Nature, 560, 639, https://doi.org/10.1038/s41586-018-0411-9, 2018.

Sulla-Menashe, D., Gray, J. M., Abercrombie, S. P., and Friedl, M. A.: Hierarchical mapping of annual global land cover 2001 to present: The MODIS Collection 6 Land Cover product, Remote sensing of environment, 222, 183-194, https://doi.org/10.1016/j.rse.2018.12.013, 2019.

Wang, C., Gao, Q., Wang, X., and Yu, M.: Spatially differentiated trends in urbanization, agricultural land abandonment and reclamation, and woodland recovery in Northern China, Scientific reports, 6, 37658, https://doi.org/10.1038/srep37658, 2016.

Zhang, B., Sun, X., Gao, L., and Yang, L.: Endmember extraction of hyperspectral remote sensing images based on the ant colony optimization (ACO) algorithm, IEEE transactions on geoscience and remote sensing, 49, 2635-2646, https://doi.org/10.1109/TGRS.2011.2108305, 2011.

Response to RC2

We thank the reviewer for the comments and thoughtful review. Please find our detailed response along with the suggested changes to our manuscript below.

General comment:

By fusing multiple existing geo-spatial datasets, the main work of this manuscript is to generate an annual dynamic product (spatial resolution: 0.5°) addressing seven kinds of land-covers (i.e., cropland, forest, grassland, shrub-land, tundra, barren land and snow/ice) from 1982 to 2015. With eye on the current existing datasets (i.e., from the perspective of classification system, period of time, and spatial/temporal resolution) the contribution is quite limited. In view of the rationality of technique and accuracy assessment, current version calls for serious revision before publication. In view of the analysis conducted on the dynamic map, rare novel findings can be captured.

Response 1:

Thanks for the comment. First of all, this is a paper describing a unique data product. It is not 0.5 degrees in resolution but 5 km. Since it is about land cover data product, it is not our attention to make novel discoveries. The purpose here is mainly to present a data set that does not exist anywhere before, for its annual frequency, 34 years long duration and high accuracy. The classification system does cover more than 90% of the land area. We did not include water, wetland, and impervious areas because wetland is extremely dynamic (more frequent than the yearly scale), water excluded from the input data source, and impervious areas already processed using more accurate source of data (e.g., annual Global Artificial Impervious Area maps, (Gong et al., 2020)). The accuracy assessment has been further improved using additional collection of test samples. We also compared our results with other data products and found that our results are superior.

Specific comments:

There are several global datasets with more rigorous production process have existed. 1) The 1992-2018 annual 300m global land-cover data (https://www.esa-landcover-cci.org/?q=node/197) with more detailed classification scheme have been released. Since the proposed product has no accuracy assessment on the annual maps from 1982-1991, it cannot be argued that the proposed work have longer period of time.

Response 2:

Thanks for your comment. We agree that ESA-CCI products have higher spatial resolution and more detailed classes. However, products with different resolution have different application purposes. In many studies, it is only necessary to use coarse-resolution land cover data, such as our 0.05 ° data, which can be used in Earth system modeling.

For Earth system modeling purposes, the 10 land cover classes mentioned in our response at the beginning are sufficient. Among the ten classes, except for wetland, impervious area, and water that occupy less than 10% of the entire land area on Earth. In the meantime, water and impervious areas can be individually obtained. Wetland is highly dynamic requiring additional types of remotely sensed data. Considering the separability and identifiability of the land cover classes under the 5 km spatial resolution, we adopted a classification system of 7 classes.

In this revision, we collected new independent test samples and performed accuracy assessment for the period of 1982-1991. In addition, we have compared our products with ESA-CCI and MODIS-based land cover data products and FAOSTAT data. The results show that our products have good reliability.

Specifically, we collected 2431 randomly distributed 5km sample points in different years around the world. According to the majority principle, we manually interpreted the land cover class of each sample as an independent test sample. Besides, in order to verify the accuracy of the change detection method, we also compared the classification accuracy before and after the change detection. The temporal distribution of the newly collected test samples is shown in Fig. 1, and the geographical distribution is shown in Fig. 2.

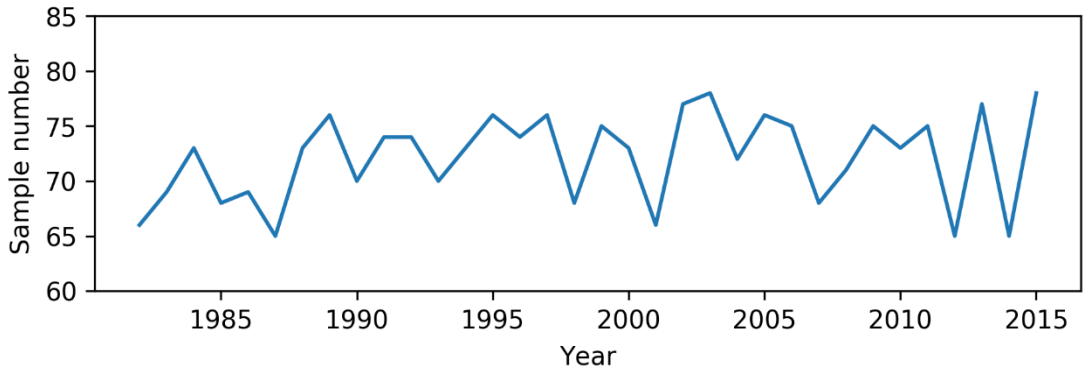

Figure 1: The temporal distribution of the newly collected test sample.

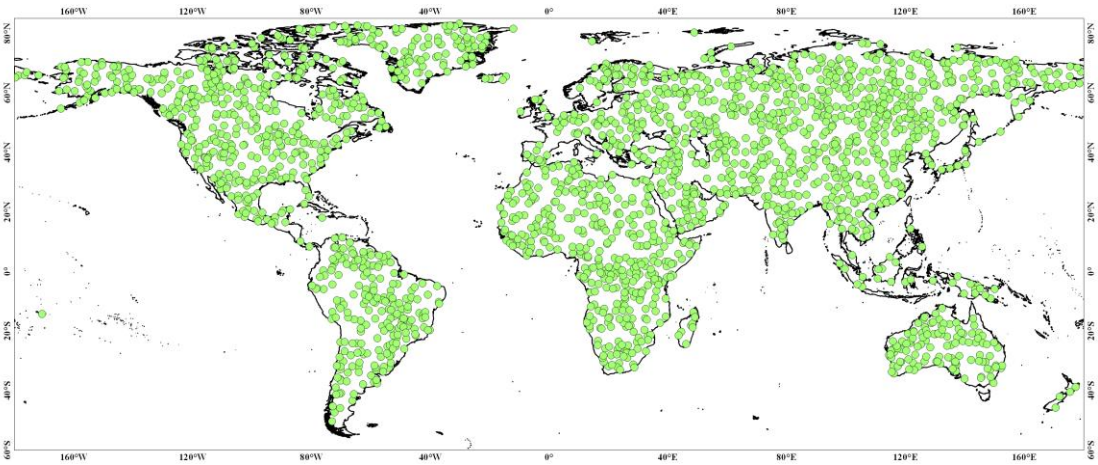

Figure 2: The geographical distribution of random test sample.

The new assessment result is shown in Table 1 and Table 2. It shows that OA of GLASS-GLC without change detection is 81.28%, and OA with change detection is 82.81%. This reflects the reliability of GLASS-GLC since the test samples are randomly distributed along the spatial and temporal dimensions, and also confirm the significance and effectiveness of the change detection method.

Table 1: Classification accuracy of GLASS-GLC without change detection under 2431 independent test samples. (Overall accuracy = 81.28 %, UA = User's Accuracy and PA = Producer's Accuracy)

Class	Cropland	Forest	Grassland	Shrubland	Tundra	Barren land	Snow/ice	Total number	UA
Cropland	257	21	34	15	0	31	0	358	71.79%
Forest	35	620	45	27	22	1	1	751	82.56%
Grassland	17	26	248	12	3	19	4	329	75.38%
Shrubland	7	6	10	154	9	12	0	198	77.78%
Tundra	0	9	11	12	250	3	0	285	87.72%
Barren land	4	1	13	14	5	355	6	398	89.20%
Snow/ice	0	4	3	0	0	13	92	112	82.14%
Total number	320	687	364	234	289	434	103	2431	
PA	80.31%	90.25%	68.13%	65.81%	86.51%	81.80%	89.32%		81.28%

Table 2: Classification accuracy of GLASS-GLC with change detection under 2431 independent test samples. (Overall accuracy =82.81 %, UA = User's Accuracy and PA = Producer's Accuracy)

Class	Cropland	Forest	Grassland	Shrubland	Tundra	Barren land	Snow/ice	Total number	UA
Cropland	262	19	32	20	0	25	0	358	73.18%
Forest	33	637	29	28	24	0	0	751	84.82%
Grassland	24	24	254	6	13	8	0	329	77.20%
Shrubland	12	3	11	159	6	7	0	198	80.30%
Tundra	0	12	9	4	250	10	0	285	87.72%
Barren land	5	1	17	8	7	357	3	398	89.70%
Snow/ice	0	5	6	0	0	7	94	112	83.93%
Total number	336	701	358	225	300	414	97	2431	
PA	77.98%	90.87%	70.95%	70.67%	83.33%	86.23%	96.91%		82.81%

We inter-compared GLASS-GLC with other available global land cover products with a relatively long time series. Land cover products from MODIS and the ESA-CCI were used. The MODIS-based global land cover products come from Collection 6 (C6) MODIS Land Cover Type (MLCT) products (Sulla-Menashe et al., 2019), and are supervised classification results from 2001 to 2016. Considering the comparability to our classification system, the FAO-Land Cover Classification System land use (LCCS2) layer was used. The corresponding relationships of classes are listed as

follows, and the class names we used are the latter: barren - barren land, permanent snow and ice – snow/ice, all kinds of forest – forest, forest/cropland mosaics and natural herbaceous/cropland mosaic – cropland, natural herbaceous and herbaceous cropland – grassland, shrubland - shrubland. The ESA-CCI global land cover products (Bontemps et al., 2013) are 300m resolution yearly products ranging from 1992 to 2015. The products were developed using the GlobCover unsupervised classification chain and merging multiple available Earth observation products based on the GlobCover products of the ESA (Liu et al., 2018). Referring to the class relationships in (Liu et al., 2018), we cross-walked classes including cropland, forest, grassland, shrubland, barren land and snow/ice.

Apart from land cover products, we also compared GLASS-GLC with the Food and Agricultural Organization of the United Nations statistical data (FAOSTAT) on cropland and forest (forest land) classes, which are the main sources of country-level land cover data for many applications. The annual FAOSTAT data set on cropland we used ranged from 1982 to 2015, and that on forest we used ranged from 1990 to 2015.

We made an inter-comparison between classes including cropland, forest, grassland, shrubland, barren land and snow/ice. The main inter-comparison is the area corresponding to the top 50 countries in each class. Besides, to compare the accuracy of different products, test samples from FLUXNET site data in 2015 are given for independent accuracy assessment.

The assessment results of MODIS-based land cover products and ESA-CCI land cover products based on test samples from FLUXNET site data are shown in Table 6 and Table 7, respectively. The overall accuracies of ESA-CCI products and MODIS-based products are 73.90% and 80.38% in 2015, respectively. Compared to these, The overall accuracy of GLASS-GLC (82.10%, Table 5) is superior. Although the cross-walk of the different classification systems may be slightly different, It can still reflect the high accuracy of our GLASS-GLC products.

Table 3: Classification accuracy of GLASS-GLC in 2015 based on FLUXNET test sample. (Overall accuracy = 82.10 %, UA = User's Accuracy and PA = Producer's Accuracy)

Class	Cropland	Forest	Grassland	Shrubland	Tundra	Barren land	Snow/ice	Total number	UA
Cropland	**63**	5	17	1	0	0	0	86	73.26 %
Forest	13	**243**	9	2	0	0	0	267	91.01 %
Grassland	8	21	**91**	2	0	2	0	124	73.39 %
Shrubland	7	3	0	**19**	0	0	0	29	65.52 %
Tundra	0	3	0	0	**14**	0	0	17	82.35 %
Barren land	0	1	0	0	0	**1**	0	2	50.00 %
Snow/ice	0	0	0	0	0	0	**0**	0	-
Total number	91	276	117	24	14	3	0	**525**	
PA	69.23 %	88.04 %	77.78 %	79.17 %	100.00 %	33.33 %	-		**82.10 %**

Table 4: Classification accuracy of the MODIS-based land cover product in 2015 based on FLUXNET test sample. (Overall accuracy = 82.10 %, UA = User's Accuracy and PA = Producer's Accuracy)

Class	Cropland	Forest	Grassland	Shrubland	Tundra	Barren land	Snow/ice	Total number	UA
Cropland	**7**	5	73	0	0	0	0	85	8.24%
Forest	1	**261**	5	0	0	0	0	267	97.75%
Grassland	1	15	**108**	1	0	0	0	125	86.40%
Shrubland	0	9	9	**11**	0	0	0	29	37.93%
Tundra	0	3	6	8	**0**	0	0	17	-
Barren land	0	0	1	0	0	**1**	0	2	50.00%
Snow/ice	0	0	0	0	0	0	**0**	0	-
Total number	9	293	202	20	0	1	0	**525**	
PA	77.78%	89.08%	53.47%	55.00%	-	100.00%	-		**73.90%**

Table 5: Classification accuracy of the ESA-CCI land cover product in 2015 based on FLUXNET test sample. (Overall accuracy = 82.10 %, UA = User's Accuracy and PA = Producer's Accuracy)

Class	Cropland	Forest	Grassland	Shrubland	Tundra	Barren land	Snow/ice	Total number	UA
Cropland	**81**	1	4	0	0	0	0	86	94.19%
Forest	11	**246**	4	5	0	1	0	267	92.13%
Grassland	28	7	**76**	5	0	8	0	124	61.29%
Shrubland	2	7	1	**19**	0	0	0	29	65.52%
Tundra	0	3	9	0	**0**	5	0	17	-
Barren land	0	0	2	0	0	**0**	0	2	0.00%
Snow/ice	0	0	0	0	0	0	**0**	0	-
Total number	122	264	96	29	0	14	0	**525**	
PA	66.39%	93.18%	79.17%	65.52%	-	0.00%	-		**80.38%**

Figure shows an inter-comparison with MODIS-based products, Figure with ESA-CCI products and Figure with FAOSTAT. The scatter plots and the linear fit lines reflect the results in 2015, and the box plots represent the distribution of R^2 of the annual linear fit lines for each class. It can be seen that various classes in several different products are relatively equivalent although they are under different classification systems. In comparison with MODIS-based products, the results of 2001-2015 for cropland, forest and snow/ice have high R^2. In comparison with ESA-CCI products, the mean R^2 of the linear fit lines of forest, grassland and snow/ice during 1992 to 2015 reach 0.99, 0.82, and 0.98, respectively, while the R^2 for shrubland is low. The inter-comparison of some other classes is poor, which may be caused by differences in class definition in various classification systems. For instance, our classification system incorporates tundra, while the other two did not. Compared with FAOSTAT, the mean R^2 of the linear fit lines of cropland and forest is 0.82, and 0.87, respectively. In general, our GLASS-GLC products have a reasonable consistency with other products and statistics and the difference are not significant.

What's more, the duration of GLASS-GLC is much longer than MODIS-based and ESA-CC land cover products (as shown in Fig. 6). The comparison with other data illustrates the reliability and superiority of GLASS-GLC.

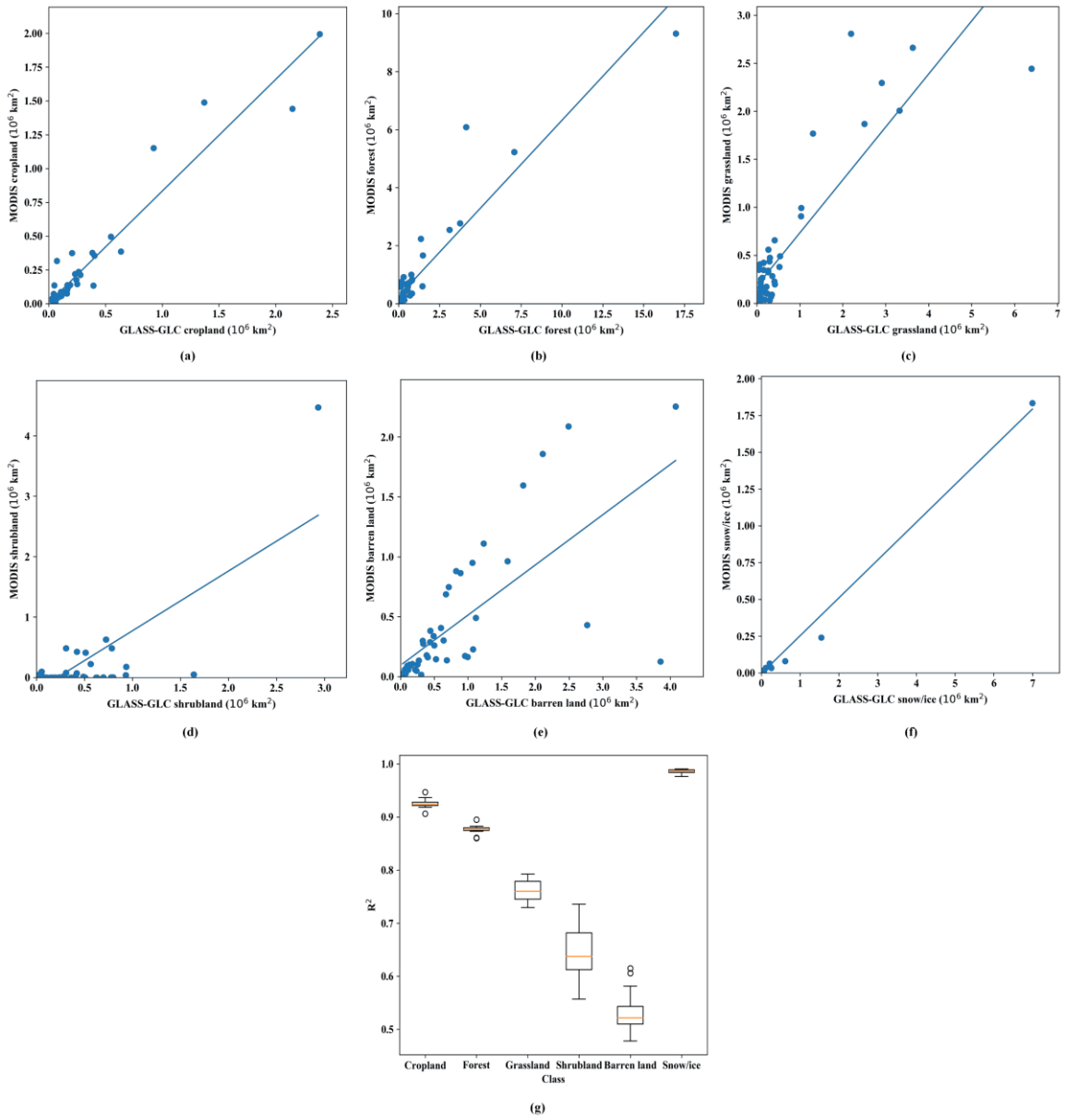

Figure 3: Inter-comparison with the MODIS-based land cover product, (a) cropland circa 2015, (b) forest circa 2015, (c) grassland circa 2015, (d) shrubland circa 2015, (e) barren land circa 2015 and (f) snow/ice circa 2015; (g) mean R2 of the annual linear fit lines for all years (2001-2015).

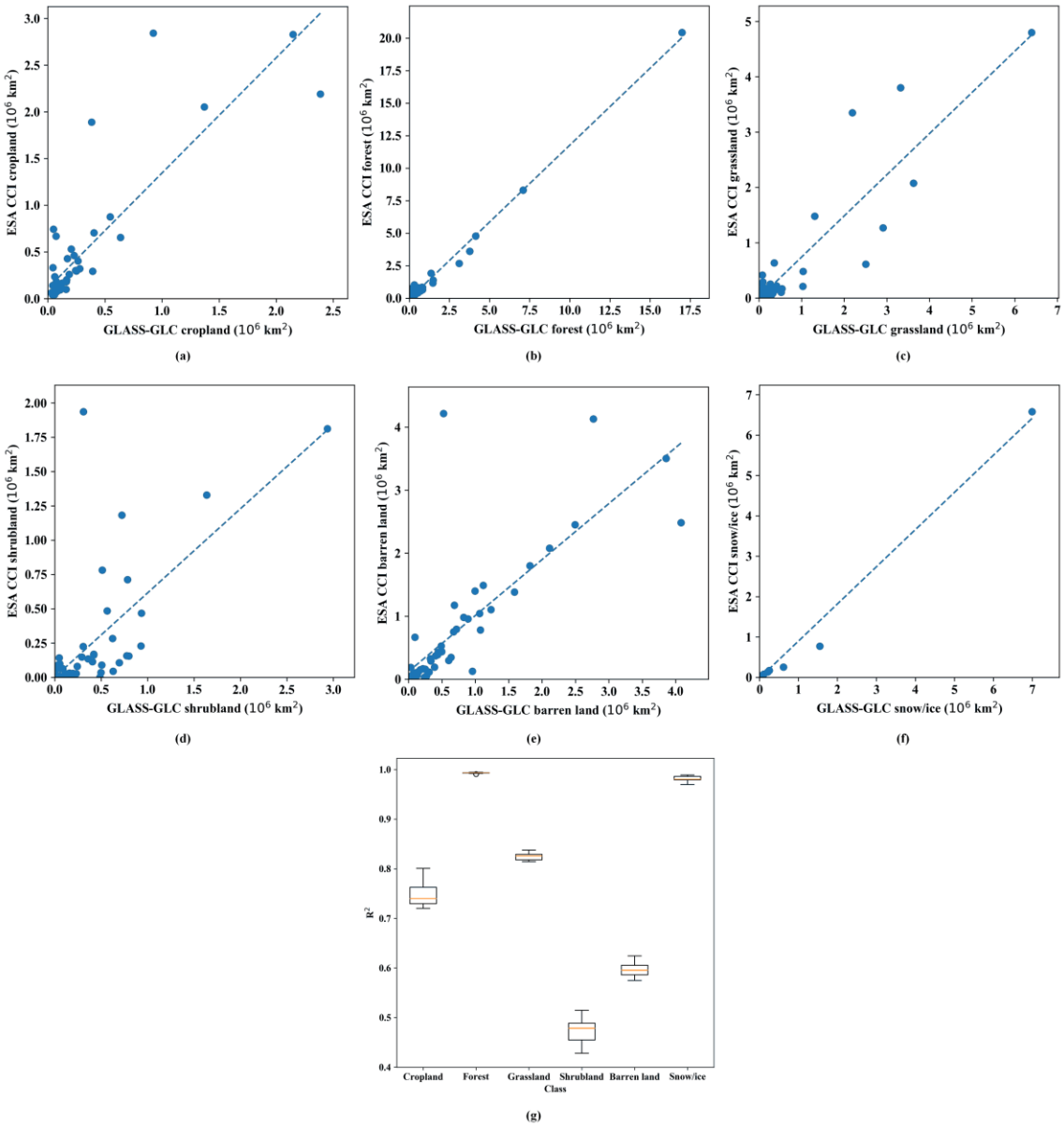

Figure 4: Inter-comparison with the ESA-CCI land cover product, (a) cropland circa 2015, (b) forest circa 2015, (c) grassland circa 2015, (d) shrubland circa 2015, (e) barren land circa 2015 and (f) snow/ice circa 2015; (g) mean R2 of the annual linear fit lines for all years (1992-2015).

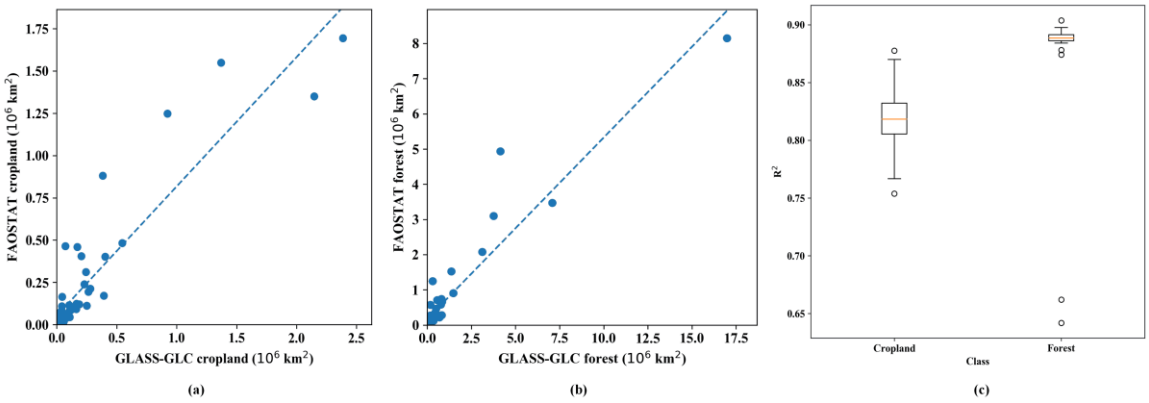

Figure 5: Inter-comparison with the FAOSTAT data set, (a) cropland circa 2015, (b) forest circa 2015, (c) mean R2 of the annual linear fit lines of cropland for years 1982-2015 and forest for years 1990-2015.

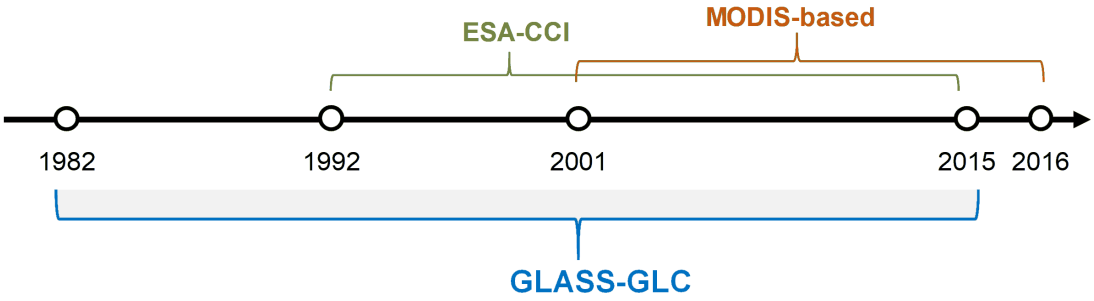

Figure 6: The duration of different land cover products, including GLASS-GLC, MODIS-based land cover products and ESA-CCI land cover products.

Change in manuscript:

We have added the new accuracy assessment results and data inter-comparison results to help show the reliability and effectiveness of GLASS-GLC.

2) The annual VCF products from 1982- 2016 have the same spatial resolution, and very similar classification scheme with the proposed work (from 1982-2015). Although the VCF product is missing in 1994 and 2000, the proposed work just directly use the data-source around the adjacent year, which cannot be viewed as a noticeable contribution. Meanwhile, since the proposed work also introduce VCF in the supervised classification, the analysis on the dynamic map is somewhat similar to this existed study (Song et al 2018a) , but more superficial.

Response 3:

Thank you for your comment. VCF is a quantitative variable. VCF data products mainly reflect vegetation cover information. Our land cover classes include multiple types of nominal variables. Again VCF and land cover information have different purposes of applications.

Here, we introduce VCF as a priori information to assist in land cover classification. VCF data is missing for two years, but this will not greatly affect the classification results. The auxiliary or supplementary data for classification and interpretation do not need to be perfect. They do not need to be in the same period or at the same resolution. As long as there is supplementary information, it will work, such as in the four-dimensional variational data assimilation.

For the analysis part of the land cover classification, the results are similar to those obtained from the analysis of VCF, which also confirm the objectivity and correctness of VCF analysis. But it is worth pointing out that our products can analyze many more detailed classes, so we can also draw some different conclusions.

Considering that the type of this paper is a data paper, our main focus is on the description of the production methods and quality control of data products, and the comparison and analysis of data quality and accuracy. More in-depth LCC analysis is out of the scope of this study.

Technical corrections

1. It is ridiculous to produce training and test set from a same product and in a same manner. In addition, it is unacceptable to conclude the applicability of the long-time period product by assessing the accuracy on only the 2015 land-cover mapping result.

Response 4:

Thank you for your comment. There may be some flaws in the way we evaluate accuracy.

Taking this into consideration, in addition to the accuracy assessment of samples taken from the FROM-GLC_v2 product, samples from FLUXNET site data are also given for independent accuracy assessment. The assessment results are shown in Table 3. The overall accuracy of GLASS-GLC reached 82.10% in 2015.

In addition, as described in response 2 above, we conducted a new independent sample test (OA=82.81%) and a comparison of multiple products (land cover products from MODIS and ESA-CCI, and FAOSTAT data), which also proved the reliability of our products.

Change in manuscript:

We have added the new accuracy assessment results and data inter-comparison results to help show the reliability and effectiveness of GLASS-GLC.

2. How to project the 30m FROM-GLC_v2 to mapping scale? How to deal with the mixed sample?

Response 5:

Thank you for your question. As the paper says, we projected the results of FROM-GLC_v2 according to the principle of majority. That is, the land cover class that accounts for the largest proportion in each grid is used as the land cover class label under the 0.05 ° grid. Generating coarse-resolution samples from high-resolution products as such is actually a common practice (Wang et al., 2016;DeFries et al., 1998).

For mixed samples, we also use the majority principle to give labels. Although percentage information is more suitable for dealing with mixed pixels, our goal here is hard classification, and we cannot avoid only doing so. This is also a problem that arises in hard land classification studies.

Considering the cost constraints, we have adopted this method of generating new samples even though it will bring some errors when producing coarse resolution samples from FROM-GLC_v2. However, the "stable classification with limited sample" theory (Gong et al., 2019) supports our approach to some extent. The theory shows that under its experimental conditions, even if 20% of the wrong samples are introduced, the classification accuracy is reduced by 1%, and it can still be stable (Fig. 7).

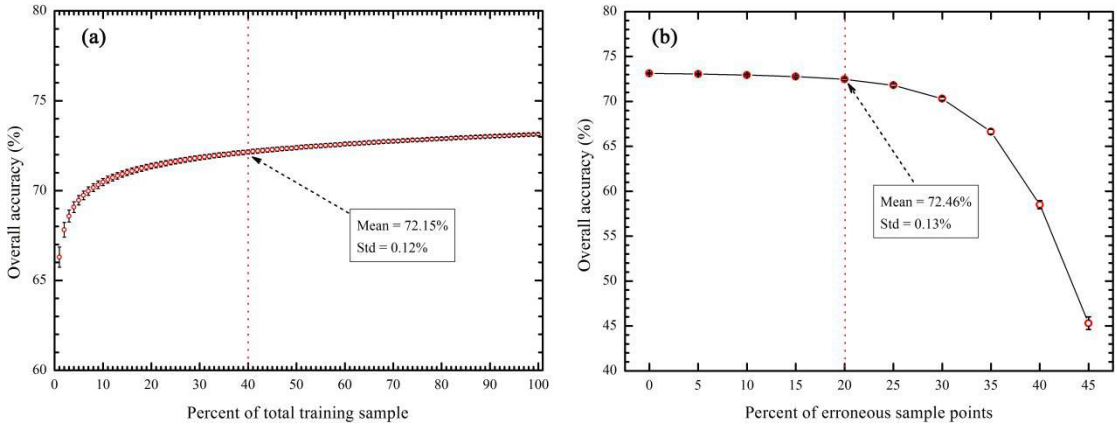

Figure 7: Sample robustness to size reduction and errors in sample. a. As sample size increases, the accuracy quickly reaches a plateau. b. As the impurity percentage of sample increases the accuracy decreases. In both cases, the 1000 times random drawing of sample points produced very stable overall classification accuracies with most standard deviations much lower than 0.5%. (Gong et al., 2019)

The newly added results of accuracy assessment have also confirmed that the samples produced in this way can meet the production needs.

3. There is no sample accuracy assessment on the produced training sample set. Please note that the accuracy of the FROM-GLC_v2 is not high enough to work as training sample.

Response 6:

Thank you for your point. The classification accuracy of FROM-GLC_v2 will surely have some impact on our results. However, FROM-GLC_v2 has been published, and it has a detailed accuracy assessment, with an OA of 73.13%. There is some complicated relationship for the use of higher resolution land cover data in producing lower-resolution land-cover products. Since there is a scaling down which requires aggregation of high-resolution land cover results. This often acts as an averaging effect that improves the accuracy in the area to some extent. Even if there is no accuracy increase during the scaling down process, the 73% accuracy would not cause a large accuracy decrease as can be seen from the figure in the right-hand side of Fig. 7.

To specifically evaluate the magnitude of the errors introduced by our training samples, we randomly selected 500 samples from the training samples for manual interpretation and evaluation, and the assessment accuracy was 92.26%. It shows that the training samples we generate this way are sufficient for our data production.

Change in manuscript:

We have added the accuracy assessment results on training samples.

4. When mapping the land-covers decades year ago, the suitability of the samples collected (mainly from 2013-2015) should be evaluated.

Response 7:

Thanks for your advice. We agree that, in the early years, the percent of land cover change may be relatively large. However, global land cover will not change by more than a few percents for decades. And these changes are primarily in urban and urban-rural fringe areas. The outdatedness of samples will not affect much of our accuracy assessment.

Concerning the reliability of sample migration, the “stable classification with limited sample” theory is specifically discussed (Gong et al., 2019).

In this study, the concept of a stable classification is defined. They use this concept to approximately determine how much reduction in training sample and how much land cover change or image interpretation error can be acceptable. If the mean accuracy of multiple runs of a classifier trained with a random drawing of a certain percentage of sample points from the total sample is within 1% of what can be achieved with the total sample set, we regard the obtained classification result “stable”. The 1% threshold is empirically chosen based on the fact that a loss of overall accuracy in 1% shall not significantly impact the application of a global land cover map.

Tens of millions of experiments suggest that it is possible to use 60% fewer sample points and even the land cover changed by 20% or the training sample contains 20% errors, we are still able to achieve “stable” classification with the random forest classifier in global land cover mapping. This conclusion well supports the effectiveness of our sample transfer method. Even for decades, it is

difficult for global land cover to change by more than 20%. Therefore, the proportion of error samples we introduced in the early years will not exceed 20%, and the classification results are still reliable and effective.

Another recent study (Huang et al., 2020) also devoted to migrating training samples to early years. They developed an automatic training sample migration method, which can successfully migrate training samples in 2015 to 2000. These studies prove the effectiveness of sample migration and provide potential solutions to resolve the problem of lack of training samples for dynamic global land cover mapping efforts.

Besides, to verify the temporal accuracy of our products, as mentioned above, we have independently collected test samples from different years and tested the accuracy of our products, with an accuracy of 82.81%. What's more, the inter-comparison results with other data have also confirmed the validity of our data using the 2015 sample for many years.

Reference

Bontemps, S., Defourny, P., Radoux, J., Van Bogaert, E., Lamarche, C., Achard, F., Mayaux, P., Boettcher, M., Brockmann, C., and Kirches, G.: Consistent global land cover maps for climate modelling communities: Current achievements of the ESA's land cover CCI, Proceedings of the ESA Living Planet Symposium, Edimburgh, 2013, 9-13,

DeFries, R. S., Hansen, M., Townshend, J. R. G., and Sohlberg, R.: Global land cover classifications at 8 km spatial resolution: the use of training data derived from Landsat imagery in decision tree classifiers, International Journal of Remote Sensing, 19, 3141-3168, https://doi.org/10.1080/014311698214235, 1998.

Gong, P., Liu, H., Zhang, M., Li, C., Wang, J., Huang, H., Clinton, N., Ji, L., Li, W., Bai, Y., Chen, B., Xu, B., Zhu, Z., Yuan, C., Suen, H. P., Guo, J., Xu, N., Li, W., Zhao, Y., Yang, J., Yu, C., Wang, X., Fu, H., Yu, L., Dronova, I., Hui, F., Cheng, X., Shi, X., Xiao, F., Liu, Q., and Song, L.: Stable classification with limited sample: transferring a 30-m resolution sample set collected in 2015 to mapping 10-m resolution global land cover in 2017, Science Bulletin, 64, 370, https://doi.org/10.1016/j.scib.2019.03.002, 2019.

Gong, P., Li, X., Wang, J., Bai, Y., Chen, B., Hu, T., Liu, X., Xu, B., Yang, J., and Zhang, W.: Annual maps of global artificial impervious area (GAIA) between 1985 and 2018, Remote Sensing of Environment, 236, 111510, https://doi.org/10.1016/j.rse.2019.111510, 2020.

Huang, H., Wang, J., Liu, C., Liang, L., Li, C., and Gong, P.: The migration of training samples towards dynamic global land cover mapping, ISPRS Journal of Photogrammetry and Remote Sensing, 161, 27-36, https://doi.org/10.1016/j.isprsjprs.2020.01.010, 2020.

Liu, X., Yu, L., Li, W., Peng, D., Zhong, L., Li, L., Xin, Q., Lu, H., Yu, C., and Gong, P.: Comparison of country-level cropland areas between ESA-CCI land cover maps and FAOSTAT data, International Journal of Remote Sensing, 1-15, https://doi.org/10.1080/01431161.2018.1465613, 2018.

Sulla-Menashe, D., Gray, J. M., Abercrombie, S. P., and Friedl, M. A.: Hierarchical mapping of annual global land cover 2001 to present: The MODIS Collection 6 Land Cover product, Remote sensing of environment, 222, 183-194, https://doi.org/10.1016/j.rse.2018.12.013, 2019.

Wang, C., Gao, Q., Wang, X., and Yu, M.: Spatially differentiated trends in urbanization, agricultural

land abandonment and reclamation, and woodland recovery in Northern China, Scientific reports, 6, 37658, https://doi.org/10.1038/srep37658, 2016.

Annual Dynamics of Global Land Cover and its Long-term Changes from 1982 to 2015

Han Liu[1], Peng Gong[1,2], Jie Wang[2,3], Nicholas Clinton[4], Yuqi Bai[1], Shunlin Liang[5,6]

[1]Ministry of Education Key Laboratory for Earth System Modeling, Department of Earth System Science, Tsinghua University, Beijing, 100084, China

[2]AI for Earth Lab, Cross-Strait Institute, Tsinghua University, Beijing, 100084, China

[3]State Key Laboratory of Remote Sensing Science, Institute of Remote Sensing and Digital Earth, Chinese Academy of Sciences, Beijing, 100101, China

[4]Google LLC, 1600 Amphitheatre Parkway, Mountain View, CA 94043 USA

[5]Department of Geographical Sciences, University of Maryland, College Park, MD 20742 USA

[6]School of Remote Sensing Information Engineering, Wuhan University, Wuhan, 430072, China

Correspondence to: Peng Gong (penggong@tsinghua.edu.cn), Jie Wang (sohuwangjie@163.com)

Abstract. Land cover (LC) is an important terrestrial variable for understanding the interaction between human activities and global change. As the cause and result of global environmental change, land cover change (LCC) influences the global energy balance and biogeochemical cycles. Continuous and dynamic monitoring of global LC is urgently needed. Effective monitoring and comprehensive analysis of LCC at the global scale are rare. Using the latest version of GLASS (The Global Land Surface Satellite) CDRs (Climate Data Records) from 1982 to 2015, we built the first record of 34-year long annual dynamics of global land cover (GLASS-GLC) at 5 km resolution using the Google Earth Engine (GEE) platform. Compared to earlier global LC products, GLASS-GLC is characterized by high consistency, more detailed, and longer temporal coverage. The average overall accuracy with 7 classes is 82.81 % based on 2431 test sample units. Comparison with other data products showed that GLASS-GLC is superior in the accuracy and the temporal range. We implemented a systematic uncertainty analysis and carried out a comprehensive spatiotemporal pattern analysis. Significant changes at various scales were found, including barren land loss and cropland gain in the tropics, forest gain in northern hemisphere, and grassland loss in Asia, etc. A global quantitative analysis of human factors showed that the average human impact level in areas with significant LCC was about 25.49 %. The anthropogenic influence has a strong correlation with the noticeable vegetation gain, especially for forest. Based on GLASS-GLC, we can conduct long-term LCC analysis, improve our understanding of global environmental change, and mitigate its negative impact. GLASS-GLC will be further applied in Earth system modeling to facilitate research on global carbon and water cycling, vegetation dynamics and climate change. The data set presented in this article is published in the Tagged Image File Format (TIFF) at https://doi.org/10.1594/PANGAEA.898096. The data set includes 34 TIFF files and one

删除了: and key information
删除了: is
删除了: set of CDRs to
删除了: the
删除了: 7 classes
删除了: 86.51
删除了: 23459 test samples in 2015
设置了格式: 字体颜色: 文字 1
设置了格式: 字体颜色: 文字 1
设置了格式: 字体颜色: 文字 1
删除了: at the global scale. In addition, we
删除了: and patterns
删除了: deforestation
删除了: agricultural land
删除了: expansion
删除了: afforestation and
删除了: expansion
删除了: high latitudes
删除了: ,
删除了: land degradation
删除了: n grassland
删除了: and reclamation in northeast China
删除了: Earth greening
删除了: gain
删除了: in order

instruction doc file.

1 Introduction

Land cover (LC) is the physical evidence on Earth. It is the result of both natural and human forces (Running, 2008;Sterling et al., 2013;Tucker et al., 1985;Gong et al., 2013;Yang et al., 2013). It is an important source of information to understand the complex interaction between human activities and global changes (Lambin et al., 2006). LC data is one of the most important variables to bring about the nine large social benefits in the field of Global Earth Observation Systems (Herold et al., 2008). Land cover change (LCC) is the cause and result of global environmental change (Turner et al., 2007), and it can change the energy balance and biogeochemical cycles (DeFries et al., 1999;Claussen et al., 2001), further affecting climate change and surface characteristics and the provision of ecosystem services (Pielke, 2005;Zhao et al., 2001;Gibbard et al., 2005;Reyers et al., 2009). Therefore, a long time series of LCC information is critical to the understanding of global environmental change (Matthews et al., 2004). LC and LCC information is also valuable to resource management, biodiversity conservation, food security, forest carbon, etc (Houghton et al., 2012;Achard et al., 2004;Andrew K et al., 2015). Therefore, more frequent land cover information at the global scale is highly desirable.

However, LC is highly dynamic due to changes in natural phenology and human activities (Lambin et al., 2001). This characteristic poses a huge challenge to mapping, monitoring (Verburg et al., 2009;Lepers et al., 2005;Rindfuss et al., 2004), and quantitative analyses of global LCC (Ramankutty et al., 2006). The traditional method of LC mapping based on field studies can hardly be applied to large areas due to the required amount of labor (Gong, 2012). In addition, any mapping results obtained in this way would be difficult to update in a timely manner. Satellite observations are the most economically feasible means of large-scale LC monitoring (Fuller et al., 2003;Rogan and Chen, 2004). Due to the development of satellite sensors, the continuous accumulation of historical satellite data, and the advancement of relevant image processing algorithms, LC monitoring can be effectively carried out (Cihlar, 2000;Pal, 2005;Gallego, 2004;Chen et al., 2018). However, previous monitoring mainly focuses on the mapping of a particular area (Liu et al., 2002;Brink and Eva, 2009;Yuan et al., 2005;Margono et al., 2012;Feng et al., 2018) or in a single time period (Homer et al., 2004), and because of the differences in data sources and mapping methods, the consistency of mapping results from different sources and times is poor and lacks comparability, making it difficult to quantify the changes effectively (Friedl et al., 2010).

Automatic mapping methods depend highly on the sample dataset for its representativeness, quantity and quality due to the considerable heterogeneity at the global level (Gong et al., 2013;Li et al., 2014). A combination of a comprehensive global sample dataset, professional interpretation and support from mapping teams are needed (Li et al., 2017). In general, sample LC data are mainly collected from field visits or manual interpretation (Li et al., 2016;Hansen et al., 2000). Generalization from higher resolution LC map products can also be useful for coarser resolution mapping purposes (Song et al., 2018a). The

删除了: needed

设置了格式: 字体颜色: 文字 1

设置了格式: 字体颜色: 文字 1

设置了格式: 字体颜色: 文字 1

设置了格式: 字体: 10 磅, 字体颜色: 文字 1, 英语(英国)

设置了格式: 字体: (默认) Times New Roman, (中文) Times New Roman, 字体颜色: 文字 1

删除了: attributes

设置了格式: 字体颜色: 文字 1

设置了格式: 字体颜色: 文字 1

设置了格式: 字体颜色: 文字 1

删除了: and

删除了: an effective

删除了: analysis

删除了: of

删除了: to

删除了: is lacking

删除了: and

删除了: between

删除了: periods

former could be more accurate and effective, but requires much manpower, resource and effort (Li et al., 2016); the latter is a feasible option and is more efficient but largely depending on the accuracy of the parent product.

A number of global LC products exists. Some examples include the 30 m Finer resolution observation and monitoring of global land cover (FROM-GLC) (Gong et al., 2013), the 1992-2015 annual 300 m global land cover data (http://maps.elie.ucl.ac.be/CCI/viewer/index.php), MODIS global land cover product (Friedl et al., 2010), 1 km International Geosphere-Biosphere Programme Data and Information System Cover map (IGBP-DISCover) (Loveland et al., 2000), 1 km University of Maryland (UMD) land-cover map (Hansen et al., 2000), 1 km Global Land Cover 2000 (GLC2000) map (Bartholome and Belward, 2005). These mapping results tend to focus on a single or short period of time, and because of their different classification systems and resolutions, they are difficult to compare (Ban et al., 2015;Grekousis et al., 2015). However, high-resolution mapping results can be used as an effective reference for low-resolution mapping (Song et al., 2018a;DeFries et al., 1998). Therefore, when performing lower-resolution global mapping, it is possible to consider directly generating training samples from high-resolution global mapping results (Wang et al., 2016).

Long time-series LC mapping requires high consistency of data sources, and also has certain requirements for multi-period samples (Huang et al., 2020). The commonly used satellite data that cover a long period of time (more than 30 years) include the Advanced Very High Resolution Radiometer (AVHRR) data and Landsat imagery (Giri et al., 2013; Franch et al., 2017; Wulder et al., 2008). Landsat data has higher resolution with some restrictions including obvious and serious cloud contamination, data inconsistency with multiple generations of sensors and relatively larger data volume (Gómez et al., 2016;Wulder et al., 2008;Xie et al., 2018). AVHRR data has a low spatial resolution, and the quality of the raw AVHRR data is poor. The requirements for pre-processing and consistency processing such as cloud removal and missing value filling are high. The GLASS CDRs based on AVHRR data tend to have better data consistency due to the systematic data production (Liang et al., 2013). Using such data for LC mapping can significantly improve the consistency and comparability of mapping results, and thus can be effective in supporting change analysis. If the consistency of the original data source used is not good enough, it may be necessary to collect annual samples for classification to ensure the reliability of change analysis (Xu et al., 2018).

Recently, some attempts have been made to map global LC over a long time series, but these have focused on a single class (such as water bodies (Wood et al., 2011;Pekel et al., 2016;Ji et al., 2018), impervious surface (Schneider et al., 2010;Zhang and Seto, 2011;Gong et al., 2020), cropland (Pittman et al., 2010), etc.) or a few classes (such as Vegetation Continuous Fields (VCF) (Song et al., 2018a), mainly depicting vegetation changes). General purpose multi-class land cover mapping over a period of over 30 years does not exist.

Due to the lack of long time-series general purpose global LC maps, using the Google Earth Engine (GEE) platform (Gorelick et al., 2017), we produced the first CDR set of consistent and reliable LC products, GLASS-GLC, covering the period from 1982 to 2015. The data used was primarily the 0.05 ° AVHRR-based GLASS CDRs. The classification system is adjusted from

删除了: is

删除了: , which will meet the mapping requirements,

删除了: (Wardlow and Egbert, 2008).

设置了格式: 字体颜色: 文字 1

删除了: , but it meets

删除了: problem

删除了: because of the high resolution

删除了: While Landsat data has higher resolution, in many areas they are more prone to cloud, consistency and data volume…

设置了格式: 字体颜色: 文字 1

设置了格式: 字体颜色: 文字 1

删除了: before

删除了: Because of

the FROM-GLC according to the data characteristics. Below, we describe the methods used, results obtained with some preliminary change analyses.

删除了: analysis

2 Data and methods

The framework for mapping GLASS-GLC is shown in Fig. 1. It includes annual feature collection and construction, training sample generation, classification and time consistency adjustment, accuracy assessment and product inter-comparison. The entire framework is implemented in the GEE. The GEE is a cloud-based platform for planetary-scale geospatial analysis that brings Google's massive computational capabilities to bear on a variety of high-impact societal issues including deforestation, drought, disaster, disease, food security, water management, climate monitoring and environmental protection (Gorelick et al., 2017). We uploaded GLASS data to GEE and did subsequent analysis in GEE.

删除了: oa

2.1 Data

The annual feature collection from 1982 to 2015 involves a variety of data products, the most important of which is the latest version of GLASS CDRs. CDRs require data with a long time series, high consistency and high continuity, which is not the same as the commonly-used remote sensing products (Hollmann et al., 2013;Cao et al., 2008). Derived from AVHRR data, the GLASS CDRs include a wide range of surface parameters that are important to LC classification (http://glass-product.bnu.edu.cn/). The products have a spatial resolution of 0.05 °, a temporal frequency of 8 days with a time span of 1982-2015. In our study, Normalized Difference Vegetation Index (NDVI), Leaf Area Index (LAI) (Xiao et al., 2016), Fraction of Absorbed Photosynthetically Active Radiation (FAPAR) (Xiao et al., 2015), Evapotranspiration (ET) (Yao et al., 2014), Gross Primary Production (GPP) (Yuan et al., 2010), Broadband Emissivity (BBE) (Cheng et al., 2016), White-sky Albedo in Visible band (ABD_WSA_VIS), White-sky Albedo in Near Infrared band (ABD_BSA_NIR) and White-sky Albedo in Shortwave band (ABD_WSA_shortwave) (Qu et al., 2014) are the variables used for subsequent classification.

删除了: for

删除了: oa

To provide further reference, vegetation cover fraction (VCF) products are used to aid classification. The VCF products decribe the surface as a combination of vegetation proportions according to information from remotely sensed data. To match the resolution of the GLASS CDRs, the VCF products used here (Song et al., 2018a) also have a spatial resolution of 0.05 °, and are obtained from the Land Processes Distributed Active Archive Center (https://lpdaac.usgs.gov/). These products are mainly based on AVHRR, and the interannual consistency has been maintained. Based on the training samples from Landsat products from around 2000 (Hansen et al., 2013;Ying et al., 2017), with a supervised regression tree model, the VCF products from 1982 to 2016 (data missing in 1994 and 2000) were generated, and were composed of the percentages of tree canopy (TC), short vegetation (SV) and bare ground (BG) in each pixel.

删除了: express

In addition, in order to enhance the discriminating capacity, we also used terrain data from Global Multi-resolution Terrain Elevation Data of 2010 (GMTED2010). Based on the elevation data, the slope information can be further calculated to reflect

删除了: distinguishing

删除了: provided by

删除了: the

the terrain and help distinguish different vegetation types growing on steep slopes to those on level ground. The dataset comes from the GEE platform and contains 2010 Earth Elevation data collected from various sources. The primary source is the Shuttle Radar Topography Mission (SRTM) Digital Terrain Elevation Data (DTED) (void-filled) 1-arc-second data. Other sources are used for filling the gaps in areas outside the SRTM coverage. As the terrain is relatively stable over years, using the data of one single year is plausible. The spatial resolution of the GMTED2010 data used is 7.5 arc seconds and it has been upsampled to 5 km in subsequent analyses.

2.2 Classification system

The classification system in FROM-GLC Version 2 (FROM-GLC_v2) defines eleven Level 1 classes that can be easily mapped to the Food and Agricultural Organization of the United Nations (FAO) LC Classification System and the International Geosphere–Biosphere Programme (IGBP) classification system (Wang et al., 2015). This classification system evolved from the classification system of FROM-GLC Version 1 (Gong et al., 2013) with addition of leaf information.

We adjusted some classes of the original classification system according to the spatial resolution and situation of the data used here. Our data are land surface products, where water surface has been masked out, the class of "water bodies" cannot be extracted from the GLASS dataset. Wetland is a highly variable class and impervious surface whose patches are small in size. They are difficult to identify at the spatial resolution of 0.05 °(Wang et al., 2015). Thus, the water body, impervious surface, and wetland classes were not included in this work, and they shall be derived with more specialized methods. While water and impervious surface mapping have achieved satisfactory results(Ji et al., 2018;Gong et al., 2020), wetland mapping remains a great challenge (Gong et al., 2013). In addition, the "cloud" class was removed. The adjusted classification system consists of seven Level 1 classes, including cropland, forest, grassland, shrubland, tundra, barren land, snow/ice, as shown in Table 1.

2.3 Training samples

In order to obtain the training samples, we adopted the majority-class synthesis strategy. First, we projected the 30m FROM-GLC_v2 results, that were created using Landsat data acquired mainly from 2013-2015 (Li et al., 2017), into a 0.05 ° coordinate system. By calculating the area ratio of each class in each 0.05 ° pixel, the class with the greatest area ratio in each pixel was used as the new class label in the aggregated 0.05 ° mapping results. Subsequently, sample points were randomly generated with greater than 0.1 ° geographical distances away. The class label for each sample unit is obtained from the aggregated FROM-GLC_v2 0.05 ° mapping result (adjusted to be consistent with the new classification system). Finally, 10,000 training sample units were obtained. The spatial distribution of training sample units is shown in Fig. 2 (a), and the percentage of training sample in each class is shown in the inner pie chart.

删除了: to

删除了: used

删除了: Because the data used here

删除了: the

删除了: (Ji et al.;Gong et al., submitted)

删除了: 7

删除了: (with a

删除了: at

删除了: an spatial limited interval

设置了格式: 字体: (默认) Times New Roman, (中文) Times New Roman

删除了:) with t

删除了: class distribution of

删除了: s

2.4 Feature collection

We constructed a feature set with a strong discrimination ability to detect LC from multiple aspects such as terrain, phenology, spectrum, and spectral index, etc. The annual percentiles (including 0, 10, 25, 50, 75, 90, 100) of all bands of the GLASS CDRs and the mean and standard deviation of the NDVI between two adjacent percentiles are calculated, as an annual feature collection from GLASS CDRs. Among them, the percentile that represents specific phenological information can provide simplified time series information, reduce the noise of annual time series, and help improve the classification accuracy (Hansen et al., 2013). By extracting the statistical information between adjacent percentiles, the time series information can be further supplemented. Due to the systematic deviation of AVHRR products (Song et al., 2018b), in order to ensure the inter-annual consistency of the GLASS features, we used the processing method developed for generating the VCF products, with the corresponding MODIS products for end-member correction, where desert and intact forest are regarded as the end-member of each pixel (Song et al., 2018a). After the correction, the inter-annual inconsistency of feature collection from the GLASS CDRs is improved. Figure S1 shows the time series of the global median value of the GLASS ABD_WSA_VIS band, where the orange one represents the curve before the correction and the grey one is the result after the correction. It can be seen that after the correction, the fluctuations of the feature become smaller, and the individual abnormal values are also adjusted.

Taking into account the time span of the GLASS CDR-based feature collection, the VCF products from 1982 to 2015 are used, with the missing 1994 and 2000 data supplemented by calculating the average of the adjacent years. There are three features of the percentage of tree cover (TC), short vegetation (SV) and bare ground (BG) for each year. Based on the GMTED2010 dataset, the slope information is calculated and finally included to obtain an average slope value for each 0.05 ° pixel. In addition, the central latitude and longitude information of each 0.05 ° pixel is also recorded as part of the input features. Finally, an annual collection of 81 input features for the period of 1982 to 2015 was constructed, including the annual GLASS CDR percentile feature (7×9), the mean and standard deviation of the NDVI annual adjacent percentiles (6×2) and VCF features (3), slope information (1), latitude (1), and longitude (1) information (Table 2).

2.5 Classification and time consistency

We used a random forest classifier for global LC mapping following the good performance of the random forest classifier in the machine learning field (Rodriguez-Galiano et al., 2012;Pal, 2005). The number of trees was 200 with out-of-bag mode turned on. The number of variables per split was set to 0, as the square root of the number of variables. The minimum size of a terminal node, the fraction of input to bag per tree, and random seed were set to be 1, 0.5 and 0, respectively. The classifier was trained using the training sample with an annual feature collection constructed as the input. The global LC maps from 1982 to 2015 were obtained using the trained classifier. The out of bag accuracy reached 87.12%.

In order to further ensure the time consistency of the mapping results, we used the “LandTrendr” method (Kennedy et al., 2010;Cohen et al., 2018) and implemented a linear regression-based algorithm for the constructed annual feature collection to

删除了: collection
删除了: element
删除了: 3
删除了:
删除了: add
删除了: assisting the
删除了: and
设置了格式: 字体颜色: 文字 1
设置了格式: 字体颜色: 文字 1
设置了格式: 字体颜色: 文字 1
删除了: ,
设置了格式: 字体: 10 磅, 字体颜色: 文字 1, 英语(英国)
设置了格式: 字体颜色: 文字 1
删除了: is
删除了: and other parameters were set as default.
设置了格式: 字体: 10 磅, 字体颜色: 文字 1, 英语(英国)
删除了: was 1
删除了: was 0.5
删除了: as
设置了格式: 字体颜色: 文字 1
设置了格式: 字体: 10 磅, 字体颜色: 文字 1, 英语(英国)
设置了格式: 字体: (默认) Times New Roman, (中文) Times New Roman, 字体颜色: 文字 1
设置了格式: 字体颜色: 文字 1
设置了格式: 字体颜色: 文字 1
删除了: OOB
设置了格式: 字体: 10 磅, 字体颜色: 文字 1, 英语(英国)
设置了格式: 字体颜色: 文字 1
设置了格式: 字体: 10 磅, 字体颜色: 文字 1, 英语(英国)
删除了: to
设置了格式: 字体颜色: 文字 1

find the breakpoints in the time series (Li et al., 2018). The class labels in the time series between adjacent breakpoints will be updated to the mode values of the class label time series for the time period. Through this strategy, we can smooth the time series of the mapping results, avoid noise interference as much as possible, and finally get the adjusted GLASS-GLC.

2.6 Accuracy assessment

To verify the reliability of GLASS-GLC CDR products from multiple perspectives, we performed accuracy assessments and uncertainty analyses. The test sample was extracted from the 30 m resolution FROM-GLC_v2 (Li et al., 2017) to evaluate the 2015 LC mapping results. First, we dropped those sample units whose classes were not included in our classification system. The remaining test sample units were then overlapped with the abovementioned aggregated 0.05 ° FROM-GLC_v2 mapping result, and only those whose class labels were consistent were kept. These were regarded as huge homogeneous sample units (H-homo sample) reserved as the final test sample. A total of 23459 H-homo test sample units from FROM-GLC_v2 were obtained to test the 2015 global LC mapping result. In addition, another 525 test sample units from the FLUXNET site data (Gong, 2009) for 2015 were selected to supplement the test sample to further test the 2015 result. The distribution of the entire test sample in 2015 is shown in Fig.Figure 2 (b), where the percentage of test sample for each class is shown in the inner pie chart.

In addition to obtaining the classification confusion matrix in 2015 based on the above test sample, in order to identify regions where classification is difficult, an uncertainty analysis was carried out. The incorrect test sample locations are marked as 1, while the correct test sample locations are marked as 0. The spatial distribution map of the uncertainty of the LC mapping result in 2015 is depicted based on a Kriging interpolation method (Oliver and Webster, 1990). The search radius parameter of Kriging interpolation is set to 12 nearby sample units, the other parameters as default. The value of the uncertainty ranges from 0 to 1. A value near 0, indicates a lower uncertainty while a value near to 1, indicates a higher uncertainty and a higher possibility of misclassification.

Other than these, we collected an independent test sample and performed accuracy assessment. Specifically, we collected 2431 randomly distributed 5 km sample points in different years around the world. According to the majority principle, we manually interpreted the land cover class of each sample as an independent test sample. To prove the impact of change detection, we further compared the accuracies with and without change detection. The geographical distribution of the independent test sample is shown in Fig.Figure 2 (c), and the temporal distribution is shown in the inner chart.

2.7 Data inter-comparison

To better reflect the product quality, We inter-compared GLASS-GLC with other available global land cover products with a relatively long time series. Land cover products from MODIS and the ESA-CCI were used. The MODIS-based global

删除了: testing sample
删除了: s
删除了: s
删除了: s
删除了: s
删除了: s
删除了: s
删除了: s
删除了: 4
删除了: class distribution of the
删除了: s
删除了: in
删除了: s
删除了: s
删除了: s
删除了: points
设置了格式: 字体颜色: 文字 1
设置了格式: 字体颜色: 文字 1
设置了格式: 字体颜色: 文字 1
设置了格式: 字体颜色: 文字 1
设置了格式: 字体: 10 磅, 字体颜色: 文字 1
设置了格式: 字体: 五号, 字体颜色: 文字 1

land cover products come from Collection 6 (C6) MODIS Land Cover Type (MLCT) products (Sulla-Menashe et al., 2019), and are supervised classification results from 2001 to 2016. Considering the comparability to our classification system, the FAO-Land Cover Classification System land use (LCCS2) layer was used. The corresponding relationships of classes are listed as follows, and the class names we used are the latter: barren - barren land, permanent snow and ice – snow/ice, all kinds of forest – forest, forest/cropland mosaics and natural herbaceous/cropland mosaic – cropland, natural herbaceous and herbaceous cropland – grassland, shrubland - shrubland. The ESA-CCI global land cover products (Bontemps et al., 2013) are 300m resolution yearly products ranging from 1992 to 2015. The products were developed using the GlobCover unsupervised classification chain and merging multiple available Earth observation products based on the GlobCover products of the ESA (Liu et al., 2018). Referring to the class relationships in (Liu et al., 2018), we cross-walked classes including cropland, forest, grassland, shrubland, barren land and snow/ice.

Apart from land cover products, we also compared GLASS-GLC with the Food and Agricultural Organization of the United Nations statistical data (FAOSTAT) on cropland and forest (forest land) classes, which are the main sources of country-level land cover data for many applications. The annual FAOSTAT data set on cropland we used ranged from 1982 to 2015, and that on forest we used ranged from 1990 to 2015.

We made an inter-comparison between classes including cropland, forest, grassland, shrubland, barren land and snow/ice. The main inter-comparison is the area corresponding to the top 50 countries in each class. Besides, to compare the accuracy of different products, test samples from FLUXNET site data in 2015 are given for independent accuracy assessment.

2.8 Statistical analysis

To extract the area of LCC, we estimated the trend of change through statistical analysis and avoided the influence of abnormal fluctuations from the obtained time series LC products. The annual area for each class on the scales of latitudinal zones, continents are summarized. A time series of the annual area for each class was generated. The boundary data of countries and continents were obtained from the Bureau of Surveying and Mapping of China. Eco-region data were obtained from the FAO global eco-region dataset (Simons et al., 2001) (http://www.fao.org/geonetwork/srv/en/metadata.show?CurrTab=simple&id=1255).

Although the inter-annual consistency has been ensured as much as possible in the above mapping framework, the effects of inter-annual changes due to climate conditions and phenological changes may still exist. To estimate the long-term trend of change, we fitted a linear trend (Theil-Sen estimator (Sen, 1968)) in area for each class, where the slope of annual change and the 95 % confidence interval of the slope is given. In addition, a Mann-Kendall test (Mann, 1945) was used to test the trend of time series with a p-value given. If $p < 0.05$, it is considered that the trend of change is significant.

Further, we obtained the change mask where all pixels showed a significant change trend (Wang et al., 2016). First, we

设置了格式 ... [1]

设置了格式 ... [2]

设置了格式 ... [3]

删除了: 7

删除了: long …ime series of global…LC products. The annual area of … ... [4]

删除了: And t

删除了: were removed by fitting…we fitted a linear trend (Theil-Sen estimator (Sen, 1968)) …in area for each classto estimate the long-term trend of change in area for each … ... [5]

删除了: slope…and the 95 % confidence interval of the slope is given. In addition, a Mann-Kendall test (Mann, 1945) was used to test the trend of time series and …ith athe…p-value is … ... [6]

删除了: got …btained the change mask where all pixels showed a significant change trend guaranteed by statistical hypothesis testing … ... [7]

downscaled the grid from 0.05 ° to 0.25 °, and the time series of the area ratio of all classes in each 0.25 ° grid was summed. Using the Mann-Kendall test, those grids showing a significant change ($p < 0.05$) were obtained. Then the slope of annual change based on area ratio for each grid with an increasing or decreasing trend was found using a Theil-Sen estimator. The change ratios were then summarized at regional scales to estimate the corresponding significant areas of change from 1982 to 2015.

2.9 LC conversion

In order to quantify the magnitude of global LCC between 1982 and 2015 and reveal the global temporal LCC pattern, we calculated the ratio of annual global LCC to the global total terrestrial LC area by different time periods. To ensure the quantified LCC to be non-accidental, we limited the computation area within the change mask in which all grids show a statistically significant loss or gain trend. We then summarized the annual LCC by 5-year and 10-year time intervals, respectively.

To further identify the direct causes of LCC, we assessed the LC conversion from 1982 to 2015. Based on the 0.05 ° LC mapping results for 1982 and 2015, a map of LC conversion can be obtained. The computation was also limited to the change mask to ensure the statistical significance. The conversion sources and destinations of LC classes were separately computed, so as to assess the direct causes of change in various LC classes.

2.10 Human impact

To further explore the role of human impact in regions with significant LCC, the results are evaluated based on data from the human impact campaign (Fritz et al., 2017), which can be downloaded from https://doi.pangaea.de/10.1594/PANGAEA.869680. The original study area was generated in the 2011 campaign to evaluate a map of land availability for biofuel production (Fritz et al., 2013), collected using a Geo-Wiki crowdsourcing platform. Pixels with a resolution of 1 km were randomly provided to volunteers. For each pixel, volunteers needed to point out the overall degree of human impact (HI, 0-100 %) which was visible from Google Earth's high-resolution satellite image and they were required to provide confidence levels in four categories: unsure; less sure; quite sure; and sure. Here, HI refers to the degree to which the landscape modified by humans visible from satellite images (Fritz et al., 2017). A total of 151942 point-records are available. To get the global distribution map of HI, we performed Kriging interpolation on the point records that had previously excluded the category of unsure confidence level. The search radius parameter of the Kriging interpolation was set to 12 nearby points and the other parameters as default. As shown in Fig. S2, we can see that the interpolation results reflect the global distribution of the intensity of human activity.

删除了： in

删除了: slope of

删除了: for the

删除了: 8

删除了: of

删除了: directly

删除了: classes of

删除了: 9

删除了: oa

删除了: 5

3 Results

3.1 Reliability of the products

3.1.1 Accuracy assessment

First of all, to evaluate the magnitude of the errors introduced by our training samples, we randomly selected 500 samples from the training sample for manual interpretation and evaluation, and the assessment accuracy was 92.26 %. It shows that the training sample we generate from 30m FROM-GLC_v2 is sufficient for our data production.

The global LC mapping result in 2015 is shown in Fig. 6. Its accuracy was tested with the H-homo sample in 2015 to obtain a confusion matrix (Table 3). The overall accuracy for the year 2015 reached 86.51 %. As for each class, the accuracies for forest, barren land and tundra are relatively high, where the user's accuracies and producer's accuracies are over 90 %. The accuracy of cropland is also high, with the user's accuracy and producer's accuracy reaching 73.54 % and 78.62 %, respectively. The user's accuracy of shrubland reached 83.62 %, while that of grassland is 67.58 %. Grassland is mainly mixed with cropland and shrubland. Table 4 shows the testing results of the FLUXNET test samples in which the number of sample units for shrubland, tundra, barren land, and snow/ice are relatively small. The overall accuracy of all classes is 82.10 % with the FLUXNET sample. Among them, the user's accuracy and the producer's accuracy for forest reach 91.01 % and 88.04 %, respectively. The producer's accuracy for cropland is 69.23 %, while its user's accuracy is 73.26 %.

Putting the test results from FROM-GLC_v2 and FLUXNET together, a spatial distribution map of the uncertainty of the 2015 LC mapping result was generated. As can be seen from Fig. 7, most of the world is shown in a green color, which means that the mapping result for most regions is most likely to be correct, and the result for 2015 is highly credible. There are still some regions showing a yellow or orange color, and a smaller number of regions showing red, representing those regions that may have been misclassified. Since there are no test samples in Greenland., the interpolation results are ignored. In general, the places with high uncertainty are Africa, East and South America, South Alaska, North and East Australia and Southwest Indonesia.

The assessment result with independent test samples is shown in Table 5 and Table 6. It shows that the overall accuracy of the GLASS-GLC without change detection is 81.28 %, and that with change detection is 82.81 %. This reflects the reliability of GLASS-GLC since the test samples are randomly distributed along the spatial and temporal dimensions, and also confirm the significance and effectiveness of the change detection method.

3.1.2 Data inter-comparison

The assessment results of MODIS-based land cover products and ESA-CCI land cover products based on test samples from FLUXNET site data are shown in Table 7 and Table 8, respectively. The overall accuracies of ESA-CCI products and MODIS-

设置了格式: 字体: (中文) Times New Roman, 10 磅
带格式的: 标题 3, 段落间距段前: 0 磅, 段后: 0 磅
设置了格式: 字体: 10 磅, 字体颜色: 自动设置
设置了格式: 字体: 10 磅, 字体颜色: 自动设置
设置了格式: 字体: 10 磅, 字体颜色: 自动设置
设置了格式: 字体: 10 磅, 字体颜色: 自动设置
设置了格式: (中文) 中文(中国), (其他) 英语(美国)
删除了:
删除了: (Table 3
删除了: of
删除了: Table 4
删除了: tested against the
删除了: s
设置了格式: 字体: 10 磅, 字体颜色: 文字 1, 英语(美国)
设置了格式: 字体颜色: 文字 1
设置了格式: 字体: 10 磅, 字体颜色: 文字 1, 英语(美国)
设置了格式: 字体颜色: 文字 1
设置了格式: 字体: 10 磅, 字体颜色: 文字 1, 英语(美国)
设置了格式: 字体: 10 磅, 字体颜色: 文字 1, 英语(美国)
带格式的: 正文, 左
设置了格式: 字体颜色: 文字 1
设置了格式: 字体: 10 磅, 字体颜色: 文字 1, 英语(美国)
设置了格式: 字体: 10 磅, 字体颜色: 文字 1, 英语(美国)
设置了格式: 字体: 10 磅, 字体颜色: 文字 1, 英语(美国)
设置了格式: 字体: 10 磅, 字体颜色: 文字 1, 英语(美国)
设置了格式: 字体颜色: 文字 1
设置了格式: 字体颜色: 文字 1
设置了格式: 字体: 10 磅, 字体颜色: 文字 1, 英语(美国)
设置了格式: 字体颜色: 文字 1
设置了格式: 字体: 10 磅, 字体颜色: 文字 1, 英语(美国)
设置了格式: 字体颜色: 文字 1
设置了格式: 字体颜色: 文字 1
设置了格式: 字体: 10 磅, 字体颜色: 文字 1
设置了格式: 字体: 10 磅, 字体颜色: 文字 1
设置了格式: 字体颜色: 文字 1
设置了格式: 字体: 10 磅, 字体颜色: 文字 1
设置了格式: 字体: 10 磅, 字体颜色: 文字 1
设置了格式: 字体颜色: 文字 1
设置了格式: 字体: 10 磅, 字体颜色: 文字 1

based products are 73.90 % and 80.38 % in 2015, respectively. Compared to these, The overall accuracy of GLASS-GLC (82.10 %, Table 4) is superior. Although the cross-walk of the different classification systems may be slightly different, It can still reflect the high accuracy of our GLASS-GLC products.

Figure 5 shows an inter-comparison with MODIS-based products, Figure 6 with ESA-CCI products and Figure 7 with FAOSTAT. The scatter plots and the linear fit lines reflect the results in 2015, and the box plots represent the distribution of R^2 of the annual linear fit lines for each class. It can be seen that various classes in several different products are relatively equivalent although they are under different classification systems. In comparison with MODIS-based products, the results of 2001-2015 for cropland, forest and snow/ice have high R^2. In comparison with ESA-CCI products, the mean R^2 of the linear fit lines of forest, grassland and snow/ice from 1992 to 2015 reach 0.99, 0.82, and 0.98, respectively, while the R^2 for shrubland is low. The inter-comparison of some other classes is poor, which may be caused by differences in the class definition in various classification systems. For instance, our classification system incorporates tundra, while the other two did not. Compared with FAOSTAT, the mean R^2 of the linear fit lines of cropland and forest is 0.82, and 0.87, respectively. In general, our GLASS-GLC products have a reasonable consistency with other products and statistics, and the difference is not significant. What's more, the duration of GLASS-GLC, 34 years, is much longer than MODIS-based and ESA-CC land cover products (as shown in Fig. 8). The comparison with other data illustrates the reliability and superiority of GLASS-GLC.

3.2 Spatiotemporal patterns in LCC

3.2.1 Global temporal patterns

Figure 9 shows the temporal changes of the global area for various LC classes from 1982 to 2015, where dotted lines are the corresponding trend lines. Overall, the global area of forest increases significantly ($p = 0.0000$) from 1982 to 2015. As for shrubland, although fluctuating, it shows a significant increasing trend ($p = 0.0017$). The global area of grassland, tundra, barren land snow/ice significantly decreases with $p = 0.0000$, $p = 0.0019$, $p = 0.0000$, and $p = 0.0003$, respectively.

Figure 10 shows the annual ratio of the global LCC to the global total terrestrial area, shown and organized in different time periods, where Fig. 10 (a) shows the results with a 5-year interval and Fig. 10 (b) with a 10-year interval. Overall, the annual ratio ranges from 0.35 % to 0.70 %, with an average of 0.52 % between 1982 and 2015. 5-year interval ratios show a relatively fluctuating trend. The average ratio reaches 0.63 % in 1991-1995, the highest among the seven intervals. The ratios have relatively large fluctuations in 2006-2010. All in all, the ratios before 1995 are generally higher, and it gradually decreases since then. With 10-year interval, ratios after 2000 are generally lower with an average of only 0.40 % in 2011-2015.

3.2.2 Patterns along latitudinal gradients

The global distribution of 0.25 ° grids with significant LCC from 1982 to 2015 is shown in Fig. 11 and Fig. S3 for the whole world, where the color depth represents the estimated change in area ratio per year. The distribution of significant LCC along

设置了格式 ... [8]

设置了格式 ... [9]
域代码已更改
设置了格式 ... [10]
域代码已更改

删除了: In comparison
设置了格式: 字体: (中文) Times New Roman, 10 磅, 字体颜色: 文字 1
删除了: ESA-CCI products…AOSTAT, the mean R^2 of the linear fit lines of forest, grassland…ropland and snow/ice…orest during 1992 to 2015 reach…s 0.99…2, 0.82, …nd 0.98…7, respectively, while the R^2 for shrubland is low… ... [11]
设置了格式 ... [12]
删除了: .
设置了格式: 字体: 10 磅, 字体颜色: 文字 1
删除了: products
设置了格式 ... [13]
删除了: our products…LASS-GLC, and also reflects the quality of our products in the time dimension to a certain extent, and the effectiveness of the change detection methods we use… ... [14]
设置了格式 ... [15]
删除了: 8
删除了: variation curves
删除了: 9
删除了: annual …lobal LCC to the global total terrestrial LC …rea, shown and calculated …rganized inby ... [16]
删除了: 9 …0 (a) shows the results with a 5-year interval and Fig. 10 9 … ... [17]

删除了: i
删除了: 10

latitudes is shown in the right, where the red curve represents a significant increase, green a significant decrease, and blue a net change.

The distribution pattern of LCC along latitudes is different, especially for cropland and forest, where it can be seen that cropland has increased significantly in the northern tropics and the southern hemisphere. It is confirmed that the significant increase in cropland has occurred mainly in the tropics and southern hemisphere (Gibbs et al., 2010). Forest has decreased significantly in the southern hemisphere and has increased significantly in the northern hemisphere, showing regional differences. In particular, in the high latitudes of the north, forest has increased significantly with a decrease of tundra. However, the increase in forest area in the northern hemisphere is significantly larger than that in the southern hemisphere, reflecting an overall increase in total forest area.

The grassland area has reduced at almost all latitudes. There might exist an increased trend in global vegetation coverage, where shrubland and forest expansion led to a reduction in the grassland area. It can be seen that shrubland has increased significantly in the southern hemisphere, corresponding to the reduction in the grassland area there. The area of barren land is decreasing, especially in the middle and high latitudes of the north, which further reflects the increase in vegetation coverage. The area of snow/ice in the northern high latitudes has reduced.

3.2.3 Continental patterns

The statistical results for each class at the continental scale are shown in Table 9, Table 10, Table 11, Table 12, Table S1, Table S2 and Table S3, where the slope and p-values are estimated according to the class area time series, while gain and loss are the computed values from 0.25 ° grids with significant LCC.

Cropland significantly increased in South America, with a growth rate of 9.1×10^3 km^2/year ($p = 0.0108$). The area of significantly increased cropland in Asia and Africa reached 67×10^3 km^2 and 23×10^3 km^2, respectively. Corresponding to the increase in cropland, forest decreased significantly in South America, at a rate of 10.8×10^3 km^2/year ($p = 0.0242$). Meanwhile, the area of forest in Africa has significantly decreased by 29×10^3 km^2. The area of forest in Asia has increased at the fastest speed. The area of forest in Europe and North America has also increased significantly. Meanwhile, the tundra area in Asia, Europe and North America decreased significantly by 132×10^3 km^2, 12×10^3 km^2 and 22×10^3 km^2, respectively. Shrubland has increased significantly in Africa at a rate of 47.4×10^3 km^2/year ($p = 0.0030$). But as shown in Fig. 3, the LC mapping result in 2015 in Africa is of high uncertainty, the trend here should be treated carefully. Shrubland also increased significantly in Oceania, by an area of 38×10^3 km^2. The decrease of grassland in Asia is serious, and the area of grassland in Asia decreased significantly by 315×10^3 km^2. Barren land in Asia also significantly decreased by 82×10^3 km^2. The global snow/ice area has decreased significantly, at a speed of 19.2×10^3 km^2/year ($p = 0.0003$).

删除了: This phenomenon may reflect the degradation of grassland. On the other hand, t

删除了:

删除了: 5

删除了: 6

删除了: 7

删除了: 8

删除了: 9

删除了: 10

删除了: 11

删除了: There is significant geographical heterogeneity among continents due to differences in latitude and longitude, as well as economic and social development differences, where significant causes of LCC are from both natural and human influences (Lambin et al., 2001). .

删除了: Many developing countries in South America, Asia and Africa have relatively poor economic and social development, rapid population growth and increasing demand for food (Barbier, 2004). At the same time, the international demand for food has increased, stimulating the export of crop products and requiring access to new land, which ultimately leads to the expansion of cropland. .

删除了: In

删除了: In addition to cropland expansion, the production of fuelwood and charcoal is also an important driving factor for deforestation (Hosonuma et al., 2012). .

删除了: The increase of forest in Asia, Europe and North America is related to afforestation projects and forest restoration policies in some regions (Aide et al., 2013;Pan et al., 2011). On the other hand, the increase of forest and the ... [18]

删除了: ure

设置了格式: 字体: (默认) Times New Roman

删除了: 7

删除了: The main source of shrubland conversion is ... [19]

删除了: degradation

删除了: .

删除了: The ar

删除了: , which may be due to drought (Dangal et al., ... [20]

删除了: , which may imply the management effects ef ... [21]

删除了: , reflecting the melting of ice and snow under ... [22]

3.3 Characteristics of LC conversion

We attempted to find out some high-frequency LC class conversions for the period 1982 to 2015 (Table 13). In addition, the conversion sources and destinations of each LC class are computed separately, as shown in Fig. 12.

Among land converted to cropland in 2015, grassland was the biggest source (Fig. 12 (b)), accounting for 67.58 %, 6.61 % of cropland was converted from forest (Fig. 12 (b)), showing the process of forest destruction. Among land converted to forest, the proportion of cropland reached 21.74 % (Fig. 12 (b)). Barren land and grassland were respectively the large sources of grassland and barren land (Fig. 12 (b)), reflecting the dynamic transformation between the two classes. Grassland accounted for 35.00 % of the increasing source of barren land (Fig. 12 (b)), indicating the process of grassland loss (Bai et al., 2008).

The most frequent direction of conversion from cropland in 1982 was forest (Fig. 12 (a)), which reached 78.22 %. At the same time, forest was also the main cause of loss of grassland and shrubland (Fig. 12 (a)). The conversion of forest to grassland accounted for 59.04 % of all conversions from forest (Fig. 12 (a)). The main conversion direction of tundra was forest, reaching 64.60 % (Fig. 12 (a)).

Overall, the increase of forest accounted for the highest proportion of all conversion processes, reaching 44.17 % (Table 13). The increase of grassland and cropland were second and third highest, reaching 19.79 % and 13.64 %, respectively (Table 13). In addition, the proportions of grassland to shrubland and barren land to grassland were 7.73 % and 5.75 %, respectively (Table 13). Cropland gain and vegetation gain were the main phenomena reflected by the changes in global LC from 1982 to 2015.

3.4 Human impact

Figure 13 (a) shows different human impact (HI) levels among different LCC areas. Overall, the average HI level in regions with significant changes in all LC classes is 25.49 %, indicating that human activity has a great impact on LCC. The highest HI level was found in those regions with significant increases in cropland, reaching an average value of 51.38 %. Meanwhile, the HI level of cropland loss reached 48.02 % while the HI level for forest loss was 26.91 %. In addition, in any change of vegetation, such as forest, grassland and shrubland, the HI level in regions of vegetation loss is higher than that of gain.

The HI levels along continents can be found in Fig. 13 (b). The highest level of HI is found in Europe and lowest in Oceania. The HI in Europe reached 46.86 %, indicating that human activity played a relatively important role in regions with significant LCC. Asia came second, with a HI level of 32.07 %. In South America and Oceania in the southern hemisphere, the overall HI level in the LCC regions is small.

As shown in Fig. 13 (c), the polar regions and the boreal conifer forest regions at northern high latitudes with significant LCC have lower HI levels. The level of HI in subtropical regions is high, among which HI levels in subtropical steppe and subtropical humid forest regions reached 38.23 % and 43.90 %, indicating that the role of LC conversion caused by human activity in subtropical climate areas is significant. In addition, in the temperate steppe regions, the HI level in the regions of significant LCC is also high, reaching 39.87 %. In the tropics the average HI level in dry forest regions is highest among regions of

删除了： Natural and human factors generally have a significant couplingjoint effect to land cover change. Whether LCC is caused by natural or human factors, there is often a significant coupling effect. …e attempted to find out some high-frequency LC class conversions for the period 1982 to 2015 (Table 12…3). In addition, the conversion sources and destinations of each LC class are computed separately, as shown in Fig. 11… ... [23]

删除了： 1… (b)), accounting for 67.58 %, which indicated that a large amount of cropland came from reclamation (Liu et al., 2005)… 6.61 % of cropland was converted from forest (Fig. 11… (b)), showing the process of forest destruction. Among land converted to forest, the proportion of cropland reached 21.74 % (Fig. 11… (b)), partly due to the fact that abandoned croplands were restored to forest… Barren land and grassland were respectively the large sources of grassland and barren land (Fig. 11… (b)), reflecting the dynamic transformation between the two classes. Grassland accounted for 35.00 % of the increasing source of barren land (Fi... [24]

删除了： land degradation

设置了格式： 字体颜色: 蓝色

删除了： 1… (a)), which reached 78.22 %, reflecting the process of forest expansion… At the same time, forest was the main cause of loss of grassland and shrubland (Fig. 11… (a)), which also confirms the process of forest expansion… conversion of forest to grassland accounted for 59.04 % of all conversions from forest (Fig. 11… (a)). The main conversion direction of tundra was forest, reaching 64.60 % (Fig. 11… (a)), indicating an expansion of forest in the high latitu... [25]

删除了： 2…), reflecting the phenomenon of forest expansion… The increase of grassland and cropland w... [26]

删除了： surface greening

删除了： 12…3 (a) shows different human impact (HI) levels among different LCC areas. Overall, the average HI le... [27]

删除了： natural

删除了： , which indicates that human activity has a relatively stronger destructive effect on natural vegetation, while ... [28]

删除了： 13

删除了： n

删除了： 14

删除了： ous

删除了： , indicating that LCC in those regions may be more related to natural factors like climate change (Buerman... [29]

significant LCC, reaching 34.04 %.

3.5 Local hotspots of LCC

Regarding LC, more attention tends to be paid to global and regional LCC. At the local scale, we can further explore the hot spots of LCC. The main regions of LCC hotspots are shown in Fig. 14, where the depth of color represents a significant change.

In the north of Eurasia, forest has increased significantly (Fig. 14 (a)), and that in Siberia has moved northward to the tundra regions. In northern North America, such as Alaska and the north of Canada, forest has also increased but the extent of the increase is weaker than that in North Eurasia. In the Great Plains of Central North America, grassland has decreased and cropland has increased (Fig. 14 (b)). In most countries of South America, croplands have expanded substantially (Fig. 14 (d)) and forests have decreased significantly (Fig. 14 (c)), especially in the southeastern part of the Amazon rainforest. In Southeast Asia, such as Cambodia, Vietnam, Indonesia and Malaysia, forest has also decreased significantly and cropland has increased. While our LCC analysis shows these trends in the Asian tropics, higher resolution data and more specific land cover mapping are needed to explicitly determine the reasons for LCC in this region (Cheng et al., 2018). In Africa, forest in the northern part of the Congo Basin has expanded while forest in the southern Miombo forest belt has decreased (Fig. 14 (e)). In China, forest has increased (Fig. 14 (f)). Some grassland in Mongolia and Inner Mongolia of China showed a trend of decrease (Fig. 14 (g)). There is an obvious increase in grassland areas in the eastern part of the Qinghai-Tibet Plateau (Fig. 14 (h)) and a decrease of grassland in central Asia and parts of Western Asia (Fig. 14 (i)). In some parts of the former Soviet Union in Eastern Europe, a decrease of cropland (Fig. 14 (j)) and an increase of forest can be observed.

4 Discussions

Based on the accuracy assessment and data inter-comparison results, it can be seen that the global LC mapping products of 1982-2015, GLASS-GLC are reliable with high accuracies, and the global long-term mapping framework we designed is effective. Using GLASS-GLC CDRs in change analysis of LC can reflect a 34-year global landscape change pattern. Many phenomena and patterns can be confirmed by existing research. In addition, we have assessed the impact of human effects within different LC classes, and have further explored local LCC hotspots.

However, there are still deficiencies in the design of the mapping framework. First, the large grid size of 0.05 °, can only reflect the average change state of LC in a large area, thus many small-area phenomena cannot be well reflected (Gómez et al., 2016). For example, the reduction of much cropland is due to urbanization, and the expansion of cities is usually sporadic. Although those changes are large at the global scale, they can hardly be reflected with 0.05 ° pixels. Moreover, due to the synthesis principle, the classification result of each pixel can only represent the class with the largest proportion in area, and the information of remaining classes is ignored even though they can sometimes be more than 50 % in total. Such a neglect, due to the famous “Scale Effect” (Turner et al., 1989) can also cause great deviations in the final statistical summary of the LC

删除了： Such HI level in this eco-region may be caused by forest destruction, deforestation, and cropland expansion.

删除了： and investigate the causes of such change by area… The main regions of LCC hotspots are shown in Fig. 1… [30]

删除了： 5… (a)), and that in Siberia has moved northward to the tundra regions, which is mainly the result of climate warming. The increase in temperature and soil moisture (thawing of the permafrost) has promoted plant growth (Berner et al., 2013)… .
In northern North America, such as Alaska and the north of Canada, forest has also increased but the extent of the increase is weaker than that in North Eurasia. Studies have shown that this may be related to an insignificant temperature rise in North America and even a slight cooling trend (Wang et al., 2011). In addition, fire disturbance in northern North America has interrupted forest succession (Alcaraz-Segura et al., 2010) and drought disasters in parts of the United States and Canada have increased tree mortality (Van Mantgem et al., 2009;Peng et al., 2011). These could also be possible reasons for the constant, or even decreasing, forest areas in these regions. In addition to climate warming, the decrease of cropland and increase of forest in the eastern part of the United States are related to forest restoration and management measures (Herrick et al., 2010). .
In the Great Plains of Central North America, grassland has decreased and cropland has increased (Fig. 15… (b)). It has been found that rising gasoline prices and the development of biofuels have led to increasing planting areas of corn and soybean in the United States (Lark et al., 2015;Wright and Wimberly, 2013). .
In most countries of South America, croplands have expanded substantially (Fig. 15… (d)) and forests have decreased… [31]

带格式的： 缩进: 首行缩进: 1.5 字符

删除了： degradation

删除了： sing

删除了： 5… (g)). There is anStudies have shown overgrazing to be the main cause of vegetation degradation in this region, while drought and soil erosion have played a secondary role (Yin et al., 2018). The…obvious increase of …n grassland… [32]

删除了： , such as the expansion of tropical agricultural land, greening in the northern region, deforestation in the southern hemisphere and melting of snow and ice… In addition, we assessed the impact of human effects within different LC… [33]

删除了： due to the coarse spatial resolution,

删除了： agricultural

area leading to uncertainties when compared with mapping results at finer resolutions.

Second, our sampling strategy for training has certain limitations. On one hand, since the training sample is generated from 30m resolution maps of more than 73 % accuracy, this will inevitably propagate and accumulate error to 5 km resolution. Of course, due to the higher signal-to-noise ratio of the high-resolution data, the sampling is still satisfactory compared to the direct visual interpretation of the coarse resolution images. On the other hand, the training sample used is only from a single year of circa 2015. Although we have implemented a time series correction for the original input features and performed a time-consistent post processing on the classification results, the effects of inter-annual fluctuations of the features cannot be completely avoided (Song et al., 2018a). On the other hand, according to the stable classification with limited sample theory (Gong et al., 2019), a representative sample collected in one year with less than 20 % in error should suffice in multiannual use at the global scale. Therefore, a multi-year sample set may not be as critical for multiannual classification provided the sample is better than 80 % accurate. In our case, although the source training data has an accuracy of 73.17 %, we are not certain if the aggregated sample set exceeds an accuracy of 80 %. While this needs further assessment, the expected loss of accuracy should be within a couple of percent (Cheng et al., 2018). According to the 92.26 % test accuracy reported in 3.1.1, the aggregated sample set can be satisfactory.

For the generation of test sample units in 2015, we have adopted the scale-up approach. That is to say, we first upscaled the 30m test sample set to 5 km by maximum area synthesis, which contains unavoidable errors because of scale transformation. Due to the difficulty of visual interpretation in coarse scale and field investigation (Gong et al., 2013), establishing a sample library at 5 km resolution is not easy. Thus, instead, we adopted the data aggregation method based on the 30m FROM-GLC_v2 results. Since mixed pixel problems for remotely sensed data are unavoidable at any scale, choosing one category for mixed pixels is inevitable and the cost of simplification in a traditional classification process. The development of LC ratio mapping products (similar to VCF products), rather than hard classification, especially for the case of coarse resolution, should be considered and further assessed. However, the independent interpreted 5 km test sample set alleviates the problem.

We have eliminated wetland and impervious surface in our classification system. This is a tradeoff when working at the 5 km scale. Patches of wetland and impervious surface are usually small, and it is difficult to achieve a pixel size of 0.05 ° for many situations, so the classification of the two types is extremely difficult. However, both are important LC types. Wetland is a transitional zone between terrestrial ecosystems and aquatic ecosystems (Davidson, 2014). The impervious surface can represent the urban area. In recent years, urban expansion has been a relatively significant phenomenon in global environmental change (Seto et al., 2011). Urban expansion reflects an important type of human activity, so the impervious surface is also one of the essential components to reflect anthropogenic influence though the total area of its change is usually small.

It should be pointed out that at a coarse resolution of 0.05 °, our definition of forest is more inclined to the tree canopy cover. Thus the changes in internal density of trees can also be reflected in the area change of forest, instead of just the stand-replacement type (Korhonen et al., 2006). In addition, the dominant-class synthesis strategy we adopted also makes it

删除了: global mapping results

删除了: oa

设置了格式: 字体: (默认) Times New Roman

删除了:

删除了: (Gong et al., submitted)

删除了: 77

删除了: This

删除了: s(Cheng et al., 2018)

删除了: actually

删除了: oa

删除了: s

删除了: The best way to verify the accuracy, of course, is to use a 0.05 ° test samples set directly derived at this resolution. However, d…

删除了: oa

删除了: of aggregation of

删除了: to 5 km scale to generate samples

删除了: with techniques of soft classification

删除了: oa

删除了: It is plausible to regard the selected test samples as “H-homo samples” that can be used for coarse resolution mapping. Although this method is feasible to a certain extent, there are inevitably errors.

删除了: oa

删除了: largest

unavoidable to include internal density change of various classes, which in turn will further affect the classification and change area calculation of forest class.

In addition, because we are mainly depicting the natural biophysical properties of vegetated areas with limitation in resolution, some artificial features cannot be distinguished, such as plantations (rubber, oil palm, and various fruit trees) and natural forest, which are uniformly included as forest in our classification system.

In the statistical analysis, although we have already conducted post-classification time-consistency processing for the original LC mapping results as much as possible, it is inevitable that there are still large fluctuations and interferences from various unknown factors unfavorable to the extraction of long-term trend of LCC. In order to ensure that the trend of the resulting time series is significant, we have to scale up the classification result from 0.05 ° to 0.25 °, converting the original class label of each 0.05 ° pixel to the class area ratio of 0.25 ° grid. The long-term time series of the area ratios is tested for statistical significance. However, in some cases this procedure will also be influenced by the “Scale Effect”.

In the analysis of anthropogenic influences, indirect effects of many human activities were ignored because the main objective was to include the effects of directly visible human activities. For example, human activities increase the concentration of carbon dioxide in the atmosphere, which in turn affects the global climate, leading to higher temperature, and thus increasing vegetation coverage (Piao et al., 2006;Bonan, 2008). This pathway of action is indirect, but it is difficult to reflect in the human impact data we use, which results in an underestimation of the assessment of anthropogenic influences.

GLASS-GLCs contain more detailed LC classes, longer temporal coverage (34 years), high consistency, which meet the requirement for CDR. GLASS-GLC CDRs are the first collection of global LC dynamics of 5 km, and fill the existing gap for high-reliability and consistency of long-term general purpose global LC products. In addition, our strategy of generating samples from high-resolution classification products can greatly reduce the cost and investment of sample collection, and can flexibly and effectively be extended to other coarse-resolution LC mapping tasks in the future.

In the future, with the advancement of technology and the accumulation of remote sensing datasets, the use of remote sensing products for LC mapping with higher resolution and longer time series will undoubtedly better reflect the global LC and its changes. However, under limited conditions, we can consider using coarse-resolution satellite data to determine the locations of potential rapid change, and then use high-resolution data in these hotspots to accurately estimate the rate and mode of change. Moreover, it is necessary to establish a multi-year sample library to assess the impact of inter-annual fluctuations in features on the accuracy of change characterization and analysis. Wetland and impervious surface are LC classes that have extremely high value. It would be useful to supplement the mapping and change analysis of these two classes when suitable data become available. For the analysis of global LCC, systematic and in-depth attribution analysis and research can be further carried out.

删除了： The result of our statistical summary shows that the global vegetated area increased significantly between 1982 and 2015, which is inconsistent with the results of FAO and some other global mapping products. This inconsistency originates from, on one hand, the above limitations of our designed mapping framework, and on the other hand, the statistics collected by FAO, and other census-based datasets, which are also affected by errors from many aspects, and its effectiveness is yet to be evaluated. Nevertheless, many studies can also confirm our results, such as (Song and Hansen, 2017;Song et al., 2018a;Piao et al., 2015;Pan et al., 2018) who have proved that the global vegetation area has increased with the increasing NDVI and LAI in time. To some extent, the sum of the global change area of forest, shrubland, and grassland is showing an increasing trend in our results, which can be seen as the sign of global vegetation growth. .

设置了格式： 字体颜色: 文字 1

删除了： oa

删除了： oa

删除了： In addition, the development of LC ratio mapping products (similar to VCF products) with techniques of soft classification, rather than hard classification, especially for the case of coarse resolution, should be considered.

5 Data availability

GLASS-GLC products at 5 km resolution from 1982 to 2015 are available to the public in the TIFF format at https://doi.org/10.1594/PANGAEA.898096 (Liu et al., 2019).

GLASS CDRs were provided by Beijing Normal University Data Center (http://glass-product.bnu.edu.cn/, last access: 27 December 2018). VCF products were obtained from the Land Processes Distributed Active Archive Center (https://lpdaac.usgs.gov/, last access: 20 December 2018). GMTED2010 were acquired from Google Earth Engine (https://code.earthengine.google.com/, last access: 24 December 2018). Geo-Wiki points came from the human impact campaign (https://doi.pangaea.de/10.1594/PANGAEA.869680, last access: 30 November 2018). Eco-region data were obtained from the FAO global eco-region dataset (http://www.fao.org/geonetwork/srv/en/metadata.show?CurrTab=simple&id=1255, last access: 3 December 2018).

6 Conclusions

In order to better reflect the global land changes, continuous and dynamic monitoring of global LC is necessary. We built GLASS-GLC, the first CDRs for global LC on the GEE platform. It can capture the global LCC information from 1982 to 2015. Compared to previous global LC products, GLASS-GLC products cover a longer time period and have higher consistency and more detailed classes. Our entire mapping framework is based on FROM-GLC_v2, including the classification system and high-quality H-homo sample generation.

Based on over ten thousand independent test samples units from both the FROM-GLC sample set and FLUXNET site data in 2015, the overall accuracy of GLASS-GLC was shown to exceed 80 %. With 2431 test sample units in different years, the overall accuracy of GLASS-GLC is also over 80 %, at 82.81 %. Using inter-comparisons with other global LC products of different resolutions from various data sources, we verified the effectiveness and reliability of GLASS-GLC from different perspectives. Systematic uncertainty analysis was also performed on a global scale based on the results of the accuracy assessment and its geographical distribution. This shows that GLASS-GLC CDR products have relatively low uncertainty in most parts of the world. Our results also indicate that GLASS CDRs have potential for multi-class LC mapping and can provide more than enough features and information to distinguish different LC classes, with relatively strong temporal and spatial consistency, which can produce extremely reliable change information.

Comprehensive spatiotemporal pattern analysis based on GLASS-GLC reflected and revealed many significant global LCC phenomena and patterns, such as forest loss and cropland gain in the tropics, forest gain in the northern regions, etc. An analysis of the global LC conversion pattern from 1982 to 2015 revealed hot spots of LCC.

Since anthropogenic influence has become one of the most important driving forces for LCC, especially after the industrial revolution, we quantified the level of human impact in areas of significant LCC. The results show that the average human

删除了: average

删除了: deforestation

删除了: agricultural land expansion

删除了: afforestation

删除了: and forest expansion

删除了: such as land degradation, forest restoration, reclamation and agricultural land abandonment

impact level in areas of significant LCC are about 25.49 %.

With increasing economic globalization, LCC has increased. Based on GLASS-GLC, effective global LC and change analysis could be conducted, enhancing our understanding of global environmental change, and even mitigating its negative impact to some extent, which is also beneficial to the achievement of sustainable development goals.

删除了: , suggesting that anthropogenic influence plays a strong role in vegetation destruction, expansion of tropical agricultural land, and degradation of grassland areas, etc. Under the current global climate change scenario with significantly elevated GHG concentrations and temperature rises, this remarkable human impact has also contributed to a noticeable greening trend of the Earth because of the effect of carbon dioxide fertilization…

删除了: Combined with field visits and literature reviews on local LCC hot spots, we can see that global LC is affected by the synergetic effect of many complicated and multi-faceted factors, including human activity, climate change, socio-economic policies, and the natural environment transition, etc., and such change could further influence global and regional climate, environment, biodiversity, etc. .

Author contribution

PG conceived the research. HL and JW designed the experiments and HL carried out experiments. NC provided GEE support. SL provided data. HL prepared the manuscript with contributions from all co-authors.

Competing interests

The authors declare that they have no conflict of interest.

Acknowledgements

This work is partially supported by the National Key Research and Development Program of China (NO.2016YFA0600103), a donation made by Delos Living LLC, and the Cyrus Tang Foundation.

References

Achard, F., Eva, H. D., Mayaux, P., Stibig, H. J., and Belward, A.: Improved estimates of net carbon emissions from land cover change in the tropics for the 1990s, Global Biogeochemical Cycles, 18, https://doi.org/10.1029/2003GB002142, 2004.

Andrew K, S., Nathalie, P., Nicholas C, C., Gary N, G., Matthew, H., Richard, L., Caspar A, M., Brian, O. C., Marc, P., and Henrique Miguel, P.: Environmental science: Agree on biodiversity metrics to track from space, Nature, 523, 403-405, https://doi.org/10.1038/523403a, 2015.

Bai, Z. G., Dent, D. L., Olsson, L., and Schaepman, M. E.: Proxy global assessment of land degradation, Soil use and management, 24, 223-234, https://doi.org/10.1111/j.1475-2743.2008.00169.x, 2008.

Ban, Y., Gong, P., and Gini, C.: Global land cover mapping using Earth observation satellite data: Recent progresses and challenges, ISPRS journal of photogrammetry and remote sensing, 103, 1-6, https://doi.org/10.1016/j.isprsjprs.2015.01.001, 2015.

Bartholome, E., and Belward, A. S.: GLC2000: a new approach to global land cover mapping from Earth observation data, International Journal of Remote Sensing, 26, 1959-1977, https://doi.org/10.1080/01431160412331291297, 2005.

Bonan, G. B.: Forests and climate change: forcings, feedbacks, and the climate benefits of forests, Science, 320, 1444-1449, https://doi.org/10.1126/science.1155121, 2008.

Bontemps, S., Defourny, P., Radoux, J., Van Bogaert, E., Lamarche, C., Achard, F., Mayaux, P., Boettcher, M., Brockmann, C., and Kirches, G.: Consistent global land cover maps for climate modelling communities: Current achievements of the ESA's land cover CCI, Proceedings of the ESA Living Planet Symposium, Edimburgh, 2013, 9-13,

Brink, A. B., and Eva, H. D.: Monitoring 25 years of land cover change dynamics in Africa: A sample based remote sensing approach, Applied Geography, 29, 501-512, https://doi.org/10.1016/j.apgeog.2008.10.004, 2009.

Cao, C., Xiong, X., Wu, A., and Wu, X.: Assessing the consistency of AVHRR and MODIS L1B reflectance for generating

fundamental climate data records, Journal of Geophysical Research: Atmospheres, 113, https://doi.org/10.1029/2007JD009363, 2008.
Chen, Y., Ge, Y., Heuvelink, G. B. M., An, R., and Chen, Y.: Object-based duperresolution land-cover mapping from remotely sensed imagery, IEEE Transactions on Geoscience and Remote Sensing, 56, 328-340, https://doi.org/10.1109/TGRS.2017.2747624, 2018.
Cheng, J., Liang, S., Verhoef, W., Shi, L., and Liu, Q.: Estimating the Hemispherical Broadband Longwave Emissivity of Global Vegetated Surfaces Using a Radiative Transfer Model, IEEE Transactions on Geoscience and Remote Sensing, 54, 905-917, https://doi.org/10.1109/TGRS.2015.2469535, 2016.
Cheng, Y., Yu, L., Xu, Y., Liu, X., Lu, H., Cracknell, A. P., Kanniah, K., and Gong, P.: Towards global oil palm plantation mapping using remote-sensing data, International Journal of Remote Sensing, 39, 5891-5906, https://doi.org/10.1080/01431161.2018.1492182, 2018.
Cihlar, J.: Land cover mapping of large areas from satellites: status and research priorities, International Journal of Remote Sensing, 21, 1093-1114, https://doi.org/10.1080/014311600210092, 2000.
Claussen, M., Brovkin, V., and Ganopolski, A.: Biogeophysical versus biogeochemical feedbacks of large-scale land cover change, Geophysical research letters, 28, 1011-1014, https://doi.org/10.1029/2000GL012471, 2001.
Cohen, W. B., Yang, Z., Healey, S. P., Kennedy, R. E., and Gorelick, N.: A LandTrendr multispectral ensemble for forest disturbance detection, Remote Sensing of Environment, 205, 131-140, https://doi.org/10.1016/j.rse.2017.11.015, 2018.
Davidson, N. C.: How much wetland has the world lost? Long-term and recent trends in global wetland area, Marine and Freshwater Research, 65, 934-941, https://doi.org/10.1071/MF14173, 2014.
DeFries, R. S., Hansen, M., Townshend, J. R. G., and Sohlberg, R.: Global land cover classifications at 8 km spatial resolution: the use of training data derived from Landsat imagery in decision tree classifiers, International Journal of Remote Sensing, 19, 3141-3168, https://doi.org/10.1080/014311698214235, 1998.
DeFries, R. S., Field, C. B., Fung, I., Collatz, G. J., and Bounoua, L.: Combining satellite data and biogeochemical models to estimate global effects of human-induced land cover change on carbon emissions and primary productivity, Global Biogeochemical Cycles, 13, 803-815, https://doi.org/10.1029/1999GB900037, 1999.
Feng, D., Yu, L., Zhao, Y., Cheng, Y., Xu, Y., Li, C., and Gong, P.: A multiple dataset approach for 30-m resolution land cover mapping: a case study of continental Africa, International Journal of Remote Sensing, 39, 3926-3938, https://doi.org/10.1080/01431161.2018.1452073, 2018.
Friedl, M. A., Sulla-Menashe, D., Tan, B., Schneider, A., Ramankutty, N., Sibley, A., and Huang, X.: MODIS Collection 5 global land cover: Algorithm refinements and characterization of new datasets, Remote Sensing of Environment, 114, 168-182, https://doi.org/10.1016/j.rse.2009.08.016, 2010.
Fritz, S., See, L., van der Velde, M., Nalepa, R. A., Perger, C., Schill, C., McCallum, I., Schepaschenko, D., Kraxner, F., and Cai, X.: Downgrading recent estimates of land available for biofuel production, Environmental Science & Technology, 47, 1688-1694, https://doi.org/10.1021/es303141h, 2013.
Fritz, S., See, L., Perger, C., McCallum, I., Schill, C., Schepaschenko, D., Duerauer, M., Karner, M., Dresel, C., and Laso-Bayas, J.-C.: A global dataset of crowdsourced land cover and land use reference data, Scientific data, 4, 170075, https://doi.org/10.1038/sdata.2017.75, 2017.
Fuller, R. M., Smith, G. M., and Devereux, B. J.: The characterisation and measurement of land cover change through remote sensing: problems in operational applications?, International Journal of Applied Earth Observation and Geoinformation, 4, 243-253, https://doi.org/10.1016/S0303-2434(03)00004-7, 2003.
Gallego, F. J.: Remote sensing and land cover area estimation, International Journal of Remote Sensing, 25, 3019-3047, https://doi.org/10.1080/01431160310001619607, 2004.
Gibbard, S., Caldeira, K., Bala, G., Phillips, T. J., and Wickett, M.: Climate effects of global land cover change, Geophysical Research Letters, 32, https://doi.org/10.1029/2005GL024550, 2005.
Gibbs, H. K., Ruesch, A. S., Achard, F., Clayton, M. K., Holmgren, P., Ramankutty, N., and Foley, J. A.: Tropical forests were the primary sources of new agricultural land in the 1980s and 1990s, Proceedings of the National Academy of

Sciences, 107, 16732-16737, https://doi.org/10.1073/pnas.0910275107, 2010.
Gómez, C., White, J. C., and Wulder, M. A.: Optical remotely sensed time series data for land cover classification: A review, ISPRS Journal of Photogrammetry and Remote Sensing, 116, 55-72, https://doi.org/10.1016/j.isprsjprs.2016.03.008, 2016.
Gong, P.: Accuracy assessment of global land cover datasets based on global field stations, Progress in Natural Science, 19, 754-759, 2009.
Gong, P.: Remote sensing of environmental change over China: A review, Chinese Science Bulletin, 57, 2793-2801, https://doi.org/10.1007/s11434-012-5268-y, 2012.
Gong, P., Wang, J., Yu, L., Zhao, Y., Zhao, Y., Liang, L., Niu, Z., Huang, X., Fu, H., and Liu, S.: Finer resolution observation and monitoring of global land cover: First mapping results with Landsat TM and ETM+ data, International Journal of Remote Sensing, 34, 2607-2654, https://doi.org/10.1080/01431161.2012.748992, 2013.
Gong, P., Liu, H., Zhang, M., Li, C., Wang, J., Huang, H., Clinton, N., Ji, L., Li, W., Bai, Y., Chen, B., Xu, B., Zhu, Z., Yuan, C., Suen, H. P., Guo, J., Xu, N., Li, W., Zhao, Y., Yang, J., Yu, C., Wang, X., Fu, H., Yu, L., Dronova, I., Hui, F., Cheng, X., Shi, X., Xiao, F., Liu, Q., and Song, L.: Stable classification with limited sample: transferring a 30-m resolution sample set collected in 2015 to mapping 10-m resolution global land cover in 2017, Science Bulletin, 64, 370, https://doi.org/10.1016/j.scib.2019.03.002, 2019.
Gong, P., Li, X., Wang, J., Bai, Y., Chen, B., Hu, T., Liu, X., Xu, B., Yang, J., and Zhang, W.: Annual maps of global artificial impervious area (GAIA) between 1985 and 2018, Remote Sensing of Environment, 236, 111510, https://doi.org/10.1016/j.rse.2019.111510, 2020.
Gorelick, N., Hancher, M., Dixon, M., Ilyushchenko, S., Thau, D., and Moore, R.: Google Earth Engine: Planetary-scale geospatial analysis for everyone, Remote Sensing of Environment, 202, 18-27, https://doi.org/10.1016/j.rse.2017.06.031, 2017.
Grekousis, G., Mountrakis, G., and Kavouras, M.: An overview of 21 global and 43 regional land-cover mapping products, International Journal of Remote Sensing, 36, 5309-5335, https://doi.org/10.1080/01431161.2015.1093195, 2015.
Hansen, M. C., DeFries, R. S., Townshend, J. R. G., and Sohlberg, R.: Global land cover classification at 1 km spatial resolution using a classification tree approach, International journal of remote sensing, 21, 1331-1364, https://doi.org/10.1080/014311600210209, 2000.
Hansen, M. C., Potapov, P. V., Moore, R., Hancher, M., Turubanova, S. A. A., Tyukavina, A., Thau, D., Stehman, S. V., Goetz, S. J., and Loveland, T. R.: High-resolution global maps of 21st-century forest cover change, science, 342, 850-853, https://doi.org/10.1126/science.1244693, 2013.
Herold, M., Mayaux, P., Woodcock, C. E., Baccini, A., and Schmullius, C.: Some challenges in global land cover mapping: An assessment of agreement and accuracy in existing 1 km datasets, Remote Sensing of Environment, 112, 2538-2556, https://doi.org/10.1016/j.rse.2007.11.013, 2008.
Hollmann, R., Merchant, C. J., Saunders, R., Downy, C., Buchwitz, M., Cazenave, A., Chuvieco, E., Defourny, P., de Leeuw, G., and Forsberg, R.: The ESA climate change initiative: Satellite data records for essential climate variables, Bulletin of the American Meteorological Society, 94, 1541-1552, https://doi.org/10.1175/BAMS-D-11-00254.1, 2013.
Homer, C., Huang, C., Yang, L., Wylie, B., and Coan, M.: Development of a 2001 national land-cover database for the United States, Photogrammetric Engineering & Remote Sensing, 70, 829-840, https://doi.org/10.14358/PERS.70.7.829, 2004.
Houghton, R. A., House, J. I., Pongratz, J., Van Der Werf, G. R., DeFries, R. S., Hansen, M. C., Quéré, C. L., and Ramankutty, N.: Carbon emissions from land use and land-cover change, Biogeosciences, 9, 5125-5142, https://doi.org/10.5194/bg-9-5125-2012, 2012.
Huang, H., Wang, J., Liu, C., Liang, L., Li, C., and Gong, P.: The migration of training samples towards dynamic global land cover mapping, ISPRS Journal of Photogrammetry and Remote Sensing, 161, 27-36, https://doi.org/10.1016/j.isprsjprs.2020.01.010, 2020.
Ji, L., Gong, P., Wang, J., Shi, J., and Zhu, Z.: Construction of the 500-m Resolution Daily Global Surface Water Change

Database (2001–2016), Water Resources Research, 54, 10,270-210,292, https://doi.org/10.1029/2018WR023060, 2018.
Kennedy, R. E., Yang, Z., and Cohen, W. B.: Detecting trends in forest disturbance and recovery using yearly Landsat time series: 1. LandTrendr—Temporal segmentation algorithms, Remote Sensing of Environment, 114, 2897-2910, https://doi.org/10.1016/j.rse.2010.07.008, 2010.
Korhonen, L., Korhonen, K. T., Rautiainen, M., and Stenberg, P.: Estimation of forest canopy cover: a comparison of field measurement techniques, Silva Fennica, 40, 577-588, https://doi.org/10.14214/sf.315, 2006.
Lambin, E. F., Turner, B. L., Geist, H. J., Agbola, S. B., Angelsen, A., Bruce, J. W., Coomes, O. T., Dirzo, R., Fischer, G., and Folke, C.: The causes of land-use and land-cover change: moving beyond the myths, Global environmental change, 11, 261-269, https://doi.org/10.1016/S0959-3780(01)00007-3, 2001.
Lambin, E. F., Geist, H., and Rindfuss, R. R.: Introduction: Local Processes with Global Impacts, in: Land-Use and Land-Cover Change: Local Processes and Global Impacts, edited by: Lambin, E. F., and Geist, H., Springer Berlin Heidelberg, Berlin, Heidelberg, 1-8, 2006.
Lepers, E., Lambin, E. F., Janetos, A. C., DeFries, R., Achard, F., Ramankutty, N., and Scholes, R. J.: A synthesis of information on rapid land-cover change for the period 1981–2000, AIBS Bulletin, 55, 115-124, https://doi.org/10.1641/0006-3568(2005)055[0115:ASOIOR]2.0.CO;2, 2005.
Li, C., Wang, J., Wang, L., Hu, L., and Peng, G.: Comparison of classification algorithms and training sample sizes in urban land classification with Landsat Thematic Mapper Imagery, Remote Sensing, 6, 964-983, https://doi.org/10.3390/rs6020964, 2014.
Li, C., Gong, P., Wang, J., Yuan, C., Hu, T., Wang, Q., Yu, L., Clinton, N., Li, M., and Guo, J.: An all-season sample database for improving land-cover mapping of Africa with two classification schemes, International Journal of Remote Sensing, 37, 4623-4647, https://doi.org/10.1080/01431161.2016.1213923, 2016.
Li, C., Gong, P., Wang, J., Zhu, Z., Biging, G. S., Yuan, C., Hu, T., Zhang, H., Wang, Q., Li, X., Liu, X., Xu, Y., Guo, J., Liu, C., Hackman, K. O., Zhang, M., Cheng, Y., Yu, L., Yang, J., Huang, H., and Clinton, N.: The first all-season sample set for mapping global land cover with Landsat-8 data, Science Bulletin, 62, 508-515, https://doi.org/10.1016/j.scib.2017.03.011, 2017.
Li, X., Zhou, Y., Zhu, Z., Liang, L., Yu, B., and Cao, W.: Mapping annual urban dynamics (1985–2015) using time series of Landsat data, Remote Sensing of Environment, 216, 674-683, https://doi.org/10.1016/j.rse.2018.07.030, 2018.
Liang, S., Zhao, X., Liu, S., Yuan, W., Cheng, X., Xiao, Z., Zhang, X., Liu, Q., Cheng, J., and Tang, H.: A long-term Global LAnd Surface Satellite (GLASS) data-set for environmental studies, International Journal of Digital Earth, 6, 5-33, https://doi.org/10.1080/17538947.2013.805262, 2013.
Liu, H., Gong, P., Wang, J., Clinton, N., Bai, Y., and Liang, S.: Annual Dynamics of Global Land Cover and its Long-term Changes from 1982 to 2015, https://doi.org/10.1594/PANGAEA.898096, 2019.
Liu, J., Liu, M., Deng, X., Zhuang, D., Zhang, Z., and Luo, D.: The land use and land cover change database and its relative studies in China, Journal of Geographical Sciences, 12, 275-282, https://doi.org/10.1007/BF02837545, 2002.
Liu, X., Yu, L., Li, W., Peng, D., Zhong, L., Li, L., Xin, Q., Lu, H., Yu, C., and Gong, P.: Comparison of country-level cropland areas between ESA-CCI land cover maps and FAOSTAT data, International Journal of Remote Sensing, 1-15, https://doi.org/10.1080/01431161.2018.1465613, 2018.
Loveland, T. R., Reed, B. C., Brown, J. F., Ohlen, D. O., Zhu, Z., Yang, L., and Merchant, J. W.: Development of a global land cover characteristics database and IGBP DISCover from 1 km AVHRR data, International Journal of Remote Sensing, 21, 1303-1330, https://doi.org/10.1080/014311600210191, 2000.
Mann, H. B.: Nonparametric tests against trend, Econometrica: Journal of the Econometric Society, 245-259, http://dx.doi.org/10.2307/1907187, 1945.
Margono, B. A., Turubanova, S., Zhuravleva, I., Potapov, P., Tyukavina, A., Baccini, A., Goetz, S., and Hansen, M. C.: Mapping and monitoring deforestation and forest degradation in Sumatra (Indonesia) using Landsat time series data sets from 1990 to 2010, Environmental Research Letters, 7, 034010, https://doi.org/10.1088/1748-9326/7/3/034010, 2012.
Matthews, H. D., Weaver, A. J., Meissner, K. J., Gillett, N. P., and Eby, M.: Natural and anthropogenic climate change:

incorporating historical land cover change, vegetation dynamics and the global carbon cycle, Climate Dynamics, 22, 461-479, https://doi.org/10.1007/s00382-004-0392-2, 2004.

Oliver, M. A., and Webster, R.: Kriging: a method of interpolation for geographical information systems, International Journal of Geographical Information System, 4, 313-332, https://doi.org/10.1080/02693799008941549, 1990.

Pal, M.: Random forest classifier for remote sensing classification, International Journal of Remote Sensing, 26, 217-222, https://doi.org/10.1080/01431160412331269698, 2005.

Pekel, J.-F., Cottam, A., Gorelick, N., and Belward, A. S.: High-resolution mapping of global surface water and its long-term changes, Nature, 540, 418, https://doi.org/10.1038/nature20584, 2016.

Piao, S., Friedlingstein, P., Ciais, P., Zhou, L., and Chen, A.: Effect of climate and CO2 changes on the greening of the Northern Hemisphere over the past two decades, Geophysical Research Letters, 33, https://doi.org/10.1029/2006GL028205, 2006.

Pielke, R. A.: Land use and climate change, Science, 310, 1625-1626, https://doi.org/10.1126/science.1120529, 2005.

Pittman, K., Hansen, M. C., Becker-Reshef, I., Potapov, P. V., and Justice, C. O.: Estimating global cropland extent with multi-year MODIS data, Remote Sensing, 2, 1844-1863, https://doi.org/10.3390/rs2071844, 2010.

Qu, Y., Liu, Q., Liang, S., Wang, L., Liu, N., and Liu, S.: Direct-estimation algorithm for mapping daily land-surface broadband albedo from MODIS data, IEEE Transactions on Geoscience and Remote sensing, 52, 907-919, https://doi.org/10.1109/TGRS.2013.2245670, 2014.

Ramankutty, N., Graumlich, L., Achard, F., Alves, D., Chhabra, A., DeFries, R. S., Foley, J. A., Geist, H., Houghton, R. A., and Goldewijk, K. K.: Global land-cover change: Recent progress, remaining challenges, in: Land-use and land-cover change, Springer, 9-39, 2006.

Reyers, B., O'Farrell, P. J., Cowling, R. M., Egoh, B. N., Le Maitre, D. C., and Vlok, J. H. J.: Ecosystem services, land-cover change, and stakeholders: finding a sustainable foothold for a semiarid biodiversity hotspot, Ecology and Society, 14, http://www.ecologyandsociety.org/vol14/iss1/art38, 2009.

Rindfuss, R. R., Walsh, S. J., Turner, B. L., Fox, J., and Mishra, V.: Developing a science of land change: challenges and methodological issues, Proceedings of the National Academy of Sciences, 101, 13976-13981, https://doi.org/10.1073/pnas.0401545101, 2004.

Rodriguez-Galiano, V. F., Ghimire, B., Rogan, J., Chica-Olmo, M., and Rigol-Sanchez, J. P.: An assessment of the effectiveness of a random forest classifier for land-cover classification, ISPRS Journal of Photogrammetry and Remote Sensing, 67, 93-104, https://doi.org/10.1016/j.isprsjprs.2011.11.002, 2012.

Rogan, J., and Chen, D.: Remote sensing technology for mapping and monitoring land-cover and land-use change, Progress in planning, 61, 301-325, https://doi.org/10.1016/S0305-9006(03)00066-7, 2004.

Running, S. W.: Ecosystem disturbance, carbon, and climate, Science, 321, 652-653, https://doi.org/10.1126/science.1159607, 2008.

Schneider, A., Friedl, M. A., and Potere, D.: Mapping global urban areas using MODIS 500-m data: New methods and datasets based on 'urban ecoregions', Remote Sensing of Environment, 114, 1733-1746, https://doi.org/10.1016/j.rse.2010.03.003, 2010.

Sen, P. K.: Estimates of the regression coefficient based on Kendall's tau, Journal of the American statistical association, 63, 1379-1389, https://doi.org/10.1080/01621459.1968.10480934, 1968.

Seto, K. C., Fragkias, M., Güneralp, B., and Reilly, M. K.: A meta-analysis of global urban land expansion, PloS one, 6, e23777, https://doi.org/10.1371/journal.pone.0023777, 2011.

Simons, H., Soto, X., Zhu, Z., Singh, K. D., Bellan, M.-F., Iremonger, S., Hirvonen, H., Smith, B., Watson, V., and Tosi, J.: Global ecological zoning for the global forest resources assessment 2000-final report, 2001.

Song, X.-P., Hansen, M. C., Stehman, S. V., Potapov, P. V., Tyukavina, A., Vermote, E. F., and Townshend, J. R.: Global land change from 1982 to 2016, Nature, 560, 639, https://doi.org/10.1038/s41586-018-0411-9, 2018a.

Song, Z., Liang, S., Wang, D., Zhou, Y., and Jia, A.: Long-term record of top-of-atmosphere albedo over land generated from AVHRR data, Remote Sensing of Environment, 211, 71-88, https://doi.org/10.1016/j.rse.2018.03.044, 2018b.

Sterling, S. M., Ducharne, A., and Polcher, J.: The impact of global land-cover change on the terrestrial water cycle,

Nature Climate Change, 3, 385, https://doi.org/10.1038/nclimate1690, 2013.
Sulla-Menashe, D., Gray, J. M., Abercrombie, S. P., and Friedl, M. A.: Hierarchical mapping of annual global land cover 2001 to present: The MODIS Collection 6 Land Cover product, Remote sensing of environment, 222, 183-194, https://doi.org/10.1016/j.rse.2018.12.013, 2019.
Tucker, C. J., Townshend, J. R. G., and Goff, T. E.: African land-cover classification using satellite data, Science, 227, 369-375, https://doi.org/10.1126/science.227.4685.369, 1985.
Turner, B. L., Lambin, E. F., and Reenberg, A.: The emergence of land change science for global environmental change and sustainability, Proceedings of the National Academy of Sciences, 104, 20666-20671, https://doi.org/10.1073/pnas.0704119104, 2007.
Turner, M. G., O'Neill, R. V., Gardner, R. H., and Milne, B. T.: Effects of changing spatial scale on the analysis of landscape pattern, Landscape ecology, 3, 153-162, https://doi.org/10.1007/BF00131534, 1989.
Verburg, P. H., Van De Steeg, J., Veldkamp, A., and Willemen, L.: From land cover change to land function dynamics: a major challenge to improve land characterization, Journal of environmental management, 90, 1327-1335, https://doi.org/10.1016/j.jenvman.2008.08.005, 2009.
Wang, C., Gao, Q., Wang, X., and Yu, M.: Spatially differentiated trends in urbanization, agricultural land abandonment and reclamation, and woodland recovery in Northern China, Scientific reports, 6, 37658, https://doi.org/10.1038/srep37658, 2016.
Wang, J., Zhao, Y., Li, C., Yu, L., Liu, D., and Gong, P.: Mapping global land cover in 2001 and 2010 with spatial-temporal consistency at 250 m resolution, ISPRS Journal of Photogrammetry and Remote Sensing, 103, 38-47, https://doi.org/10.1016/j.isprsjprs.2014.03.007, 2015.
Wood, E. F., Roundy, J. K., Troy, T. J., Van Beek, L. P. H., Bierkens, M. F. P., Blyth, E., de Roo, A., Döll, P., Ek, M., and Famiglietti, J.: Hyperresolution global land surface modeling: Meeting a grand challenge for monitoring Earth's terrestrial water, Water Resources Research, 47, https://doi.org/10.1029/2010WR010090, 2011.
Wulder, M. A., White, J. C., Goward, S. N., Masek, J. G., Irons, J. R., Herold, M., Cohen, W. B., Loveland, T. R., and Woodcock, C. E.: Landsat continuity: Issues and opportunities for land cover monitoring, Remote Sensing of Environment, 112, 955-969, https://doi.org/1016/j.rse.2007.07.004, 2008.
Xiao, Z., Liang, S., Sun, R., Wang, J., and Jiang, B.: Estimating the fraction of absorbed photosynthetically active radiation from the MODIS data based GLASS leaf area index product, Remote Sensing of Environment, 171, 105-117, https://doi.org/10.1016/j.rse.2015.10.016, 2015.
Xiao, Z., Liang, S., Wang, J., Xiang, Y., Zhao, X., and Song, J.: Long-time-series global land surface satellite leaf area inde. Product Derived From MODIS and AVHRR Surface Reflectance, IEEE Trans. Geoscience and Remote Sensing, 54, 5301-5318, https://doi.org/10.1109/TGRS.2016.2560522, 2016.
Xie, S., Liu, L., Zhang, X., and Chen, X.: Annual land-cover mapping based on multi-temporal cloud-contaminated landsat images, International Journal of Remote Sensing, 1-23, https://doi.org/10.1080/01431161.2018.1553320, 2018.
Xu, Y., Yu, L., Zhao, F. R., Cai, X., Zhao, J., Lu, H., and Gong, P.: Tracking annual cropland changes from 1984 to 2016 using time-series Landsat images with a change-detection and post-classification approach: Experiments from three sites in Africa, Remote Sensing of Environment, 218, 13-31, https://doi.org/10.1016/j.rse.2018.09.008, 2018.
Yang, J., Peng, G., Rong, F., Zhang, M., Chen, J., Liang, S., Bing, X., Shi, J., and Dickinson, R.: The role of satellite remote sensing in climate change studies, Nature Climate Change, 3, 875-883, https://doi.org/10.1038/nclimate1908, 2013.
Yao, Y., Liang, S., Li, X., Hong, Y., Fisher, J. B., Zhang, N., Chen, J., Cheng, J., Zhao, S., and Zhang, X.: Bayesian multimodel estimation of global terrestrial latent heat flux from eddy covariance, meteorological, and satellite observations, Journal of Geophysical Research: Atmospheres, 119, 4521-4545, https://doi.org/10.1002/2013JD020864, 2014.
Ying, Q., Hansen, M. C., Potapov, P. V., Tyukavina, A., Wang, L., Stehman, S. V., Moore, R., and Hancher, M.: Global bare ground gain from 2000 to 2012 using Landsat imagery, Remote sensing of environment, 194, 161-176, https://doi.org/10.1016/j.rse.2017.03.022, 2017.
Yuan, F., Sawaya, K. E., Loeffelholz, B. C., and Bauer, M. E.: Land cover classification and change analysis of the Twin Cities (Minnesota) Metropolitan Area by multitemporal Landsat remote sensing, Remote sensing of Environment, 98,

317-328, https://doi.org/10.1016/j.rse.2005.08.006, 2005.
Yuan, W., Liu, S., Yu, G., Bonnefond, J.-M., Chen, J., Davis, K., Desai, A. R., Goldstein, A. H., Gianelle, D., and Rossi, F.: Global estimates of evapotranspiration and gross primary production based on MODIS and global meteorology data, Remote Sensing of Environment, 114, 1416-1431, https://doi.org/10.1016/j.rse.2010.01.022, 2010.
Zhang, Q., and Seto, K. C.: Mapping urbanization dynamics at regional and global scales using multi-temporal DMSP/OLS nighttime light data, Remote Sensing of Environment, 115, 2320-2329, https://doi.org/10.1016/j.rse.2011.04.032, 2011.
Zhao, M., Pitman, A. J., and Chase, T.: The impact of land cover change on the atmospheric circulation, Climate Dynamics, 17, 467-477, https://doi.org/10.1038/nclimate3004, 2001.

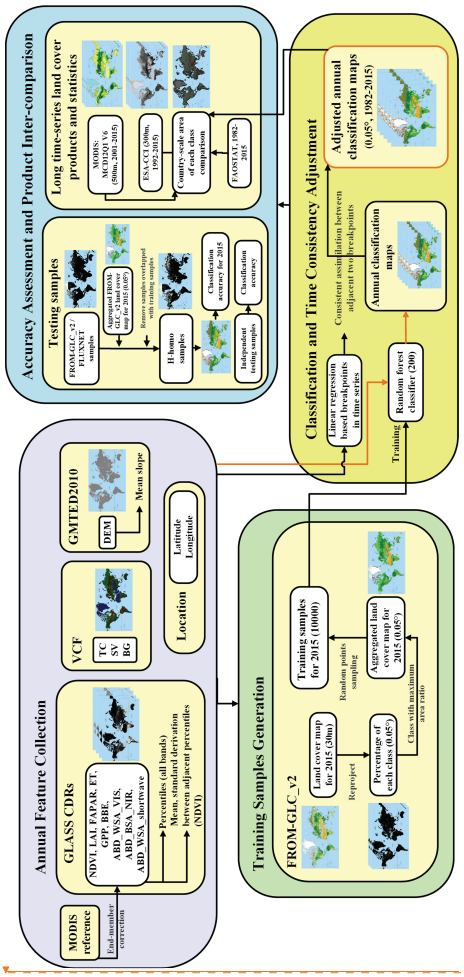

Figure 1: The framework for building GLASS-GLC (annual dynamics of global land cover) CDRs (Climate Data Records).

1485

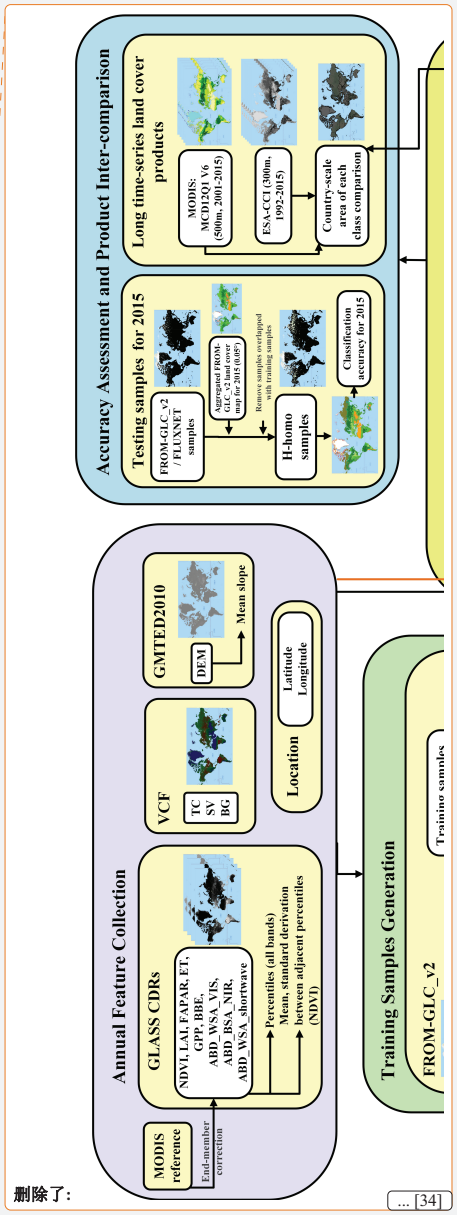

Table 1: Classification system, with 7 Level 1 classes and 21 Level 2 classes.

Level 1 class	Level 2 class	Description
Cropland	Rice paddy	—
	Greenhouse	—
	Other farmland	—
	Orchard	—
	Bare farmland	—
Forest	Broadleaf, leaf-on	Tree cover≥10%; Height≥5m; For mixed leaf, neither coniferous nor broadleaf types exceed 60%
	Broadleaf, leaf-off	
	Needle-leaf, leaf-on	
	Needle-leaf, leaf-off	
	Mixed leaf type, leaf-on	
	Mixed leaf type, leaf-off	
Grassland	Pasture, leaf-on	Canopy cover≥20%
	Natural grassland, leaf-on	
	Grassland, leaf-off	
Shrubland	Shrub cover, leaf-on	Canopy cover≥20%; Height≤5m
	Shrub cover, leaf-off	
Tundra	Shrub and brush tundra	
	Herbaceous tundra	
Barren land	Barren land	Vegetation cover<10%
Snow/Ice	Snow	
	Ice	

设置了格式: 字体颜色: 文字 1

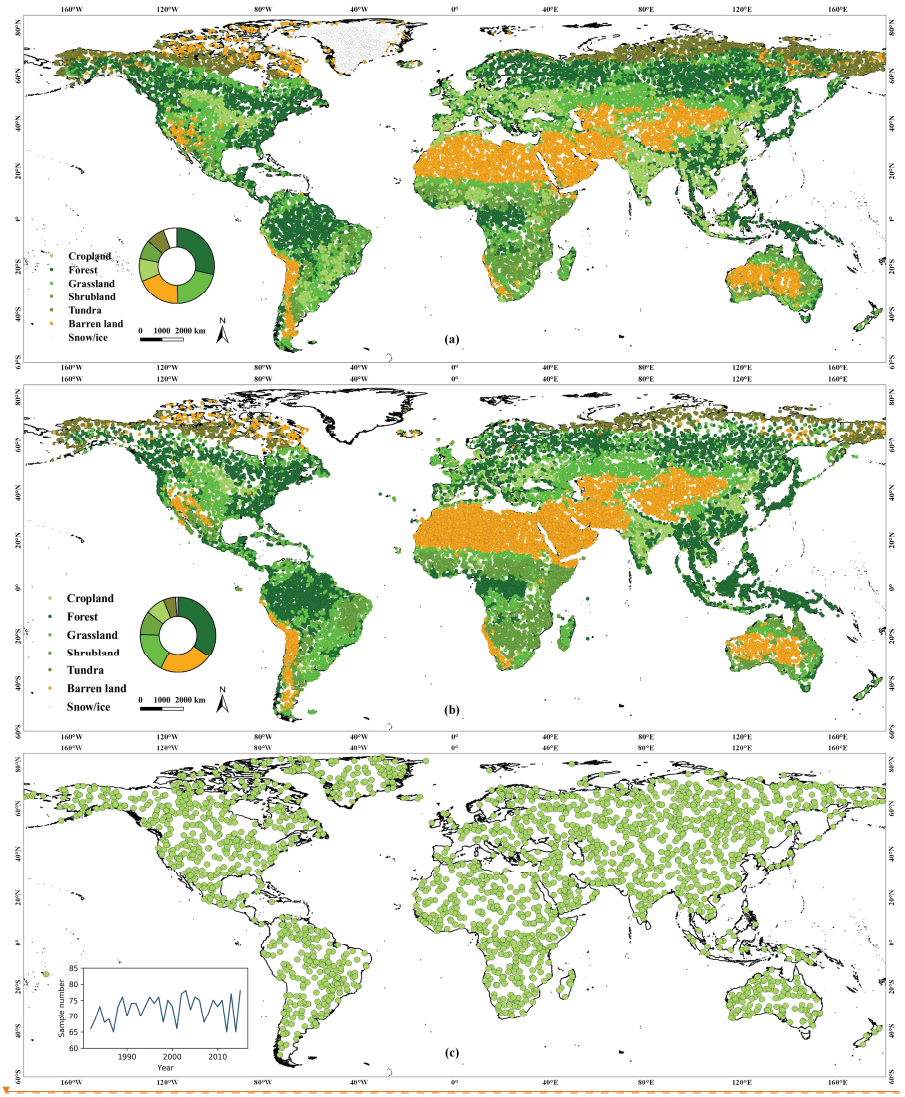

Figure 2: The geographical distribution training and test sample. (a) training sample in 2015, where different colors represent the different classes. (b) huge homogeneous test samples (H-homo sample) in 2015, where the different colors represent the source of the sample units, either FROM-GLC v2 or FLUXNET. (c) independent test sample in different years, where the temporal distribution is shown in the inner chart.

删除了:

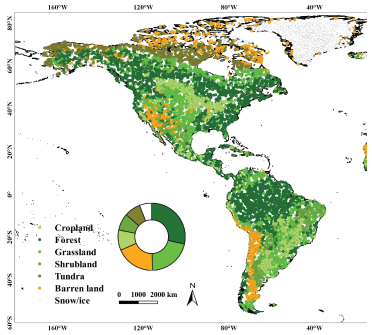

删除了: The geographical distribution of

删除了: s

删除了: years

设置了格式: 字体: 小五, 字体颜色: 自动设置

删除了: 分页符

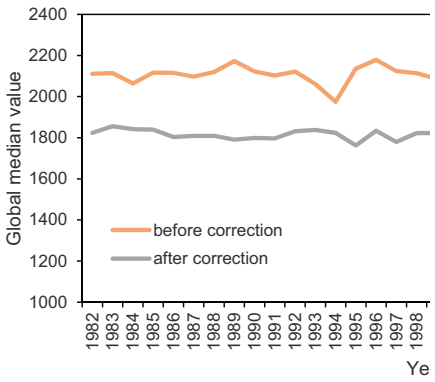

Figure 3: Global median value time series of GLASS ABD_WSA_VIS before and after the end-member correction with reference to MODIS.

Table 2: The explanatory table of the constructed feature collection, with a total 81 features each year.

Product	Band	Feature	Number of features
GLASS CDR, 0.05 °, 1982-2015	NDVI LAI FAPAR ET GPP	Percentiles [0, 10, 25, 50, 75, 90, 100] of all 10 bands	63
	BBE ABD_WSA_VIS ABD_BSA_NIR ABD_WSA_shortwave	Mean, standard derivation of NDVI between adjacent two percentiles of NDVI	12
VCF, 0.05 °, 1982-2015	TC SV BG	TC SV BG	3
GMTED2010, 7.5 s, 2010	DEM	Mean slope in each 0.05 ° pixel	1
Location	Latitude, longitude	Center latitude, longitude of each 0.05 ° pixel	2
Total number of features			81

删除了: 分页符

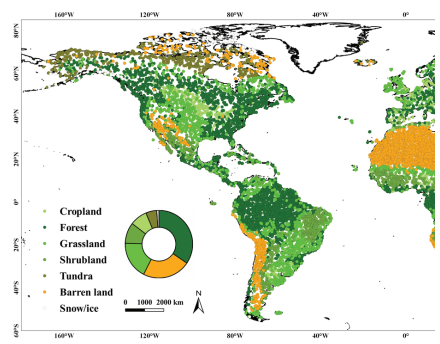

Figure 4: The geographical distribution of different types of huge homogeneous test samples (H-homo sample), where the different colors represent the source of the sample units, either FROM-GLC_v2 or FLUXNET.

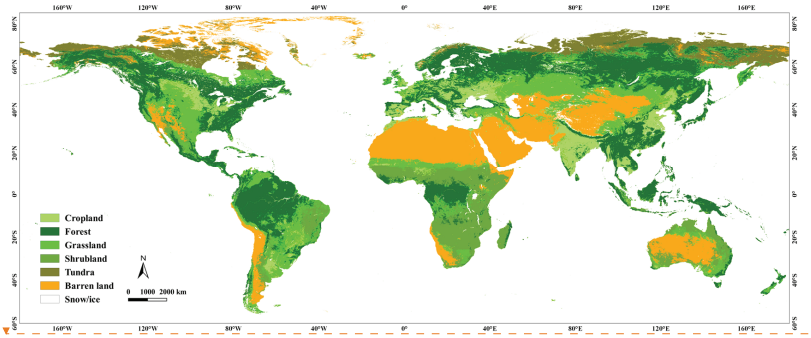

Figure 3: GLASS-GLC (annual dynamics of global land cover) CDRs (Climate Data Records) result in 2015.

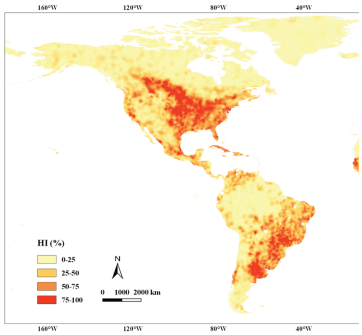

删除了:

Figure 5: The geographical distribution of the spatial interpolation results of human impact where the darker color indicates a value closer to 100 and a higher human impact. .

分页符

.

带格式的: 左, 行距: 单倍行距, 孤行控制

删除了: 6

Table 3: Classification accuracy of GLASS-GLC in 2015 based on FROM-GLC_v2 test samples. (Overall accuracy = 86.51 %, UA = User's Accuracy and PA = Producer's Accuracy)

Class	Cropland	Forest	Grassland	Shrubland	Tundra	Barren land	Snow/ice	Total	UA
Cropland	**1390**	166	221	101	0	12	0	1890	73.54 %
Forest	115	**7427**	279	145	18	0	3	7987	92.99 %
Grassland	199	431	**2820**	534	45	141	3	4173	67.58 %
Shrubland	47	65	185	**1986**	0	92	0	2375	83.62 %
Tundra	0	32	36	0	**1157**	24	2	1251	92.49 %
Barren land	17	5	91	27	48	**5336**	20	5544	96.25 %
Snow/ice	0	2	10	0	7	41	**179**	239	74.90 %
Total	1768	8128	3642	2793	1275	5646	207	**23459**	
PA	78.62 %	91.38 %	77.43 %	71.11 %	90.75 %	94.51 %	86.47 %		**86.51 %**

设置了格式：字体颜色: 文字 1

删除了：.

Table 4: Classification accuracy of GLASS-GLC in 2015 based on FLUXNET test samples. (Overall accuracy = 82.10 %, UA = User's Accuracy and PA = Producer's Accuracy)

Class	Cropland	Forest	Grassland	Shrubland	Tundra	Barren land	Snow/ice	Total number	UA
Cropland	**63**	5	17	1	0	0	0	86	73.26 %
Forest	13	**243**	9	2	0	0	0	267	91.01 %
Grassland	8	21	**91**	2	0	2	0	124	73.39 %
Shrubland	7	3	0	**19**	0	0	0	29	65.52 %
Tundra	0	3	0	0	**14**	0	0	17	82.35 %
Barren land	0	1	0	0	0	**1**	0	2	50.00 %
Snow/ice	0	0	0	0	0	0	**0**	0	-
Total number	91	276	117	24	14	3	0	**525**	
PA	69.23 %	88.04 %	77.78 %	79.17 %	100.00 %	33.33 %	-		**82.10 %**

删除了: testing sample

删除了: 分页符

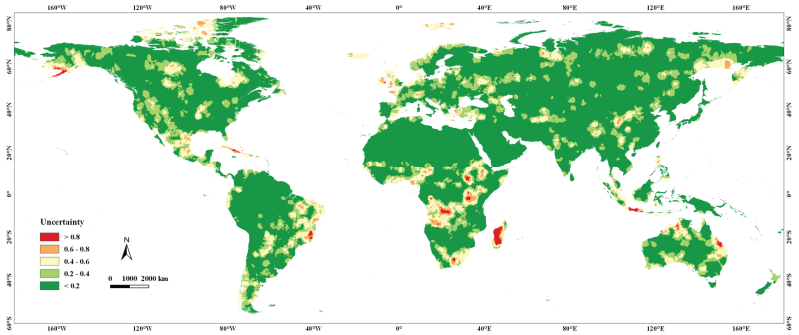

Figure 4: The geographical distribution of uncertainty for GLASS-GLC (annual dynamics of global land cover) CDRs (Climate Data Records) in 2015, where regions in red represent higher uncertainty levels while those in green represent lower uncertainty levels.

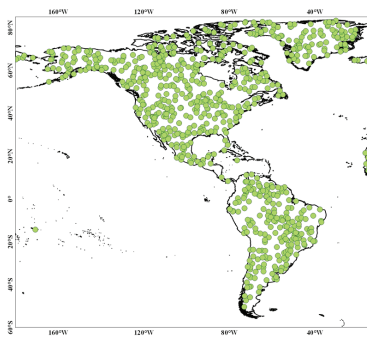

删除了:

Figure 4: The geographical distribution of random test samples. .

分页符

.

Table 4: Classification accuracy without change detection under 2431 independent testing samples. (Overall accuracy = 81.28 %, UA = User's Accuracy and PA = Producer's Accuracy) .

Class

... [35]

设置了格式: 字体颜色: 文字 1

设置了格式: 字体颜色: 文字 1

设置了格式: 字体颜色: 文字 1

设置了格式: 字体颜色: 文字 1

带格式表格

设置了格式: 字体颜色: 文字 1

删除了: 7

Table 5: Classification accuracy of GLASS-GLC without change detection under independent test samples. (Overall accuracy = 81.28 %, UA = User's Accuracy and PA = Producer's Accuracy)

Class	Cropland	Forest	Grassland	Shrubland	Tundra	Barren land	Snow/ice	Total number	UA
Cropland	**257**	21	34	15	0	31	0	358	71.79%
Forest	35	**620**	45	27	22	1	1	751	82.56%
Grassland	17	26	**248**	12	3	19	4	329	75.38%
Shrubland	7	6	10	**154**	9	12	0	198	77.78%
Tundra	0	9	11	12	**250**	3	0	285	87.72%
Barren land	4	1	13	14	5	**355**	6	398	89.20%
Snow/ice	0	4	3	0	0	13	**92**	112	82.14%
Total number	320	687	364	234	289	434	103	**2431**	
PA	80.31%	90.25%	68.13%	65.81%	86.51%	81.80%	89.32%		**81.28%**

设置了格式: 字体颜色: 文字 1
删除了: testing sample
设置了格式: 字体颜色: 文字 1
设置了格式: 字体颜色: 文字 1
设置了格式: 字体颜色: 文字 1
设置了格式: 字体颜色: 文字 1
设置了格式: 字体: 加粗, 字体颜色: 文字 1
设置了格式: 字体颜色: 文字 1
设置了格式: 字体颜色: 文字 1
设置了格式: 字体: 加粗, 字体颜色: 文字 1
设置了格式: 字体颜色: 文字 1
设置了格式: 字体颜色: 文字 1
设置了格式: 字体: 加粗, 字体颜色: 文字 1
设置了格式: 字体颜色: 文字 1
设置了格式: 字体颜色: 文字 1
设置了格式: 字体: 加粗, 字体颜色: 文字 1
设置了格式: 字体颜色: 文字 1
设置了格式: 字体颜色: 文字 1
设置了格式: 字体: 加粗, 字体颜色: 文字 1
设置了格式: 字体颜色: 文字 1
设置了格式: 字体颜色: 文字 1
设置了格式: 字体: 加粗, 字体颜色: 文字 1
设置了格式: 字体颜色: 文字 1
设置了格式: 字体颜色: 文字 1
设置了格式: 字体: 加粗, 字体颜色: 文字 1
设置了格式: 字体颜色: 文字 1
设置了格式: 字体颜色: 文字 1
设置了格式: 字体颜色: 文字 1
设置了格式: 字体: 加粗, 字体颜色: 文字 1
设置了格式: 字体颜色: 文字 1
设置了格式: 字体: 加粗, 字体颜色: 文字 1
设置了格式: 字体颜色: 文字 1

Table 6: Classification accuracy of GLASS-GLC with change detection under independent test samples. (Overall accuracy =82.81 %, UA = User's Accuracy and PA = Producer's Accuracy)

Class	Cropland	Forest	Grassland	Shrubland	Tundra	Barren land	Snow/ice	Total number	UA
Cropland	**262**	19	32	20	0	25	0	358	73.18%
Forest	33	**637**	29	28	24	0	0	751	84.82%
Grassland	24	24	**254**	6	13	8	0	329	77.20%
Shrubland	12	3	11	**159**	6	7	0	198	80.30%
Tundra	0	12	9	4	**250**	10	0	285	87.72%
Barren land	5	1	17	8	7	**357**	3	398	89.70%
Snow/ice	0	5	6	0	0	7	**94**	112	83.93%
Total number	336	701	358	225	300	414	97	**2431**	
PA	77.98%	90.87%	70.95%	70.67%	83.33%	86.23%	96.91%		**82.81%**

删除了: 7
删除了: testing sample
设置了格式: 字体颜色: 文字 1
设置了格式: 字体颜色: 文字 1
设置了格式: 字体颜色: 文字 1
设置了格式: 字体颜色: 文字 1
设置了格式: 字体颜色: 文字 1
设置了格式: 字体: 加粗, 字体颜色: 文字 1
设置了格式: 字体颜色: 文字 1
设置了格式: 字体颜色: 文字 1
设置了格式: 字体: 加粗, 字体颜色: 文字 1
设置了格式: 字体颜色: 文字 1
设置了格式: 字体颜色: 文字 1
设置了格式: 字体: 加粗, 字体颜色: 文字 1
设置了格式: 字体颜色: 文字 1
设置了格式: 字体颜色: 文字 1
设置了格式: 字体: 加粗, 字体颜色: 文字 1
设置了格式: 字体颜色: 文字 1
设置了格式: 字体颜色: 文字 1
设置了格式: 字体: 加粗, 字体颜色: 文字 1
设置了格式: 字体颜色: 文字 1
设置了格式: 字体颜色: 文字 1
设置了格式: 字体: 加粗, 字体颜色: 文字 1
设置了格式: 字体颜色: 文字 1
设置了格式: 字体颜色: 文字 1
设置了格式: 字体: 加粗, 字体颜色: 文字 1
设置了格式: 字体颜色: 文字 1
设置了格式: 字体颜色: 文字 1
设置了格式: 字体颜色: 文字 1
设置了格式: 字体: 加粗, 字体颜色: 文字 1
设置了格式: 字体颜色: 文字 1
设置了格式: 字体: 加粗, 字体颜色: 文字 1
设置了格式: 字体颜色: 文字 1

Table 7: Classification accuracy of the MODIS-based land cover product in 2015 based on FLUXNET test samples. (Overall accuracy = 82.10 %, UA = User's Accuracy and PA = Producer's Accuracy)

Class	Cropland	Forest	Grassland	Shrubland	Tundra	Barren land	Snow/ice	Total number	UA
Cropland	**7**	5	73	0	0	0	0	85	8.24%
Forest	1	**261**	5	0	0	0	0	267	97.75%
Grassland	1	15	**108**	1	0	0	0	125	86.40%
Shrubland	0	9	9	**11**	0	0	0	29	37.93%
Tundra	0	3	6	8	**0**	0	0	17	-
Barren land	0	0	1	0	0	**1**	0	2	50.00%
Snow/ice	0	0	0	0	0	0	**0**	0	-
Total number	9	293	202	20	0	1	0	**525**	
PA	77.78%	89.08%	53.47%	55.00%	-	100.00%	-		**73.90%**

删除了: 7

设置了格式: 字体颜色: 文字 1

设置了格式: 字体颜色: 文字 1

设置了格式: 字体颜色: 文字 1

设置了格式: 字体颜色: 文字 1

设置了格式: 字体颜色: 文字 1

设置了格式: 字体颜色: 文字 1

设置了格式: 字体颜色: 文字 1

设置了格式: 字体颜色: 文字 1

设置了格式: 字体颜色: 文字 1

Table 8: Classification accuracy of the ESA-CCI land cover product in 2015 based on FLUXNET test samples. (Overall accuracy = 82.10 %, UA = User's Accuracy and PA = Producer's Accuracy)

Class	Cropland	Forest	Grassland	Shrubland	Tundra	Barren land	Snow/ice	Total number	UA
Cropland	**81**	1	4	0	0	0	0	86	94.19%
Forest	11	**246**	4	5	0	1	0	267	92.13%
Grassland	28	7	**76**	5	0	8	0	124	61.29%
Shrubland	2	7	1	**19**	0	0	0	29	65.52%
Tundra	0	3	9	0	**0**	5	0	17	-
Barren land	0	0	2	0	0	**0**	0	2	0.00%
Snow/ice	0	0	0	0	0	0	**0**	0	-
Total number	122	264	96	29	0	14	0	**525**	
PA	66.39%	93.18%	79.17%	65.52%	-	0.00%	-		**80.38%**

带格式的: 题注, 与下段同页

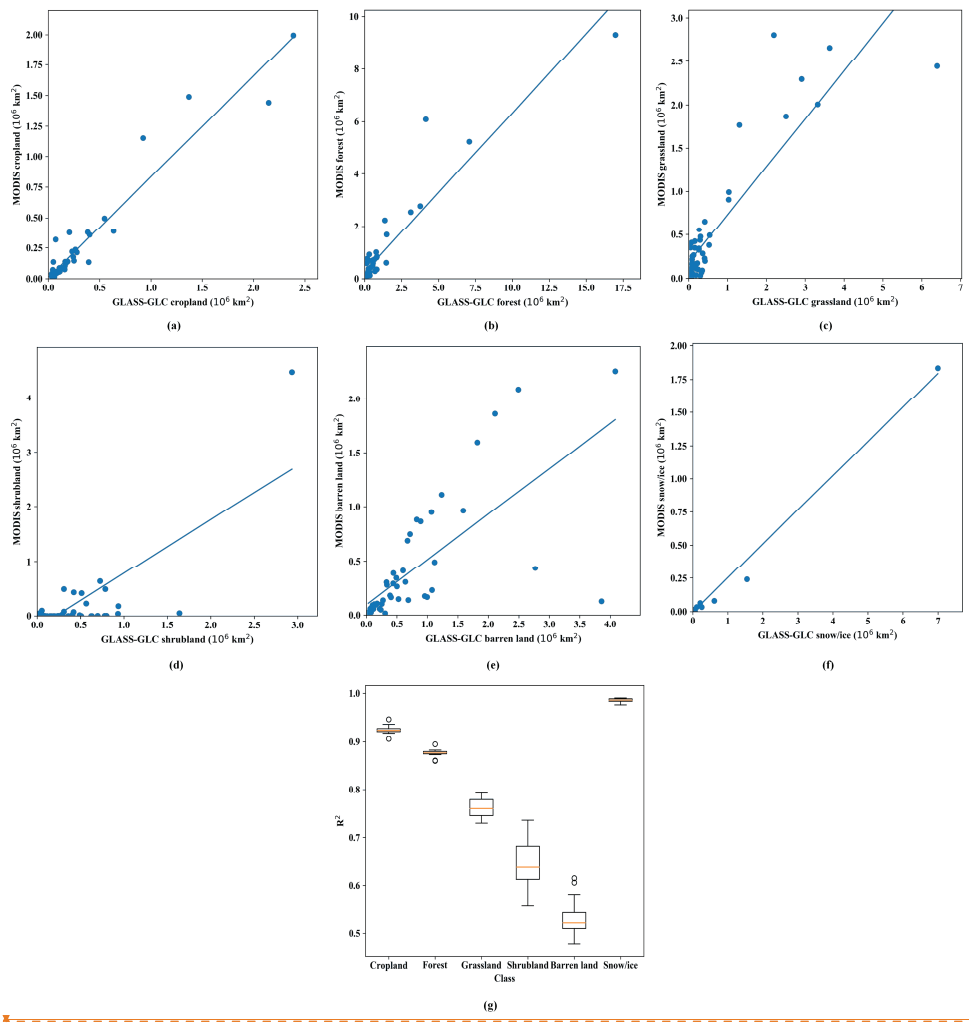

Figure 5: Inter-comparison with the MODIS-based land cover product, (a) cropland circa 2015, (b) forest circa 2015, (c) grassland circa 2015, (d) shrubland circa 2015, (e) barren land circa 2015 and (f) snow/ice circa 2015; (g) mean R2 of the annual linear fit lines for all years (2001-2015).

删除了: ----------分页符----------

设置了格式: 字体颜色: 文字 1

设置了格式: 字体颜色: 文字 1

带格式的: 题注

设置了格式: 字体颜色: 文字 1

设置了格式: 字体: 小五, 字体颜色: 文字 1

设置了格式: 字体颜色: 文字 1

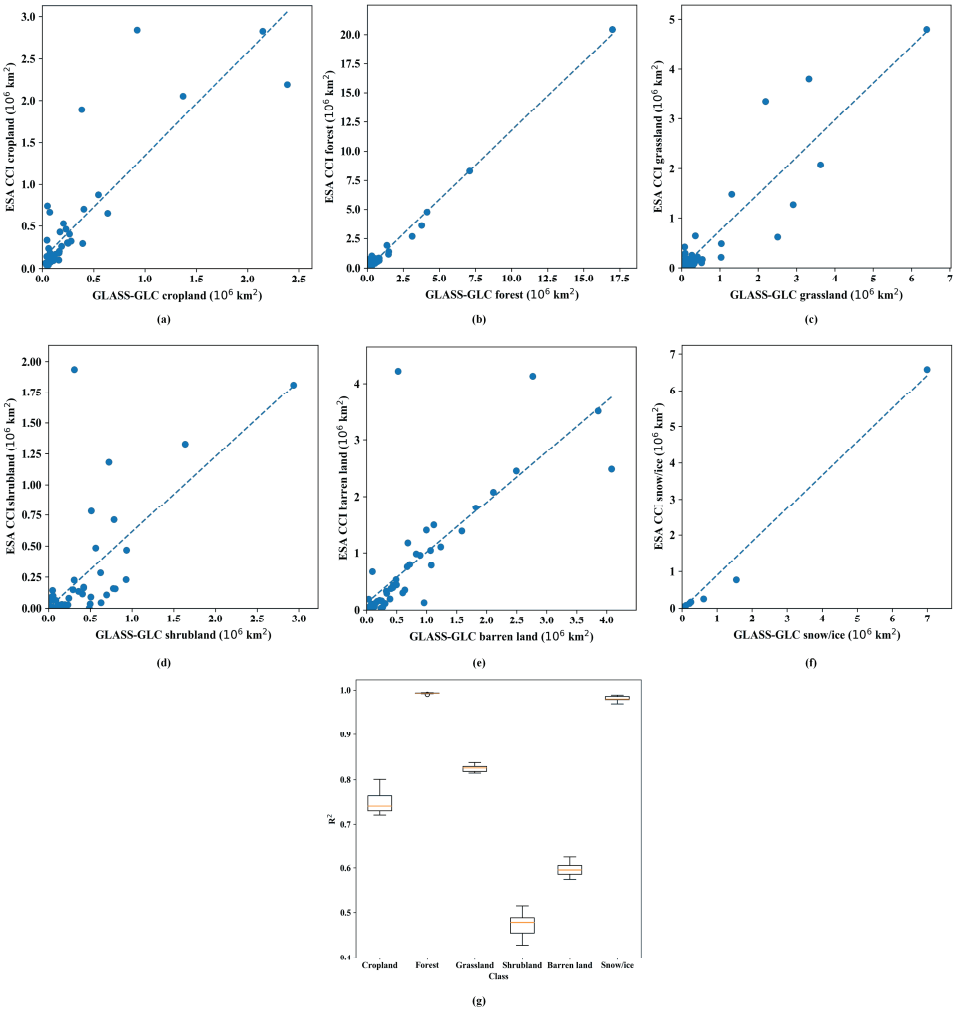

Figure 6: Inter-comparison with the ESA-CCI land cover product, (a) cropland circa 2015, (b) forest circa 2015, (c) grassland circa 2015, (d) shrubland circa 2015, (e) barren land circa 2015 and (f) snow/ice circa 2015; (g) mean R2 of the annual linear fit lines for all years (1992-2015).

带格式的：与下段同页

设置了格式：字体颜色：文字 1

设置了格式：字体颜色：文字 1

设置了格式：字体：小五，字体颜色：文字 1

带格式的：题注

设置了格式：字体颜色：文字 1

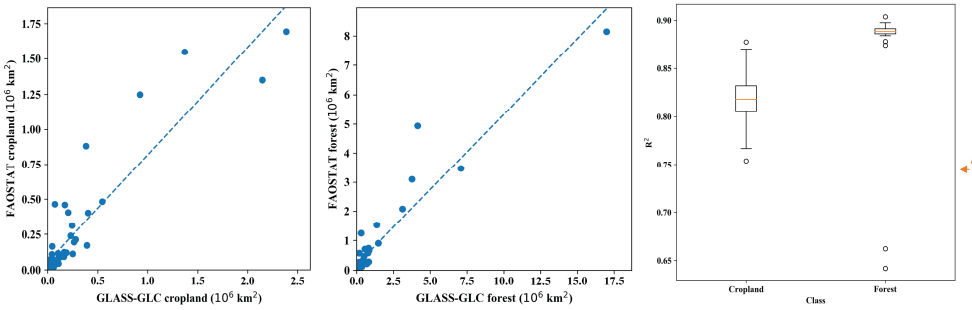

Figure 7: Inter-comparison with the FAOSTAT data set, (a) cropland circa 2015, (b) forest circa 2015, (c) mean R2 of the annual linear fit lines of cropland for years 1982-2015 and forest for years 1990-2015.

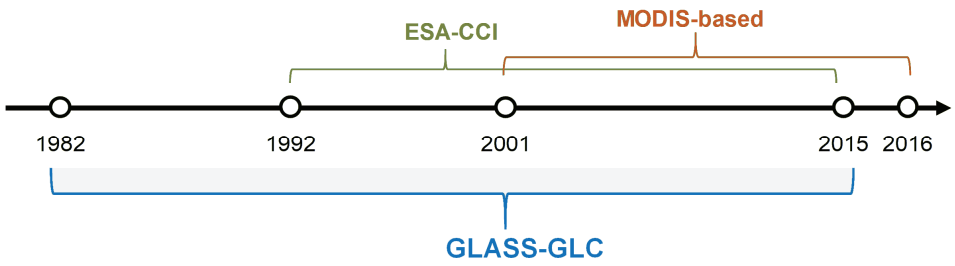

Figure 8: The duration of different land cover products, including GLASS-GLC, MODIS-based land cover products and ESA-CCI land cover products.

带格式的: 左

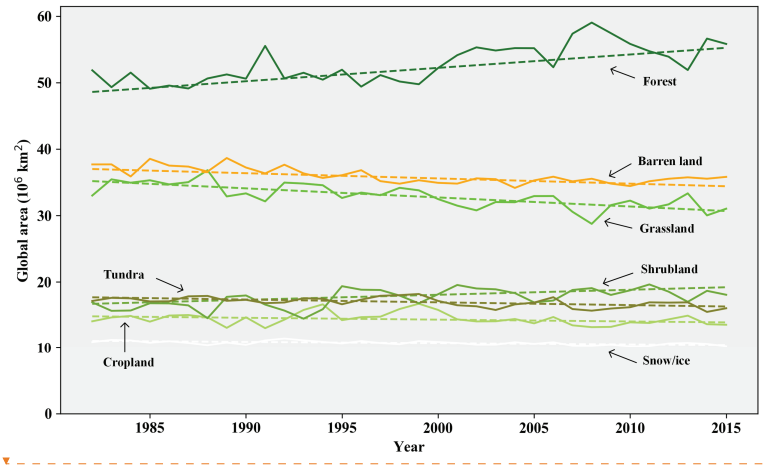

Figure 9: Area curves of global annual land cover change from 1982 to 2015.

删除了：.

删除了: 8

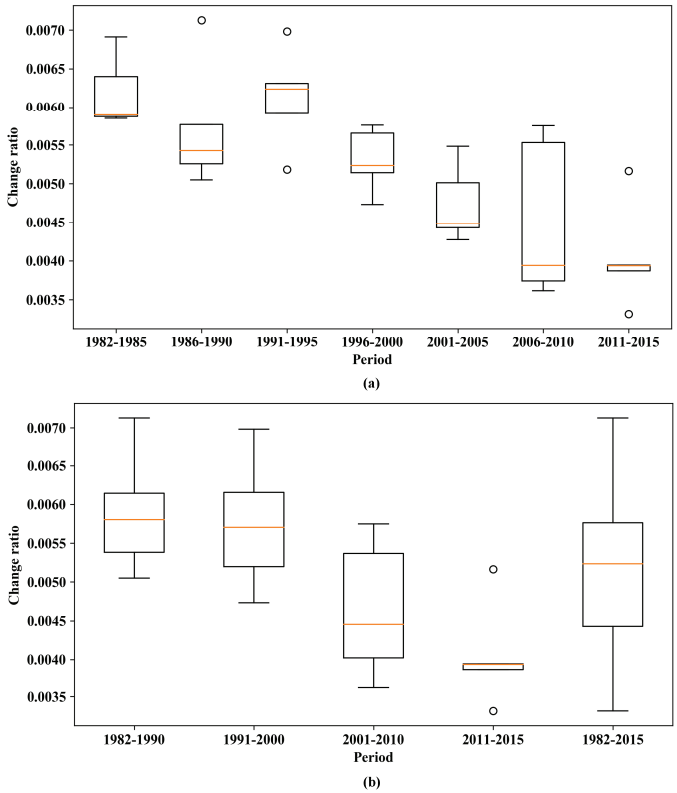

Figure 10: Comparison and distribution of ratios of annual global land cover change (LCC) to the global total terrestrial land cover (LC) area by different time periods and time intervals (a) 5-year interval, (b) 10-year interval. The box extends from the first quartile (Q1) to third quartile (Q3) values of the data, with a orange line at the median. The upper whisker extends to last datum less than Q3 + 1.5 * IQR, and the lower whisker extends to the first datum greater than Q1 - 1.5 * IQR. Flier points are those past the end of the whiskers.

删除了: 9

删除了:

设置了格式: 英语(美国)

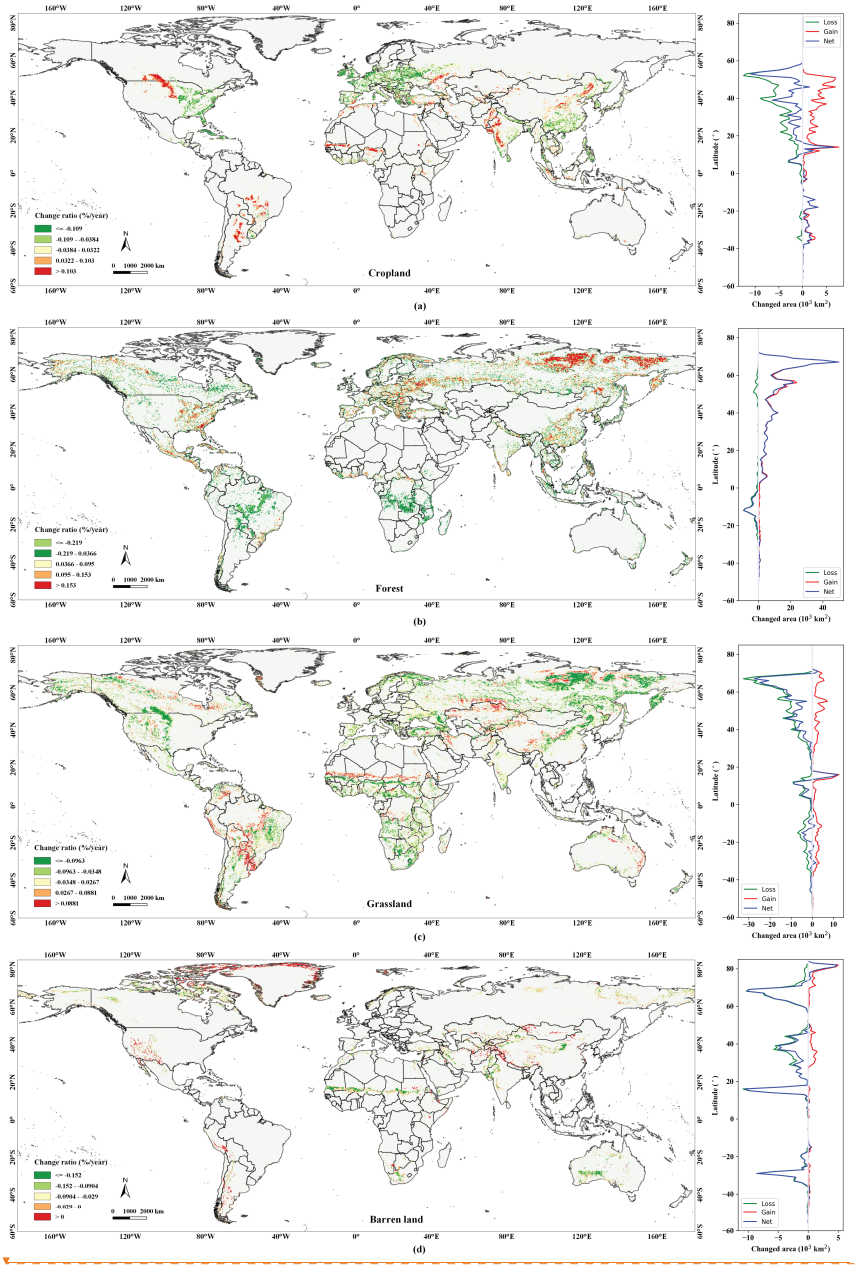

删除了：

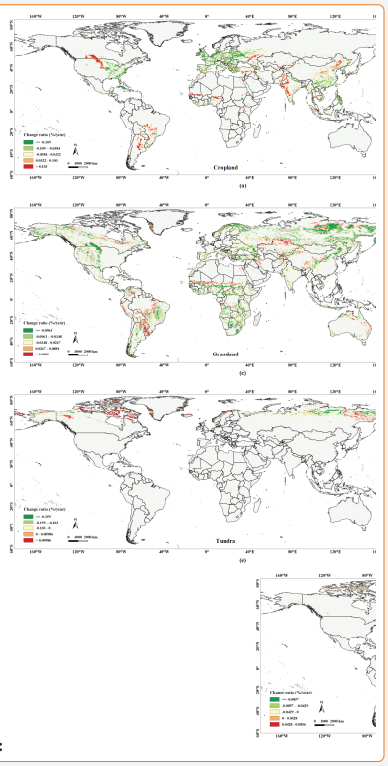

Figure 11: The geographical distribution of global regions with significant land cover change during 1982-2015, and the summarized results along latitudinal gradients for each class, (a) cropland, (b) forest, (c) grassland and (d) barren land.

删除了: 10

删除了: , (d) shrubland, (e) tundra,

删除了: f

删除了: and (g) snow/ice

删除了: .

Table 9: Statistical results of change analysis for cropland (on the scale of continents). Annual change slope and its 95 % confidence interval are given by Thei-sen estimator, p-value and trend information from a Mann-Kendall test. Gain and Loss areas are summarized results relating to the whole time series.

Continent	Slope (10^3 km^2/year)	Lower (10^3 km^2/year)	Upper (10^3 km^2/year)	p	Trend	Gain (10^3 km^2)	Loss (10^3 km^2)
Africa	5.3	1.5	10.0	0.0099	increasing	23	-6
Asia	-1.7	-9.2	7.1	0.6999	no trend	67	-70
Europe	-30.4	-43.6	-17.9	0.0005	decreasing	12	-99
North America	-4.9	-10.9	2.8	0.1635	no trend	37	-54
South America	9.1	2.1	19.3	0.0108	increasing	35	-4
Oceania	-0.5	-1.8	0.6	0.3580	no trend	1	-1
Global	-27.5	-54.7	3.1	0.0968	no trend	175	-238

1620

Table 10: Statistical results of change analysis for forest (on the scale of continents) . Annual change slope and its 95 % confidence interval are given by Thei-sen estimator, p-value and trend information from a Mann-Kendall test. Gain and Loss areas are summarized results relating to the whole time series.

Continent	Slope (10^3 km^2/year)	Lower (10^3 km^2/year)	Upper (10^3 km^2/year)	p	Trend	Gain (10^3 km^2)	Loss (10^3 km^2)
Africa	-8.4	-18.6	2.6	0.1463	no trend	15	-29
Asia	128.6	86.8	165.0	0.0000	increasing	365	-12
Europe	53.1	34.9	67.4	0.0000	increasing	131	-1
North America	45.1	24.7	65.0	0.0000	increasing	132	-16
South America	-10.8	-19.6	-1.4	0.0242	decreasing	23	-49
Oceania	1.4	-0.1	2.6	0.0802	no trend	6	-1
Global	201.3	120.9	278.1	0.0000	increasing	680	-109

Table 11: Statistical results of change analysis for grassland (on the scale of continents) . Annual change slope and its 95 % confidence interval are given by Thei-sen estimator, p-value and trend information from a Mann-Kendall test. Gain and Loss areas are summarized results relating to the whole time series.

Continent	Slope (10^3 km^2/year)	Lower (10^3 km^2/year)	Upper (10^3 km^2/year)	p	Trend	Gain (10^3 km^2)	Loss (10^3 km^2)
Africa	-18.9	-36.4	3.0	0.0855	no trend	50	-108
Asia	-52.7	-67.1	-38.1	0.0000	decreasing	85	-315
Europe	-11.8	-21.7	-2.0	0.0207	decreasing	6	-59
North America	-39.6	-48.4	-26.9	0.0000	decreasing	25	-114
South America	-16.1	-29.0	-4.7	0.0070	decreasing	68	-54
Oceania	-4.6	-9.5	0.7	0.1029	no trend	9	-11
Global	-136.6	-172.9	-86.4	0.0000	decreasing	246	-663

删除了: 7

Table 12: Statistical results of change analysis for barren land (on the scale of continents) . Annual change slope and its 95 % confidence interval are given by Thei-sen estimator, p-value and trend information from a Mann-Kendall test. Gain and Loss areas are summarized results relating to the whole time series.

Continent	Slope (10^3 km^2/year)	Lower (10^3 km^2/year)	Upper (10^3 km^2/year)	p	Trend	Gain (10^3 km^2)	Loss (10^3 km^2)
Africa	-26.1	-37.4	-17.7	0.0000	decreasing	2	-43
Asia	-28.3	-40.6	-18.1	0.0000	decreasing	12	-82
Europe	-2.8	-3.5	-1.8	0.0000	decreasing	0	-6
North America	-8.8	-21.3	-1.0	0.0353	decreasing	26	-49
South America	1.6	-2.3	5.3	0.3737	no trend	4	-5
Oceania	-16.8	-32.2	4.0	0.1161	no trend	0	-25
Global	-78.5	-116.4	-48.8	0.0001	decreasing	48	-213

1640

删除了: Table 8: Statistical results of change analysis for shrubland (on the scale of continents) . Annual change slope and its 95 % confidence interval are given by Thei-sen estimator, p-value and trend information from a Mann-Kendall test. Gain and Loss areas are summarized results relating to the whole time series. .

Continent ... [36]

删除了: 10

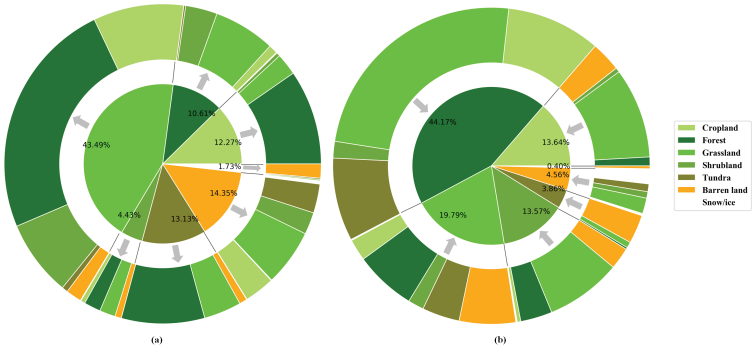

Figure 12: Land cover conversions with significant land cover change (LCC) between 1982 and 2015. The inner pie in (a) shows the percentages of different gross gain for each land cover, and the outer ring indicates which land cover the gross gain came from. The inner pie in (b) shows the percentage of different gross loss for each land cover, and the outer ring in indicates which land cover the gross loss went to.

删除了: **Table 11: Statistical results of change analysis for snow/ice (on the scale of continents) . Annual change slope and its 95 % confidence interval are given by Thei-sen estimator, p-value and trend information from a Mann-Kendall test. Gain and Loss areas are summarized results relating to the whole time series.** .

Continent ... [37]

删除了: **11**

Table 13: Area ratio (%) of land cover conversions from 1982 to 2015, where the red color denotes a higher ratio, and the blue color represents a lower ratio.

Class		2015						
		Cropland	Forest	Grassland	Shrubland	Tundra	Barren land	Snow/ice
1982	Cropland	-	9.6	2.22	0.37	0	0.09	0
	Forest	0.9	-	6.26	3.24	0.19	0.01	0.01
	Grassland	9.22	24.27	-	7.73	0.6	1.6	0.06
	Shrubland	0.45	1.7	1.62	-	0	0.66	0
	Tundra	0	8.48	3.82	0	-	0.79	0.04
	Barren land	3.07	0.07	5.75	2.23	2.93	-	0.29
	Snow/ice	0	0.05	0.13	0	0.13	1.43	-

删除了: 12

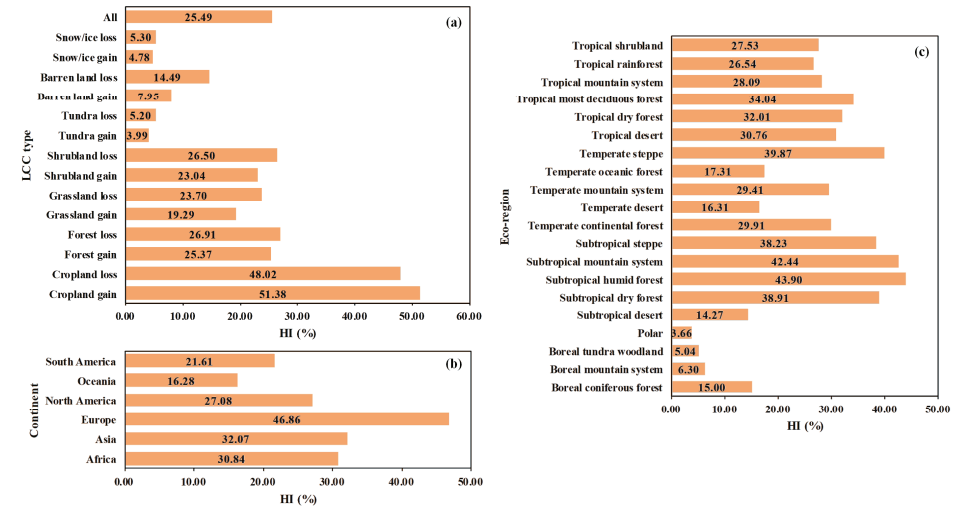

Figure 13: The mean human impact (HI) of regions with significant land cover change on the scale of (a) LCC, (b) continents and (c) eco-regions.

删除了:

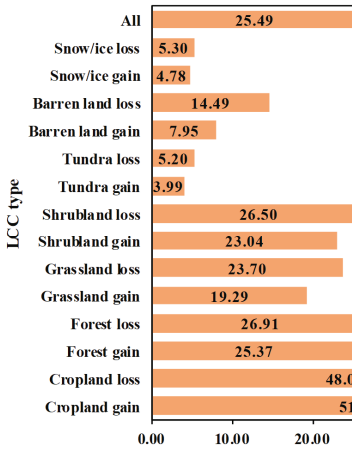

删除了: 12

删除了: (on the scale of

删除了:).

设置了格式: 字体: (默认) Times New Roman

删除了: .

分页符

.

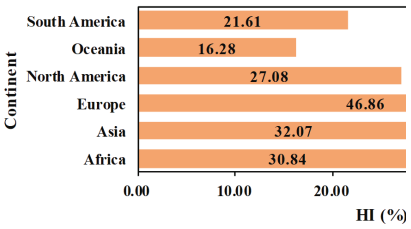

Figure 13: The mean human impact (HI) of regions with significant land cover change (on the scale of continents).

分页符

.

... [38]

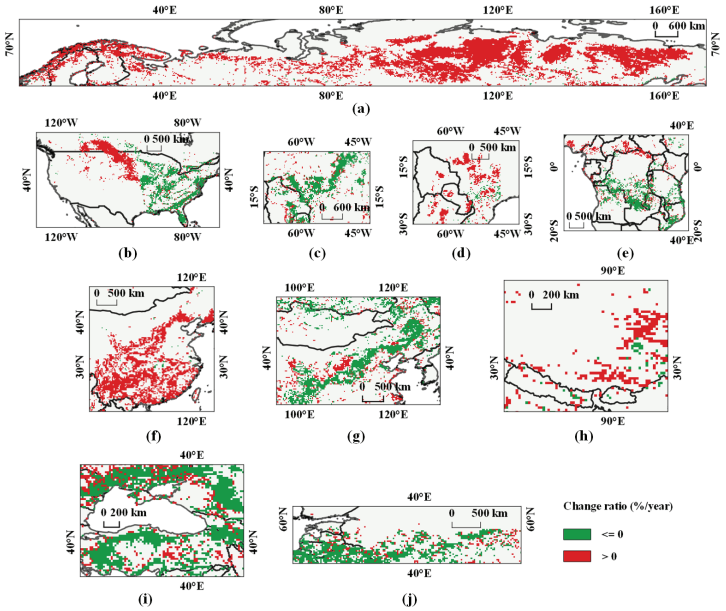

Figure 14: Visualization of local hotspots of land cover change, (a) north Eurasia, forest, (b) Great Plains of Central North America, cropland, (c) South America, forest, (d) South America, cropland, (e) Africa, forest, (f) China, forest, (g) Mongolia and Inner Mongolia of China, grassland, (h) Qinghai-Tibet Plateau, grassland, (i) central Asia, grassland, (j) the former Soviet Union in Eastern Europe, cropland.

删除了: 15

删除了: 分页符

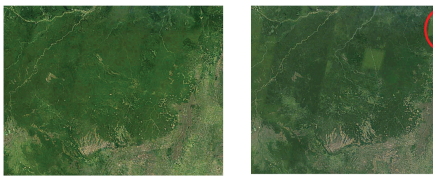

Figure 16: Example visualization for the cropland expansion and deforestion phenomenon in the southeastern part of the Amazon rainforest from Google Earth images in (a) 1984, (b) 1994, (c) 2000, (d) 2015, where the phenomenon is significant in area within red circles.

设置了格式: 英语(英国)